12-10-2005

A Micro-Cooling, Heating, And Power (M-CHP) Instructional Module

Jason Ryan Oliver

A micro-COOLING, HEATING, AND POWER

(m-CHP) INSTRUCTIONAL MODULE

By

Jason Ryan Oliver

A Thesis
Submitted to the Faculty of
Mississippi State University
in Partial Fulfillment of the Requirements
for the Degree of Master of Science
in Mechanical Engineering
in the Department of Mechanical Engineering

Mississippi State, Mississippi

December 2005

Name: Jason Ryan Oliver

Date of Degree: December 9, 2005

Institution: Mississippi State University

Major Field: Mechanical Engineering

Major Professor: Dr. B.K. Hodge

Title of Study: A micro-COOLING, HEATING, AND POWER (m-CHP) INSTRUCTIONAL MODULE

Pages in Study: 209

Candidate for Degree of Master of Science

Cooling, Heating, and Power (CHP) is an emerging category of energy systems consisting of power generation equipment coupled with thermally activated components. The application of CHP systems to residential and small commercial buildings is known as micro-CHP (m-CHP). This instructional module has been developed to introduce engineering students to m-CHP. In the typical engineering curriculum, a number of courses could contain topics related to m-CHP. Thermodynamics, heat transfer, HVAC, heat and power, thermal systems design, and alternate energy systems courses are appropriate m-CHP topics. The types of material and level of analysis for this range of courses vary. In thermodynamics or heat transfer, basic problems involving a m-CHP flavor are needed, but in an alternate energy systems course much more detail and content would be required. This instructional module contains both lecture material and a compilation of problems/exercises for both m-CHP systems and components.

TABLE OF CONTENTS

CHAPTER Page

CHAPTER Page

CHAPTER Page

LIST OF TABLES

TABLE Page

LIST OF FIGURES

FIGURE Page

FIGURE Page

FIGURE Page

NOMENCLATURE

C	capacity ratio
C_c	capacity of the cold fluid
C_h	capacity of the hot fluid
COP	coefficient of performance
cp	constant pressure specific heat
cv	constant volume specific heat
G	Gibbs energy
h	specific enthalpy
i	enthalpy
k	ratio of specific heats
m	mass
$\dot{m}$	mass flow rate
n	the number of moles of gas
NTU	number of transfer units
p	pressure
Qin	heat addition to the system during the cycle
Qout	heat rejected from the system during the cycle
Q′in	heat added in the generator

Q′out	heat rejected in the absorber
$\dot{q}$	rate of heat transfer
r	compression ratio
R	the gas constant
rc	cutoff ratio
s	specific entropy
T	temperature
u	specific internal energy
UA	conductance
v	specific volume
V	Volume
W	work of a given cycle
$\dot{W}_P$	power requirement for pump operation
x	concentration

Greek

$\overline{\Delta T}$	log mean temperature difference
ΔT	change in temperature between two states
ξ	heat exchanger effectiveness
ξ_{rec}	recuperator effectiveness
η	efficiency

Subscripts

HX	denotes heat exchanger
MAX	denotes maximum rate of heat transfer of the heat exchanger
evaporator	rate of heat transfer in the evaporator
generator	rate of heat transfer in the condensor
C	denotes compressor
in	indicates a quantity is input to the system
Diesel	denotes the Diesel cycle
net	indicates a net quantity of a given cycle
Otto	denotes the Otto cycle
p	denotes a pump
Stirling	denotes the Stirling cycle
T	denotes a turbine
fc	the electrical conversion efficiency of a fuel cell
i	indicates the current efficiency of a fuel cell
Rank	denotes the Rankine cycle
th	indicates the thermal efficiency of a fuel cell
v	indicates the voltage efficiency of a fuel cell

CHAPTER I:

micro-CHP

Micro-cooling, heating, and power (m-CHP) is decentralized electricity generation coupled with thermally activated components for residential and small commercial applications. m-CHP systems can simultaneously produce heat, cooling effects, and electrical power. The “micro” regime is typically designated as less than fifteen kilowatts electric (< 15 kWe).

The concept of m-CHP is illustrated in Figure 1.1. A prime mover, such as a reciprocating engine, drives a generator which produces electrical power. The waste heat from the prime mover is recovered and used to drive thermally activated components, such as an absorption chiller or desiccant dehumidifier, and to produce hot water or warm air through the use of heat exchangers.

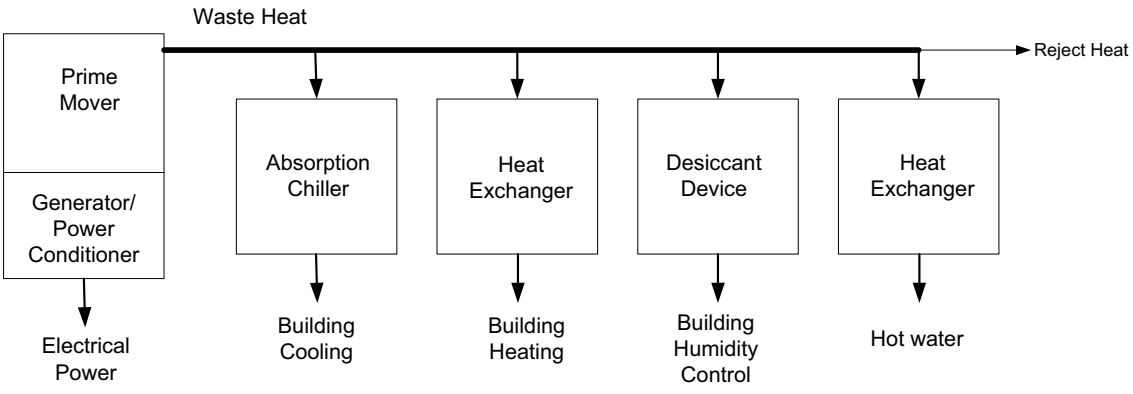

Figure 1.1: Schematic of an m-CHP System

Cooling, heating, and power (CHP) has proven beneficial in many industrial situations by increasing the overall thermal efficiency, reducing the total power requirement, and providing higher quality, more reliable power. Applying CHP technology to smaller scale residential and small commercial buildings is an attractive option because of the large potential market.

The residential and small commercial sectors account for 40% of the electrical usage in the U.S. As can be seen from Figure 1.2, the residential and small commercial sectors make up the largest portion of the utility electricity market.

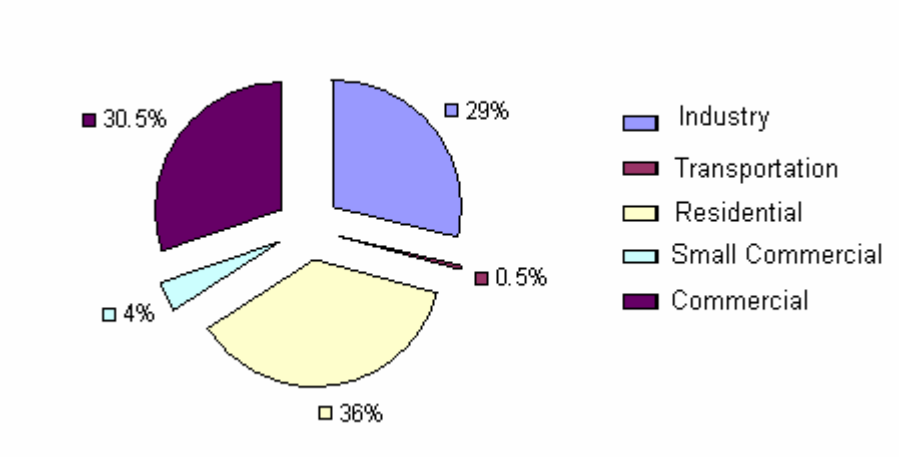

Figure 1.2: 2001 U.S. Electrical Consumption by Building Sector (http://www.eia.doe.gov)

The residential energy consumption is not only the largest portion of the pie, but it is also the fastest growing segment. Between 1978 and 1997, the number of U.S households has increased by over 30%. At the same time, space heating expenditures have increased by 75%, air conditioning by 140%, and

water heating by 184%. The largest increase in household energy expenditures was for home appliances, which increased by 210%.

As a result of such large increases, residential energy consumption is projected to increase 25% from 2001-2025. The question is: Why should m-CHP be considered a viable option to meet the needs of the U.S. residential and small commercial market?

The basis of this answer can be found by applying the “wells to wheels” analysis concept to the energy production for a single residence. The idea of “wells to wheels” is that the whole system must be considered from fuel harvesting to the energy (in some final form) that is used. In addition, each time that fuel is converted, packaged, or transported, there is an associated loss of energy. The more conversion and transportation steps in a process, the greater the associated energy losses.

In the U.S. as of 2004, electricity is generated by coal (50%), nuclear (20%), natural gas (18%), hydro (7%), petroleum (3%), and various renewable energy methods (2%). The traditional method of electrical power generation and distribution is based on large, centrally-located power plants. Central means that the power plant is located on a hub surrounded by major electric load centers.

Once the electricity is produced, the power must be delivered to the end user. Delivery is achieved by a utility transmitting the electricity to a substation through a high-voltage electrical grid. At the substation, the high-voltage electricity is transformed, or stepped down, to a lower voltage to be distributed to

individual customers. The electricity is then stepped down a final time by an on site transformer before being used by the customer. The number of times that the electricity must be transformed depends largely upon the distance the power is transmitted and the number of substations used in distributing the electricity.

Inefficiencies are associated with the traditional methods of electrical power generation and delivery. To begin, the majority of the energy content of the fuel is lost at the power plant through the discharge of waste heat. Traditional power plants convert about 30% of a fuel's available energy into electric power. Highly efficient combined-cycle power plants convert about 50% of the available energy into electric power. Further energy losses occur in the transmission and distribution of electric power to the individual user. Inefficiencies and pollution issues associated with conventional power plants have provided the motivation for new developments in on-site power generation. The overall efficiencies of central power generation and distributed combined-cycle power generation are shown in Figures 1.3 and 1.4.

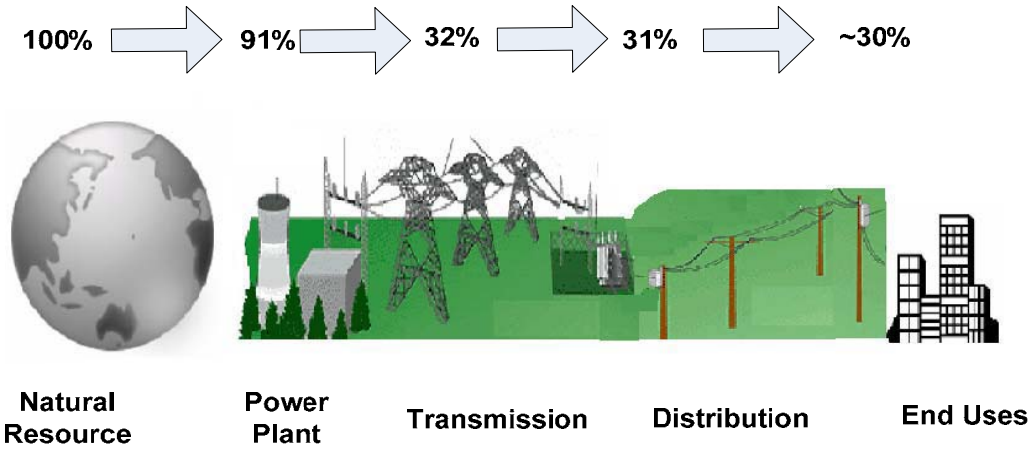

Figure 1.3: Efficiency of Central Power Generation

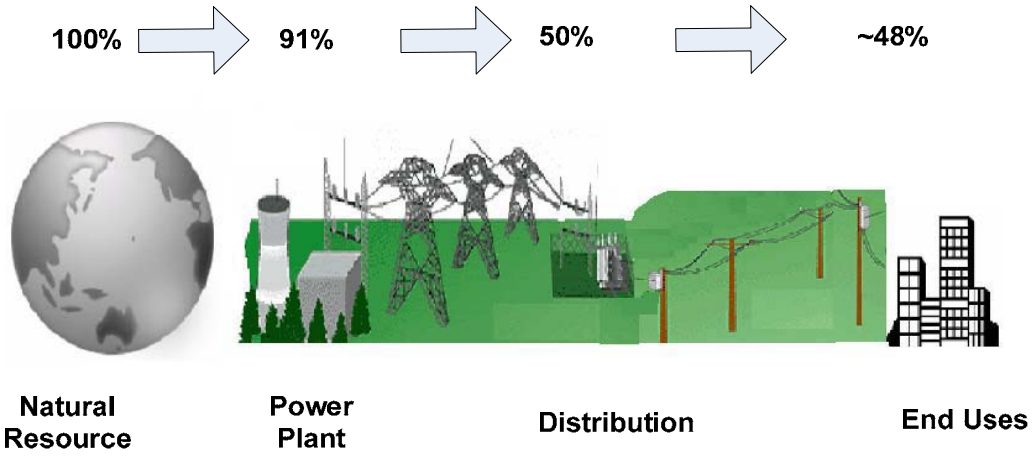

Figure 1.4: Efficiency of Combined-Cycle Power Generation

Once the electric power reaches the end user, the electricity is used to run central heat and air conditioners, appliances, lighting, and in some cases, water heating. These are the same end uses that could be provided by an m-CHP system at a greater overall thermal efficiency. Micro-combined heat and power units utilize waste heat while simultaneously producing electric power for a

residence or building. The waste heat is used to meet space and water heating requirements and to provide cooling if an absorption chiller is incorporated into the system. Heating and cooling are major end uses of residential energy. Because the heating and cooling loads of the space are being met without total dependence on electrically-driven thermal components, the overall electric load of the residence will be reduced.

Another advantage of m-CHP is that there are no losses associated with power distribution and transmission as opposed to the traditional power generation method. m-CHP systems can utilize about 75% of the fuels available energy to provide electric and thermal energy. A m-CHP system can produce an overall efficiency of about 75% while a modern combined-cycle power plant will have an overall efficiency of around 50%. The overall efficiencies of a m-CHP system is shown in Figure 1.5.

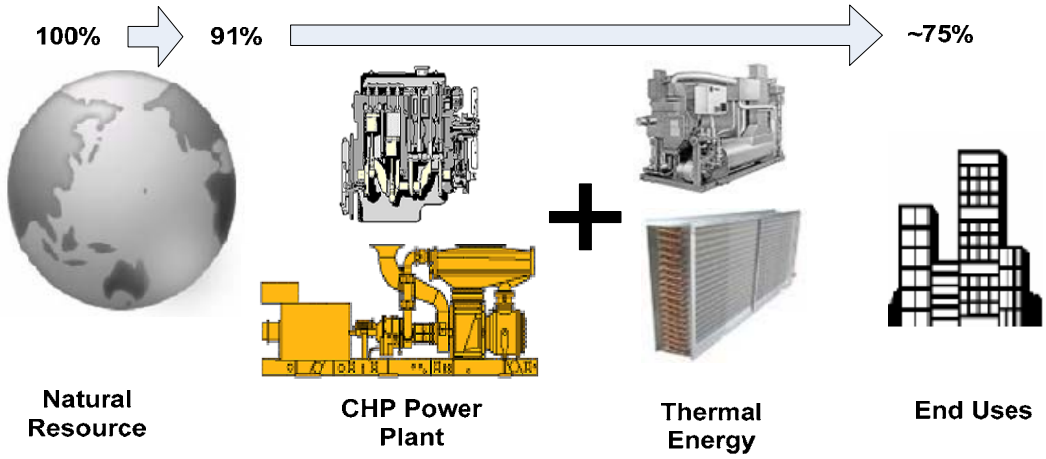

Figure 1.5: Efficiency of m-CHP System

Larger homes, higher energy costs, volatile fuel markets, electricity blackouts, power security, power quality, and increasing concern for environmental issues have all helped open the door for m-CHP. RKS, a leading market research firm, found that more than 38% of high-income households, (i.e., incomes greater than $50,000) are interested in generating their own electricity. (Micro-CHP Technologies Roadmap, U.S. DOE)

CHAPTER II:

EUROPEAN EXPERIENCES WITH m-CHP

Many factors have spurred the European community to explore alternative methods for power generation. The blackouts in North America and Europe placed a focus on reducing consumer dependence on traditional grid-distributed electricity. At the same time, many European nations set carbon-dioxide reduction targets in accordance with the Kyoto Protocol. One of the methods identified capable of helping nations achieve both goals is domestic CHP.

Feasibility studies for the use of m-CHP in Europe began in the early 1990s and since that time, several m-CHP technologies have been developed and investigated. However, since m-CHP is viewed differently in Europe and because differences in markets and climatic conditions exist in Europe, the technologies developed and used in Europe may not be directly applicable to the U.S. market.

To begin, European m-CHP is typically viewed as “A direct replacement for a boiler in a hydronic heating system, which simultaneously produces heat and electrical power.” (Harrison, 2003a) Basically, the unit replaces the boiler in the conventional central heating system and the electricity produced is considered a by-product. Also, until recently, most technologies and applications

identified as having potential for m-CHP have focused on natural gas fired applications. Because of the manner in which m-CHP is viewed, units have been designed for ease of implementation into the majority of European homes. This has lead to great market potential for m-CHP units in the European residential sector.

m-CHP systems have the potential to have an installed capacity of 22 GWe in the United Kingdom and a potential of 60 GWe installed capacity in Europe by 2010. Approximately 40 million homes have been identified as suitable candidates for m-CHP. In the UK, 14 – 18 million of the 24 million households have been identified as candidates for m-CHP. Around 18 million homes in the UK are provided with gas-fired central heating. Based on the rate for replacing standard boilers in the UK, an estimated 600,000 new m-CHP systems could be installed or retrofitted in place of conventional boilers each year. Over a 25 year span, this technology could reach 16 million UK homes. "At present, the marginal cost of replacing boilers [with m-CHP units] suggests a payback period of 5 – 8 years." Current goals are to have one million units installed in Europe by 2010 (Flin, 2005).

With one-third of the UK's carbon dioxide emissions coming from domestic energy consumption, the prospect of reduced emissions by implementing m-CHP has great appeal. When replacing a natural gas-fired boiler, a typical m-CHP unit with 1 kW of electrical output could potentially save 1.7 tons per year of carbon dioxide emissions (Harrison, 2003a). Potentially, the UK could reduce carbon

dioxide emissions by 9 – 12 million tons per year through m-CHP (Flin, 2005). The potential is to reduce carbon dioxide emissions in Europe by 40 million tons per year using natural gas fired m-CHP (Harrison, 2003a).

Because of the existing market potential, several companies, such as SenerTec, Power Plus Technologies, Whisper Tech, Siemens Westinghouse, Honda, and Plug Power have developed m-CHP units with the intention of mass marketing. The prime movers used in the m-CHP units range from internal combustion engines and micro-turbines to Stirling engines and fuel cells. Though the technology differs and considerations for each system are different, common characteristics needed by all prime movers are

- Low noise and vibration
- Low maintenance – essentially maintenance free
- Small size and low weight
- Reliable and simple operation
- Easy installation
- Low capital cost

Common challenges have also been identified in the European market. Many of these challenges stem from the incorporation of m-CHP systems into the current infrastructure of the electrical utilities and from the variation of electric and thermal loads due to geographic location. Other challenges arise from overcoming the inertia of the utility market. “Three major obstacles currently existing to market penetration are cost, the requirement for market

transformation, and developing the necessary maintenance skill base (Flin, 2005)." Some of these challenges also exist for the U.S. market. Other challenges include

- Control of the unit and a network of units to ensure optimal performance
- Selecting the right technology for the environment in which the unit is to be placed
- Developing units with the ability to be controlled and diagnosed remotely
- Designing the entire system for minimum costs (Flin, 2005)

Several lessons can be drawn from the success and failure of the technologies developed in Europe. When selecting a prime mover for a system, two of the most important considerations are the heat-to-power ratio and operating cost (Harrison, 2003c). Experience has shown that, "m-CHP operation follows thermal demand and generates electricity according to that demand profile (Harrison, 2003b)." Because of this, many of the prime movers with higher efficiencies did not perform as well as less efficient prime movers that provided a suitable match of thermal and electric loads. Also, high efficiency corresponds to higher stresses and temperatures, which in turn leads to high material and production costs and issues with service life (Harrison, 2003c).

The European experience has also shown that gaining the cooperation and participation of the distributed network operators (European equivalent of local utility providers) is crucial (Harrison, 2003c). Due to the high price of energy storage and the need to draw power from the grid at peak times, m-CHP units need to be grid connected. If an m-CHP unit is not grid connected, then the

systems must either be oversized for base load operation (thus requiring energy storage in the form of batteries) or be provided with a peaking load generator (to accompany the base load generator). In either case, the cost of the m-CHP system increases drastically, decreasing market appeal.

By involving the network operators and the electric utilities, the issue of buying from the grid and selling electricity to the grid raises the problem of metering. To fully utilize m-CHP, energy companies must develop means that would allow them to aggregate and dispatch electricity remotely and measure the flow of electricity into and out of a location (Flin, 2005).

Another widely recognized concern of implementing m-CHP into the European market is quality installation and professional service support. Service support has been a vital component in the success or failure of several European technologies. As stated by Harrison, “Poor initial support has led to some products, such as heat pumps and condensing boilers being considered unreliable and undesirable by the general public in some states (Harrison, 2003c).”

In conclusion, Halliday-Pegg (Cambridge Consultants) states, “It is clear that domestic CHP will shake up the home energy market, but there are still fundamental questions which must be addressed, and much development and cost reduction is required to transform promising technology into viable products and services for the mass market. Market penetration will only be possible when the systems are at a cost the market can bear (Flin, 2005).”

CHAPTER III:

THE m-CHP SYSTEM

Micro-cooling, heating, and power combines distributed power generation with thermally activated components to meet the cooling, heating, and power needs of residential and small commercial buildings. The success of CHP systems for large-scale application coupled with the development of power generation equipment and thermally activated components on a smaller scale have contributed to the development of m-CHP applications. Distributed power generation technologies and thermally activated components will be introduced and briefly discussed.

Distributed Power Generation

A number of technologies are commercially available or under development for generating electric power (or mechanical shaft power) onsite or near site where the power is used. Distributed power generation is a required component of m-CHP systems. Fuel cells, reciprocating engines, Stirling engines, Rankine cycle engines, and microturbines are prime movers that have the most potential for distributed power generation for m-CHP systems.

Reciprocating Engines

Reciprocating engines can be used to produce shaft power. The shaft power can then be used to drive a generator to produce electrical power. The shaft power can also be used to operate equipment such as compressors and pumps. The application of reciprocating engines is widespread and highly developed. Reciprocating engines use natural gas, propane, gasoline, diesel and biofuels to produce 0.5 kW to 10 MW of power. A diesel fuel engine generator set is shown in Figure 3.1.

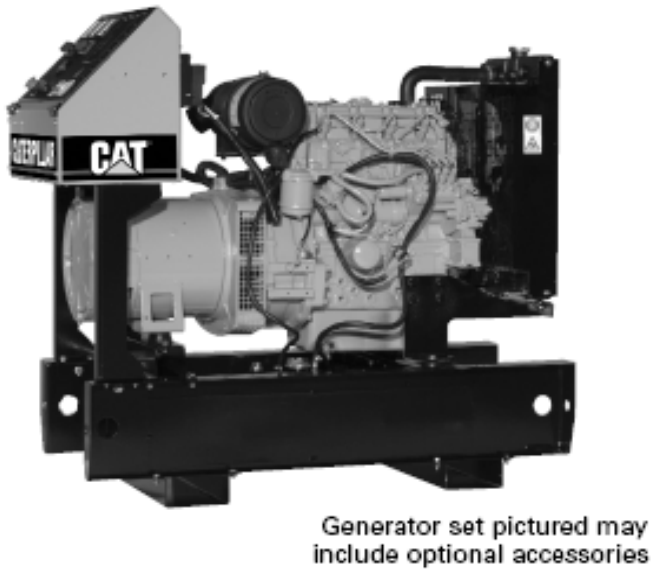

Figure 3.1: Model D13-2, 12-kW Diesel Engine Generator Set from Caterpillar. (http://www.cat.com)

Reciprocating engines exhibit characteristics that are advantageous for m-CHP applications. Reciprocating engines used for power generation have proven reliability, good load-following characteristics, low capital cost, fast startup, and significant heat

recovery potential. Recent advances in combustion design and exhaust catalyst have also helped reduce overall emissions of reciprocating engines. Currently, reciprocating engines are the most widely used distributed energy technology. Typical electrical conversion efficiencies are in the range of 25% to 40%. The overall thermal efficiencies of these systems increase with the incorporation of thermally activated components.

The thermal energy in the engine cooling system and exhaust gases from reciprocating engines can often be recaptured and used for space heating, for hot water heating and for driving thermally activated components. Shaft power from the engine can also be used to power thermal components, such as gas vapor compression chillers. Such chillers are very similar to electric-driven chillers with the exception that the compressor is driven by the reciprocating engine rather than an electric motor.

Emissions of reciprocating engines tend to be higher than that of other distributed generation equipment. Due to the emissions and noise emitted by these engines, care must be exercised in the location of the engine with respect to the occupants of the building. In some areas, local air quality standards may limit the use of reciprocating engines.

Microturbines

Microturbines were derived from turbocharger technologies found in large trucks or the turbines in aircraft auxiliary power units (APUs) and have a capacity range of 25 kW to 500 kW. Microturbines utilize a variety of fuels including

natural gas, propane, and biofuels. Electrical energy efficiencies of 25% to 30% are capable with the use of regenerators. Microturbines have fewer moving parts than other generation equipment of similar capacity, creating the potential for reduced maintenance intervals and cost. Though the generating capacity of microturbines is above the range defined in the m-CHP regime, microturbines have considerable potential in on-site power generation applications such as apartment complexes and clusters of small commercial buildings.

The waste heat from a microturbine is primarily in the form of hot exhaust gases. This heat is suitable for powering a steam generator, indirect heating of a building, allocation to thermal storage devices, or use in heat-driven cooling systems. Most designs incorporate recuperators that limit the amount of heat available for m-CHP applications.

Microturbines have relatively low emissions and noise and also have low maintenance costs. Another advantage is that microturbines are relatively small in size or footprint. The fuel flexibility and quantity of hot exhaust gases make microturbines an advantageous technology for m-CHP and cogeneration applications. The Capstone C30, a 30-kW microturbine, is pictured in Figure 3.2.

Figure 3.2: Capstone C30 Microturbine. (www.capstone.com)

Stirling Engines

The Stirling engine is a type of external combustion piston engine which uses a temperature difference to produce motion. The cycle is based on the behavior of a fixed volume of gas. The heat source used to provide the temperature difference can be supplied by a wide variety of fuels or solar energy. The Stirling engine has only seen use in specific and somewhat limited applications. However, recently many companies have begun research and development related to Stirling engines due to their potential for m-CHP applications and solar power stations.

Stirling engines typically have an electrical efficiency in the range of 12% to 25%. This efficiency can be increased with the use of recuperators. The operation of a Stirling engine requires that one side of the engine remain hot

while the other side remains cool. This requirement makes heat recovery an integral part of the operation of a Stirling engine. Heat can be recovered from dissipation of the heat source and through the use of heat exchangers on the cool side of the engine. Stirling engines have low emissions and create low noise levels. These engines are also mechanically simple, and because there is no internal combustion, the maintenance requirements of Stirling engines are relatively low. However, due to design, Stirling engines are heavy and large for the amount of power generated. Stirling engines also have one of the higher capital costs of distributed power generation technologies. The SOLO 9-kW Stirling engine based m-CHP unit is shown in Figure 3.3.

Figure 3.3: SOLO 9-kW Stirling Engine
(http://www.stirling-engine.de/engl/index.html)

Rankine Cycle Engines

Rankine cycle engines are based upon the well known thermodynamic cycle that is used in most commercial electric power plants. The shaft power from a Rankine cycle engine is used to drive an electric generator in the same

manner as reciprocating or Stirling engines. Rankine cycle engines have relatively low electrical conversion efficiency. However, as m-CHP technologies are designed to follow the thermal load, this low electrical efficiency becomes less of a drawback because significant thermal energy that can be recovered from a Rankine cycle engine. The durability and performance characteristics of Rankine cycle engines are also well known, and low production costs are a potential benefit.

The construction of a Rankine cycle engine allows heat to be recaptured easily through the use of a condenser, which is already a component in the engine cycle. Currently, Rankine cycle engines for m-CHP applications are in the development stage. As a result, cost and specific performance characteristics are not yet defined. A Cogen Microsystems 2.5-kW m-CHP unit based on a Rankine cycle engine is pictured in Figure 3.4.

Figure 3.4: Cogen Microsystems 2.5-kW Rankine Cycle m-CHP Unit (www.cogenmicro.com)

Fuel Cells

Fuel cells are electrochemical energy conversion devices that produce electrical power rather than shaft power. Unlike the technologies discussed previously, fuel cells have no moving parts and, thus, no mechanical inefficiencies. Four major types of fuel cells will be discussed: proton exchange membrane (PEMFC), solid oxide (SOFC), phosphoric acid (PAFC), and molten carbonate (MCFC) fuel cells. Each of these fuel cell types operate differently and exhibit different performance characteristics.

In general terms, fuels cells combine a hydrogen based fuel input and gaseous stream containing oxygen in the presence of a catalyst to initiate a chemical reaction. The products of this reaction vary for each type of fuel cell but typically are electrical power, heat, and water. In some instances, other product gases such as carbon dioxide are formed. As a pure hydrogen-rich fuel is required by most fuel cells, hydrogen reformers are often included in a fuel cell system.

Like batteries, fuel cells produce direct current (DC) electrical power. This requires that an inverter and power conditioner be used to transform the DC current into alternating current (AC) at the appropriate frequency for use in the majority of applications.

Fuel cells can achieve high electrical efficiencies as compared to other distributed power generation equipment. Fuel cells exhibit quiet operation and low emissions. Also, the absence of mechanical components decreases

maintenance. Unfortunately, the costs of fuel cells are relatively high as compared to other technologies. The fuel flexibility of fuel cells is also low as very pure streams of hydrogen are the only suitable fuel for certain types of fuel cells. In some instances, the energy required to reform the input fuel greatly decreases the overall efficiency of a fuel cell system. Still, fuel cells are a promising technology that hold potential for m-CHP applications. A Plug Power fuel cell is shown in Figure 3.5.

Figure 3.5: Plug Power Fuel Cell Unit (www.plugpower.com)

Heat Recovery

In most m-CHP applications, heat recovery is accomplished by ducting the exhaust gas from a prime mover to a heat exchanger to capture the thermal energy in the gas stream. Generally, these heat exchangers are air-to-water heat exchangers, where the exhaust gases flow over a fin-tube heat exchanger surface and the heat is used to produce hot water, or in some cases, steam. For

prime movers that include a cooling jacket that circulates engine coolant, a liquid-to-liquid heat exchanger can also be used to recover waste heat in the form of hot water. The hot water can then be used directly or used to operate thermally activated components, such as desiccant dehumidifiers and absorption chillers. Many of the thermal technologies used in the construction of an m-CHP system require hot water at pressures of 15 – 150 psig. If needed, additional heat can be supplied through a duct burner to provide additional steam or hot water.

Depending on the amount of waste heat available and the emission concentrations of the prime mover, air-to-air heat exchangers can be used for space heating for a building. However, air-to-air heat exchangers often have lower effectivenesses than air-to-liquid heat exchangers.

In most m-CHP installations, a flapper damper or diverter valve is used to control the flow of exhaust gases to the recovery heat exchanger. The flapper can be used to divert a portion of the exhaust to the atmosphere to maintain desired design conditions at the recovery heat exchanger. Exhaust gases can also be used to drive an enthalpy wheel or desiccant dehumidifier in an m-CHP system. An enthalpy wheel uses the exhaust gases to heat one side of a rotating wheel with a medium that absorbs the heat and then transfers the heat to the incoming air flow on the opposite side of the wheel. Temperature has a strong relationship to the usefulness of waste heat. The term “quality” is often used to describe the usefulness of waste heat in these terms.

Thermally Activated Devices

Thermally activated devices are technologies that utilize thermal energy rather than electric energy to provide heating, cooling, or humidity control. The primary thermally activated components used in m-CHP systems are desiccant dehumidifiers and absorption chillers.

Desiccant Dehumidifiers

The comfort level of a conditioned space is determined by the temperature and the relative humidity. Humidity control is also important to protect the health of the occupants inhabiting the conditioned space. The humidity level should remain below 60% Relative Humidity (RH) to prevent growth of mold, bacteria, and other harmful organisms in buildings and to prevent adverse health effects.

Traditionally, a single piece of equipment, a cold coil, has been used for both the temperature and humidity control for a conditioned space. Dehumidification effects have been achieved by reducing the temperature of the process air below its dew point. Moisture in the air condenses on the surface of cooling coils over which the air passes. Cooler air containing less moisture can then be sent to the conditioned space. However, in some cases, the temperature of the air leaving the cooling coils is below the comfort level and the air must be reheated to the desired temperature.

Desiccants are materials that directly absorb moisture from air. Desiccant dehumidifiers can be used to reduce the moisture content of air. In an m-CHP

system, recovered heat is used for regenerating the desiccant material in dehumidifiers. Desiccant dehumidifiers satisfy the latent load by reducing the relative humidity of the air. Sensible cooling is provided by a cold coil from absorption chillers or conventional air conditioning units. Desiccant dehumidifiers operate in series or parallel with other cooling system components. A Bry-Air, MiniPAC^{TM} desiccant dehumidifier is pictured in Figure 3.6.

Figure 3.6: MiniPAC Desiccant Dehumidifier by Bry-Air (http://www.bry-air.com/)

Absorption Chillers

Absorption chillers use heat as the primary energy source for driving an absorption refrigeration cycle. Little electrical power is needed for most absorption chiller designs (0.02 kW/ton) as compared to electric driven chillers (0.47 to 0.88 kW/ton). Absorption chillers also have fewer moving parts as compared to electric chillers and exhibit quieter operation than electric chillers.

Commercially available absorption chillers can utilize steam, hot water, exhaust gases, and direct combustion as heat sources. Absorption chillers that utilize hot water and exhaust gases are prime candidates for providing some or

all of the cooling load in an m-CHP system. Modern absorption chillers can also provide heat in the winter and feature electronic controls that allow quick start-up, automatic purge, and greater turndown capacity than many electric chillers. Maintenance contracts and warranties, comparable to those for electric chillers, are also available for absorption chillers.

Absorption chillers come in single-effect and multiple-effect configurations. Multiple-effect absorption chillers have higher capital cost than single-effect chillers. However, multiple effect absorption chillers are more energy efficient and, therefore, are less expensive to operate. The attractiveness of absorption chillers for m-CHP applications depends on capital costs, operational costs, and cooling load requirements. A Yazaki Energy Systems, Inc. 10-ton capacity WFC-S Series absorption chiller is shown in Figure 3.7.

Figure 3.7: Yazaki Energy Systems WFCS Series 10-ton Absorption Chiller. (www.yazakienergy.com)

CHAPTER IV:

PRIME MOVERS

Reciprocating Engines

Technology Overview

Fossil fueled internal combustion (IC) engines are in widespread and diverse use. Available IC engines range from small portable gasoline engines to large 50,000 horsepower diesel engines. An IC engine is powered by the expansion of the hot combustion products of fuel directly acting within the engine. IC engines require air, fuel, compression, and a combustion source to function. The two types of combustion engines which are most significant to stationary power generation are the spark-ignition, four-stroke reciprocating IC engines and the compression-ignited engines, typically using diesel fuel.

Basic engine terminology is schematically illustrated in Figure 4-1. The bore is the cylinder diameter. The piston is at top dead center (TDC) when the cylinder volume is a minimum. When the piston is moved to the position where the cylinder volume is at a maximum, the piston is at bottom dead center (BDC). The stroke is the distance between TDC and BDC. The displacement volume, usually just called the displacement, is the volume displaced as the piston moves from TDC to BDC - the area of the bore times the stroke

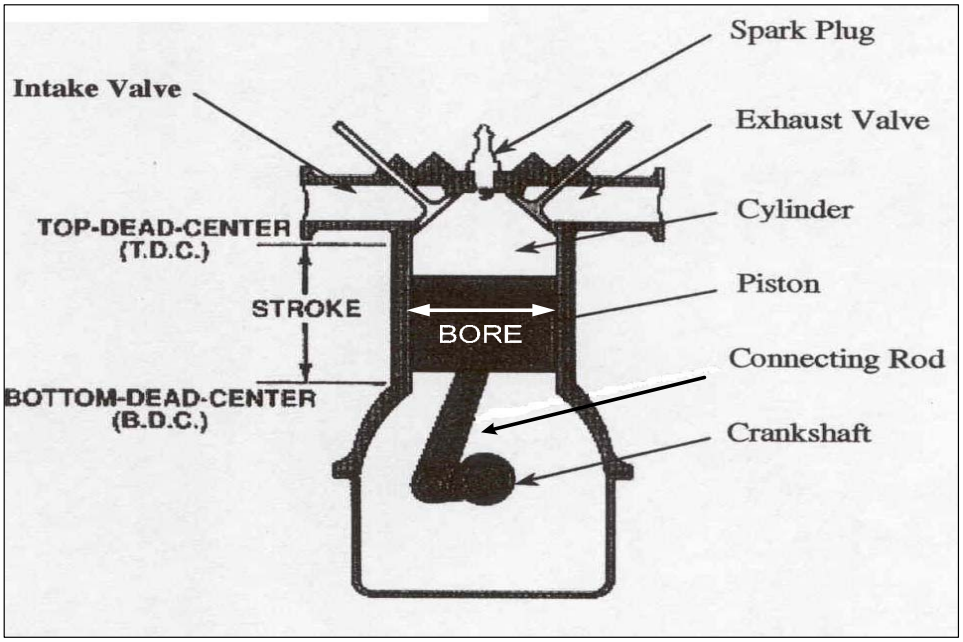

Figure 4.1: Four-stroke Reciprocating IC Engine
(www.personal.washtenaw.cc.mi.us)

The four-stroke IC engine is a spark-ignited reciprocating engine that operates on the basis of the Otto cycle. The major components of the four-stroke IC engine are an ignition source (spark plug), cylinder, piston, connecting rod, intake and exhaust valves, and a crankshaft shown in Figure 4.1. The basic IC engine model is the air-standard Otto cycle, in which heat is added instantaneously while the piston is at top dead center and in which heat is rejected at constant volume.

The air-standard Otto cycle consists of four internally reversible processes in series. The pressure-specific volume (pv) and temperature-entropy (Ts) diagrams for the air-standard Otto cycle are shown in Figure 4.2. As the piston moves from BDC to TDC, an isentropic compression of air comprises Process 1

– 2. Process 2 – 3 is a constant volume heat transfer to the air from an external source. Combustion begins as the heat is added to the compressed working fluid. The piston moves from TDC to BDC in Process 3 – 4 through an isentropic expansion, the power stroke. Process 4 – 1 is constant volume heat rejection with the piston at bottom dead center to complete the cycle.

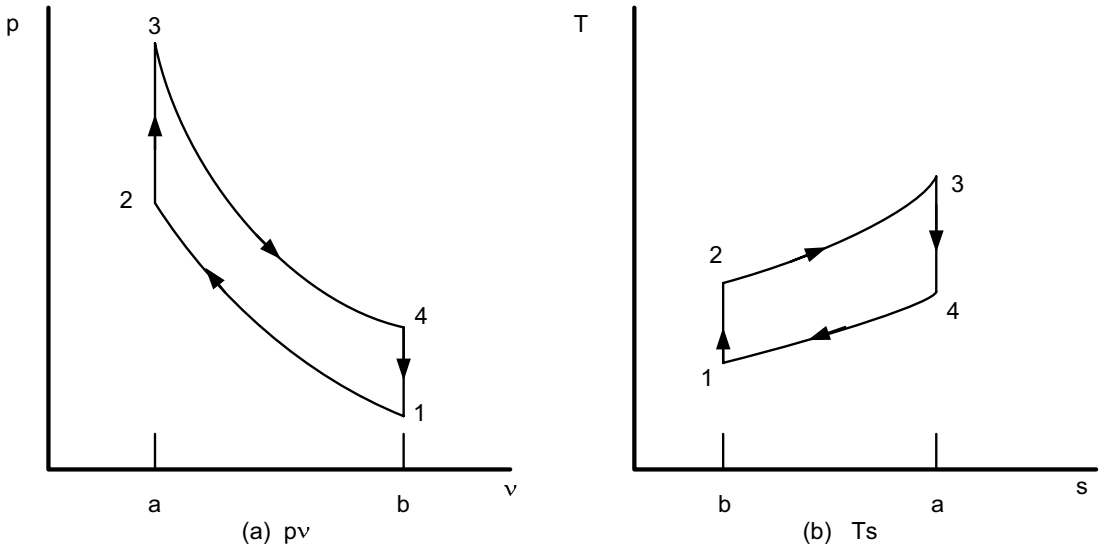

Figure 4.2: Pressure-Specific Volume and Temperature-Entropy Diagrams for the Air-Standard Otto Cycle.

The expressions for the work accomplished by the cycle (W_{Otto}), the heat added (Q_{in}), and the thermal efficiency (η_{Otto}) can be determined through the application of the first law of thermodynamics. Applying the air-standard assumptions of constant specific heats and ideal gas properties, the following relationships are employed.

$$W_{Otto} = m \cdot (u_{34} - u_{12}) \tag{4-1a}$$

$$W_{Otto} = m \cdot (u_3 - u_4) - m \cdot (u_2 - u_1) \tag{4-1b}$$

$$W_{Otto} = m \cdot c_v \cdot (T_3 + T_2 - T_4 - T_1) \quad (4\text{-}1c)$$

$$Q_{in} = m \cdot (u_3 - u_2) \quad (4\text{-}2a)$$

$$Q_{in} = c_v \cdot m \cdot (T_3 - T_2) \quad (4\text{-}2a)$$

$$\eta_{Otto} = \frac{W_{Otto}}{Q_{in}} \quad (4\text{-}3a)$$

$$\eta_{Otto} = \frac{c_v \cdot m \cdot (T_3 + T_2 - T_4 - T_1)}{c_v \cdot m \cdot (T_3 - T_2)} \quad (4\text{-}3b)$$

$$\eta_{Otto} = 1 - \frac{T_1}{T_2} \cdot \left(\frac{(T_4 / T_1 - 1)}{(T_3 / T_2 - 1)} \right) \quad (4\text{-}3c)$$

For the isentropic compression and expansion process, the compression ratio (r) is the ratio of the volume of the working fluid when the piston is at BDC to the volume of the working fluid when the piston is at TDC. Noting from Figure 4-2 that $V_2 = V_3$ and $V_1 = V_4$, the expression for the compression ratio can be expressed as

$$r = \frac{V_1}{V_2} = \frac{V_4}{V_3} \quad (4\text{-}4)$$

For an air-standard analysis, the isentropic relationships for pressure, temperature, and volume are as follows:

$$\frac{p_1}{p_2} = \left(\frac{V_2}{V_1} \right)^k = \frac{1}{r^k} \; and \; \frac{p_3}{p_4} = \left(\frac{V_4}{V_3} \right)^k = r^k \quad (4\text{-}5)$$

$$\frac{T_1}{T_2} = \left(\frac{V_2}{V_1} \right)^{k-1} = \frac{1}{r^{k-1}} \; and \; \frac{T_4}{T_3} = \left(\frac{V_3}{V_4} \right)^{k-1} = \frac{1}{r^{k-1}} \quad (4\text{-}6)$$

where k is the ratio of the specific heats (C_p/C_v). For an air-standard analysis, k is 1.4. Since $T_3/T_2 = T_4/T_1$, the thermal efficiency becomes

$$\eta_{Otto} = 1 - \frac{T_1}{T_2} \tag{4-7}$$

The efficiency can also be expressed in terms of the compression ratio and ratio of specific heats as

$$\eta_{Otto} = 1 - \frac{1}{r^{k-1}} \tag{4-8}$$

For a working fluid with constant specific heats, the thermal efficiency will increase with an increase in the compression ratio. The ideal Otto cycle thermal efficiency is shown as a function of the compression ratio in Figure 4.3. The figure demonstrates that the change in the compression ratio from 1 to 10 has the greatest effect on the thermal efficiency of an Otto engine.

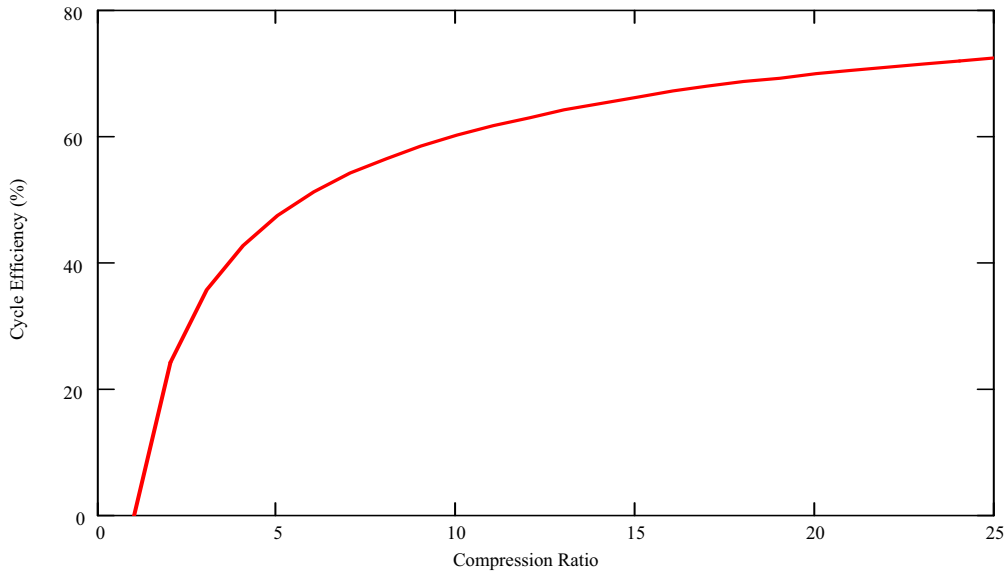

Figure 4.3: Otto Cycle Thermal Efficiency as a Function of Compression Ratio

Example 4-1.

The temperature at the beginning of the compression of an air-standard Otto cycle with a compression ratio of 9 is 550 R, the pressure is 1 atm and the cylinder volume is 0.9 ft^3. The maximum temperature during the cycle is 1600 R. For air, c_v = 0.171 Btu/lb-R and c_p = 0.24 Btu/lb-R. Determine (a) the temperature and pressure at the end state of each cycle, (b) the thermal efficiency, (c) the net work per cycle, (d) the amount of heat rejected per cycle, and (e) the maximum temperature and pressure of the rejected heat.

Solution:

Schematic

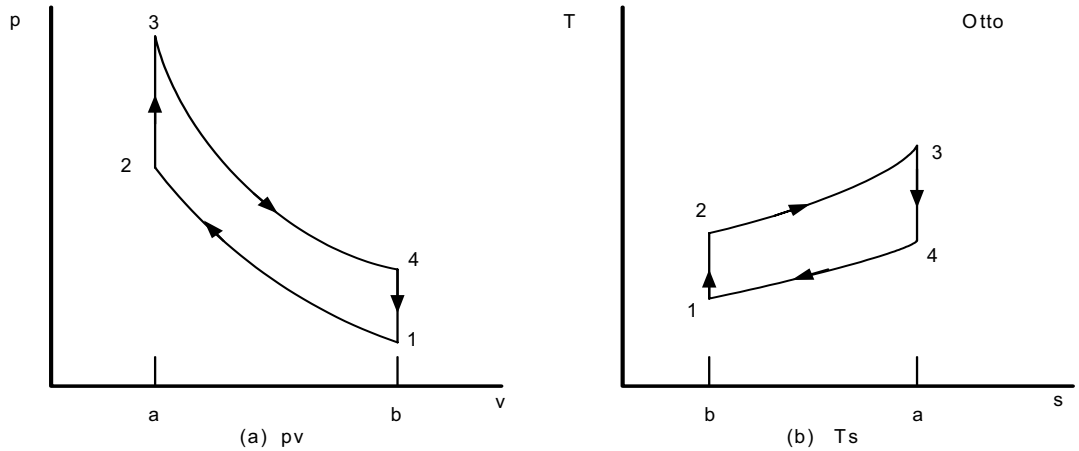

Given Data:

$T_1 := 550R$	Temperature before compression stroke
$T_3 := 1600R$	Maximum temperature
$r := 9$	Compression ratio
$P_1 := 1atm$	Pressure before the compression stroke
$V_1 := 0.02ft^3$	Cylinder volume
$c_v := 0.171\frac{BTU}{lb \cdot R}$	Constant volume specific heat
$c_p := 0.24\frac{BTU}{lb \cdot R}$	Constant pressure specific heat
$R_g := 0.06855\frac{BTU}{lb \cdot R}$	Gas constant of air

Figure 4.4: Example 4-1

Characteristics of the air-standard Otto cycle:
1. The air in the piston cylinder assembly is a closed system.
2. The compression and expansion processes are adiabatic.
3. All processes are internally reversible.
4. The air is modeled as an ideal gas with an air-standard analysis.
5. Kinetic and potential energy effects are negligible.

(a) Determine the temperature, pressure, and specific internal energy (u) at each principal state in the cycle.

Using T_1,

$u_1 := c_v \cdot T_1$ $\quad u_1 = 94.05 \frac{BTU}{lb}$ Internal Energy at State 1

For an isentropic compression (Process 1-2)

$T_2 := T_1 \cdot \left(r^{k-1}\right)$ $\quad T_2 = 1.325 \times 10^3 R$ Temperature at State 2

and

$P_2 := P_1 \cdot r^k$ $\quad P_2 = 21.674 atm$ Pressure at State 2

Using T_2,

$u_2 := c_v \cdot T_2$ $\quad u_2 = 226.494 \frac{BTU}{lb}$ Internal Energy at State 2

Process 2-3 occurs at constant volume. Using the ideal gas equation,

$V_3 = \frac{m \cdot R \cdot T_3}{P_3}$ and $V_2 = \frac{m \cdot R \cdot T_2}{P_2}$ with $V_2 = V_3$ yields

$P_3 := P_2 \cdot \frac{T_3}{T_2}$ $\quad P_3 = 26.182 atm$ Pressure at State 3

Using T_3,

$u_3 := c_v \cdot T_3$ $\quad u_3 = 273.6 \frac{BTU}{lb}$ Internal energy at State 3

For an isentropic compression (Process 3-4)

$T_4 := \frac{T_3}{r^{k-1}}$ $\quad T_4 = 664.39 R$ Temperature at State 4

and

$P_4 := P_3 \cdot \frac{1}{k^k}$ $\quad P_4 = 16.346 atm$ Pressure at State 4

Using T_4,

$u_4 := c_v \cdot T_4$ $\quad u_4 = 113.611 \frac{BTU}{lb}$ Internal energy at State 4

Figure 4.4 (continued)

(b) The thermal efficiency is determined based on the compression ratio.

Equation 4-8 gives the thermal efficiency of the air-standard Otto cycle as

$\eta_{Otto} := 1 - \frac{1}{r^{k-1}}$ $\eta_{Otto} = 58.476\%$ Thermal efficiency

(c) The net work produced per cycle can be calculated with the internal energy known at each point in the cycle.

The mass (m) is calculated using the ideal gas law.

$m_1 := \frac{P_1 \cdot V_1}{(R_g) \cdot T_1}$ $m_1 = 1.443 \times 10^{-3}\,lb$

Equation 4-1b expresses the net work per cycle as

$W_{Otto} := m_1 \cdot [(u_3 - u_4) - (u_2 - u_1)]$ $W_{Otto} = 0.04BTU$ Net work per cycle

(d) The heat rejected per cycle is

$Q_{rej} := m_1 \cdot (u_4 - u_1)$ $Q_{rej} = 0.028BTU$ Reject heat per cycle

(e) The pressure and temperature of the rejected heat is at the maximum at the beginning of the heat rejected process.

$P_4 = 16.346atm$ Maximum pressure of Q_{rej}

$T_4 = 664.39R$ Maximum temperature of Q_{rej}

Figure 4.4 (continued)

Compression-ignition reciprocating engines operate on the basis of the Diesel cycle. An illustration of a combustion-ignition cylinder is shown in Figure 4.5. The ideal, air-standard Diesel cycle is similar to the model of the ideal, air-standard Otto cycle.

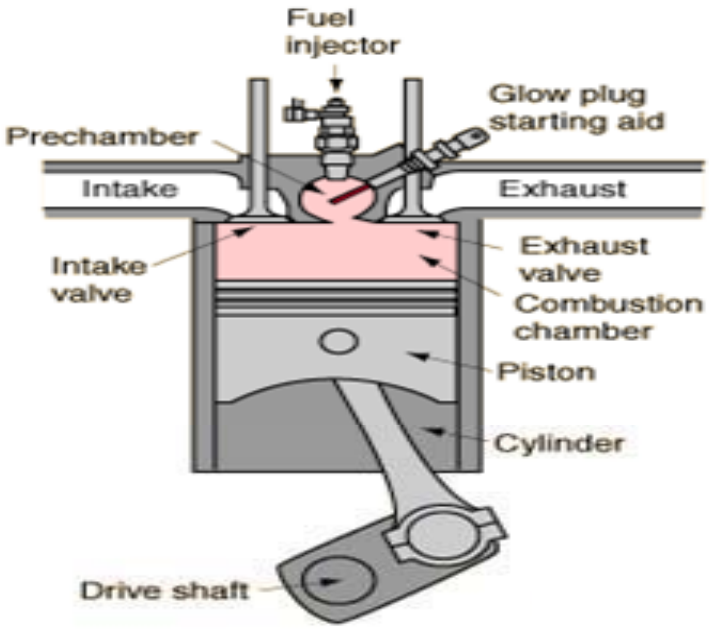

Figure 4.5: Compression-ignition Engine.
(hyperphysics.phy-astr.gsu.edu/hbase/thermo/diesel.html)

The air-standard Diesel cycle is a cycle in which the heat addition occurs during the constant pressure process that begins with the piston at top dead center. The pressure-specific volume (pv) and temperature-entropy (Ts) diagrams for the air-standard Diesel cycle are shown in Figure 4.6. The cycle consists of four internally reversible processes in series. Process 1 – 2 is an isentropic compression, the same as the Otto cycle. In Process 2 – 3, heat is transferred to the working fluid at constant pressure, and Process 2 – 3 also makes up the first part of the power stroke. The remainder of the power stroke is completed through an isentropic expansion in Process 3 – 4. In Process 4 – 1, heat is rejected from the air while the piston is at bottom dead center.

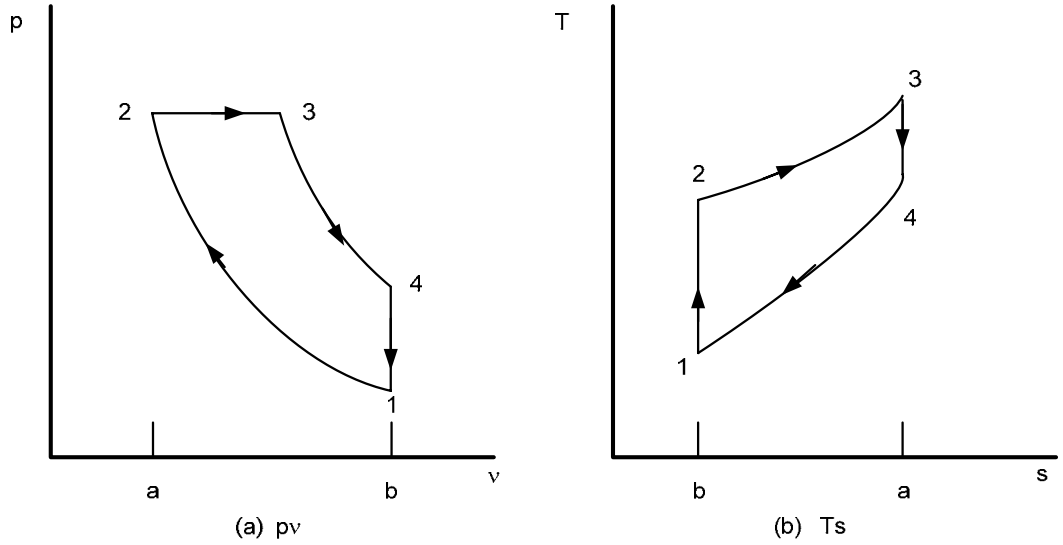

Figure 4.6: Pressure-Specific Volume and Temperature-Entropy Diagrams for the Air-Standard Diesel Cycle.

While the spark-ignition engine compresses a fuel/air mixture, the compression-ignition engine requires the working fluid to be compressed to a high temperature and pressure before fuel is added. The addition of the fuel to the high temperature, high pressure working fluid initiates combustion.

Application of the first law to the ideal Diesel cycle yields the expressions for the net work accomplished by the cycle, (W_{Diesel}), the heat added (Q_{in}), and the heat rejected (Q_{out}), and the thermal efficiency (η_{Diesel}).

$$Q_{in} = m \cdot (h_3 - h_2) \qquad (4\text{-}8a)$$

$$Q_{in} = m \cdot c_p \cdot (T_3 - T_2) \qquad (4\text{-}8b)$$

$$Q_{out} = m \cdot (u_4 - u_1) \qquad (4\text{-}9a)$$

$$Q_{out} = m \cdot c_p \cdot (T_4 - T_1) \qquad (4\text{-}9b)$$

$$W_{Diesel} = Q_{in} - Q_{out} \quad \text{(4-10a)}$$

$$W_{Diesel} = m \cdot c_p \cdot (T_3 - T_2) - c_p \cdot (T_4 - T_1) \quad \text{(4-10b)}$$

$$\eta_{Diesel} = \frac{W_{Diesel}}{Q_{in}} \quad \text{(4-11)}$$

Both a compression ratio (r) and a cutoff ratio (r_c) are defined for the Diesel cycle. The cutoff ratio is the ratio of the volume when the fuel flow is cut off to the volume when the fuel flow is started.

$$r = \frac{V_1}{V_2}$$

$$r_c = \frac{V_3}{V_2}$$

The compression ratio for the Diesel cycle is based only on the isentropic compression and not the isentropic expansion. The air-standard thermal efficiency of the Diesel cycle is

$$\eta_{Diesel} = 1 - \frac{1}{r^{k-1}}\left[\frac{r_c^k - 1}{k(r_c - 1)}\right] \quad \text{(4-12)}$$

The thermal efficiency of the Diesel cycle differs from the thermal efficiency of the Otto cycle by the bracketed term in the equation (4.12). Diesel engines must always have a cutoff ratio greater than unity ($r_c > 1$). Otto engines typically have higher thermal efficiencies than Diesel engines at the same compression ratio. Still, better overall thermal efficiencies are achieved by Diesel engines because they can operate at higher compression ratios than Otto engines. Diesel engines can achieve compression ratios as high as 25:1 and

exhibit higher thermal efficiencies than Otto cycles, which are limited to compression ratios of 12:1. A comparison of the thermal efficiencies of the Otto and Diesel cycles is presented in Figure 4.7.

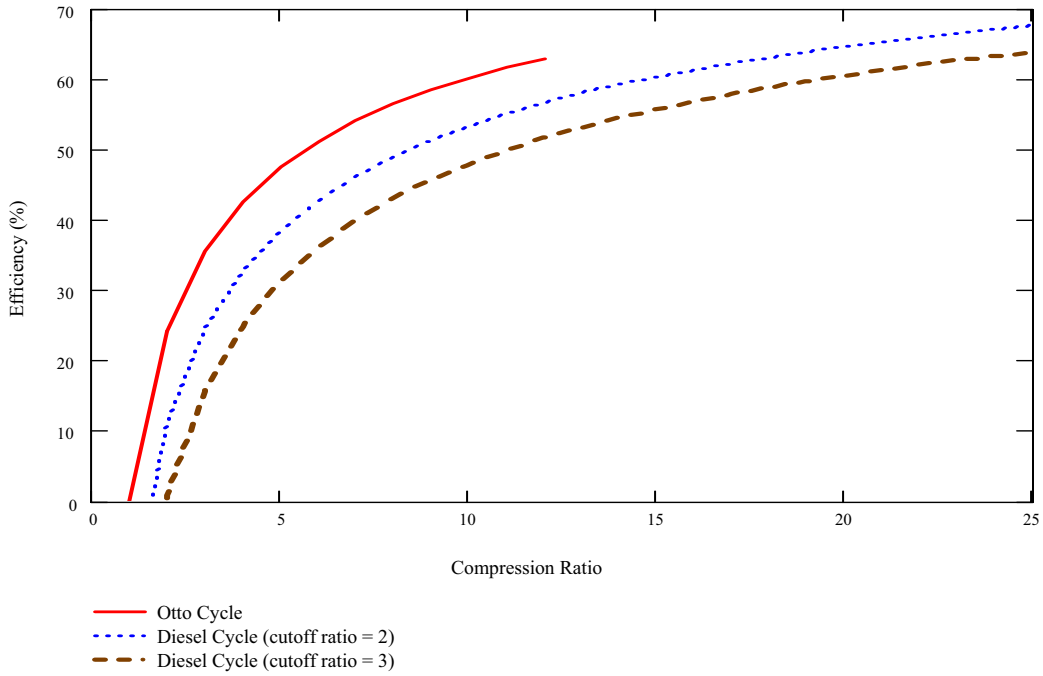

Figure 4.7: Otto and Diesel Cycle Thermal Efficiencies as Functions of Compression Ratio

Application

Reciprocating engine generator sets are the most common and most technically mature of all DER technologies. Reciprocating engines are available from small sizes (0.5 kW) to large generators (7 MW). Reciprocating engines use commonly available fuels such as gasoline, natural gas, and diesel fuel. Reciprocating engines can be used for a variety of applications due to their small size, low unit costs, and useful thermal output. Applications for reciprocating engines in power generation include continuous or prime-power generation, peak

shaving, back-up power, premium power, remote power, standby power, and mechanical drive use. An overview of reciprocating engine characteristics is presented in Table 4.1.

Table 4.1: Overview of Reciprocating Engine Technology (http://www.energy.ca.gov/distgen/)

Reciprocating Engines Overview	
Commercially Available	Yes
Size Range	0.5 kW – 7 MW
Fuels	Natural gas, diesel, landfill gas, digester gas
Efficiency	25 – 45%
Environmental	Emission controls required for NOx and CO
Other Features	Cogeneration (some models)
Commercial Status	Products are widely available

Reciprocating engines are an ideal candidate for applications in which there is a substantial need for hot water or low pressure steam. The thermal output can be used in an absorption chiller to provide cooling. Comparatively low installation costs, suitability for intermittent operation, and high temperature exhaust make combustion engines an attractive option for m-CHP. Internal combustion engines utilize proven technologies with a well established infrastructure for mass production and marketing. The development of combustion engines has also formed a maintenance infrastructure with certified technicians and relatively inexpensive and available parts are available. Due to the long history and widespread application, internal combustion engines are a more developed technology than most prime movers considered for m-CHP.

Heat Recovery

Traditional large-scale electric power generation is typically about 30% efficient, while combined cycle plants are typically 48% efficient. In either case, the reject heat is lost to the atmosphere with the exhaust gases. In an internal combustion engine, heat is released from the engine through coolant, surface radiation, and exhaust. Engine-driven m-CHP systems recover heat from the jacket water, engine oil, and engine exhaust. Low pressure steam or hot water can be produced from the recovered heat, and can be used for space heating, domestic hot water, and absorption cooling.

Heat from the engine jacket coolant is capable of producing 200 F (93 C)hot water and accounts for approximately 30 % of the energy input from the fuel. Engines operating at high pressure or equipped with ebullient cooling systems can operate at jacket temperatures of up to 265 F (129 C). Engine exhaust heat can account for 10 – 30 % of the fuel input energy and exhaust temperatures of 850 F –1200 F (455 C – 649 C) are typical. Because exhaust gas temperatures must be kept above condensation thresholds, only a portion of the exhaust heat can be recovered. Heat recovery units are typically designed for a 300 F – 350 F exhaust outlet temperature to avoid corrosive effects of condensation in the exhaust piping. Low-pressure steam (~15 psig) and 230 F (110 C) hot water are typically generated using exhaust heat from the engine. The combined heat recovery of the coolant and exhaust in conjunction with the work produced by combustion can utilize approximately 70 – 80% of the fuel energy.

Cost

Reciprocating internal combustion (IC) engines are the traditional technology for emergency power all over the world. They have the lowest first costs among DER technologies. The capital cost of a basic gas-fueled generator set (genset) package ranges from $300-$900/kW, depending on size, fuel type, and engine type. Generally speaking, the overall engine cost increases as power output increases. The total installed cost can be 50-100% more than the engine itself. Additional costs include balance of plant (BOP) equipment, installation fees, engineering fees, and other owner costs. Installed costs of m-CHP projects using IC engines typically range between $800/kW - $1500/kW.

The maintenance costs over the life of IC engines can be significant. The core of the engine maintenance is in the periodic replacement of engine oil, coolant, and spark plugs (if spark ignition). Routine inspections and/or adjustments are also necessary. Maintenance costs of gas and diesel IC engines range between $0.007-$0.015/kWh and $0.005-$0.010/kWh respectively. (http://www.energy.ca.gov/distgen/equipment/.html)

Advantages and Disadvantages

Reciprocating engines are generally less expensive than competing technologies. They also have start-up times as low as ten seconds, compared to other technologies that may take several hours to reach steady-state operation. Through years of technology advancements, reciprocating engines have climbed

in efficiency from under 20% to over 30%. Today's most advanced natural gas-fueled IC engines have electrical efficiencies (based on lower heating value, LHV) close to 45% and are among the most efficient of the commercially available prime mover technology. Lower heating values neglect the energy in the water vapor formed by the combustion of hydrogen in the fuel. This water vapor typically represents about 10% of the energy content. Therefore the lower heating values for natural gas are typically 900 - 950 Btu per cubic foot.

Advantages of reciprocating engines include:

- Available in a wide range of sizes to match the electrical demand.
- Fast start-up and adjustable power output “on the fly.”
- Minimal auxiliary power requirements, generally only batteries are required.
- Demonstrated availability in excess of 95%.
- In load following applications, high part-load efficiency of IC engines maintains economical operation.
- Relatively long life and reliable service with proper maintenance.
- Very fuel flexible.
- Natural gas can be supplied at low pressure.

Disadvantages of IC engines are:

- Noisy operation.
- Require maintenance at frequent intervals.
- Relatively high emissions to the atmosphere.

Exercises

For air-standard analysis c_v = 0.171 Btu/lb-R and c_p = 0.24 Btu/lb-R.

1. A piston-cylinder arrangement has a cylinder diameter (bore) of 60 mm and performs a 100 mm stroke. If the clearance volume, the volume above top-dead-center, is 75 cm^3, what is the compression ratio?

2. A four-cylinder, four-stroke IC engine has a bore of 3.0 in. and a stroke of 2.7 in. The clearance volume is 14 % of the cylinder volume when the piston is at bottom dead center. What are (a) the compression ratio, (b) the cylinder displacement (volume displaced by cylinder), and (c) the engine displacement?

3. An air-standard analysis is to be performed on a spark-ignited IC engine with a compression ratio of 9.0. At the start of compression, the pressure and temperature are 100 kPa and 300 K, respectively. The heat addition per unit mass of air is 600 kJ/kg. Determine (a) the net work, (b) the thermal efficiency, (c) the heat rejected during the cycle, and (d) the maximum temperature and pressure of the rejected heat.

4. An Otto cycle operates on an air-standard basis. The properties of the air prior To compression are p_1 = 1 bar, T_1 = 310 K, and V_1 = 100 cm^3. The compression ratio of the cycle is 8 and the maximum temperature is 900 K. Determine (a) the heat addition in kJ, (b) the net work in kJ, (c) the thermal efficiency, and (d) the availability transfer from the air accompanying the heat rejection process, in kJ, for T_0 = 310 K, p_0 = 1 bar.

5. Consider a four-stroke, spark-ignited engine with four cylinders. Each cylinder undergoes a process like the cycle in Problem 2. If the engine operates at 1500 rpm, determine the net power output in kW.

6. Prior to the compression stroke in an Otto cycle, the pressure and temperature are 14.7 psi and 540 R, respectively. The compression ratio is 6, and the heat addition per unit mass of air is 250 Btu/lb. Find (a) the maximum temperature of heat rejection, in R, (b) the maximum pressure of heat rejection, in psi, and (c) the thermal efficiency if the cycle is modeled on a cold-air standard basis with specific heats evaluated at 540 R.

7. A four-stroke two-cylinder Otto engine has a bore of 2.5 in, a stroke of 3.5 in, and a compression ratio of 7.2:1. The intake air is at 14.7 psi and 40 F with compression and expansion processes that are reversible and adiabatic. If 300 Btu/lbm air is added and the engine speed is 300 rpm, determine (a) the

net work per cycle, (b) the work per minute, and (c) the rate of heat rejection in Btu/hr.

8. A four-cylinder, four-stroke IC engine has a bore of 1.7 in. and a stroke of 3.1 inches. The clearance volume is 16 % of the cylinder volume when the piston is at bottomdead center and the crankshaft rotates at 1100 rpm. The processes in the cylinders are modeled as a cold air-standard Otto cycle with a pressure of 14.7 psi and a temperature of 80 F at the beginning of compression. The maximum temperature in the cycle is 1800 R. Based on this model, calculate (a) the net work per cycle, (b) the power developed by the engine, (c) the amount of heat rejected, (d) the maximum temperature and pressure of heat rejection, and (e) the thermal efficiency of the cycle.

9. A diesel cycle is modeled on a cold air-standard basis with specific heats calculated at 300 K. At the beginning of compression, the pressure and temperature are 112 kPa and 273 K, respectively. After heat addition, the pressure is 1.2 MPa and the temperature is 1200 K. Determine (a) the compression ratio, (b) the cutoff ratio, (c) the heat rejected by the cycle, and (d) the thermal efficiency of the cycle.

10. An air standard diesel cycle has a compression ratio of 16 and a cutoff ratio of 2. Before compression, p_1 = 14.7 psi, V_1 = 0.4 ft^3, and T_1 = 320 R. Calculate (a) the heat added, (b) the heat rejected, (c) the thermal efficiency, (d) the maximum temperature and pressure of the rejected heat, and (e) the availability transfer from the air accompanying the heat rejection process for $T_0 = T_1$ and $p_0 = p_1$.

11. The maximum temperature of a cold air-standard diesel cycle is 1200 K. The pressure and temperature before compression are 84 kPa and 290 K, respectively. With an air mass of 6 grams and compression ratios of 14, 19, and 21, calculate (a) the net work of the cycle, (b) the heat rejected during the cycle, and (b) the thermal efficiency of the cycle.

Manufacturers

- Generac Power Systems, Inc. headquartered in Waukesha, Wisconsin manufactures a complete line of residential/light commercial standby generators that can be installed during new construction or retrofitted into existing homes and businesses. These systems range from 7 to 40 kilowatts of output, in both air- and liquid-cooled models. All models are factory-built for natural gas operation and can be reconfigured for liquid propane (LP gas) operation. The 15-kW liquid cooled Generac model MMC 4G15 Engine is pictured in Figure 4.8.

Figure 4.8: Generac Model MMC 4G15 15-kW Reciprocating Engine Generator (http://www.generac.com)

- Caterpillar headquartered in Peoria, Illinois, manufactures diesel generator sets from 7 to 16,200 kW, and gas-powered generator sets, from 9 to 6,000 kW. Figure 4.9 shows a model D13-2, 12-kW diesel engine generator set from Caterpillar.

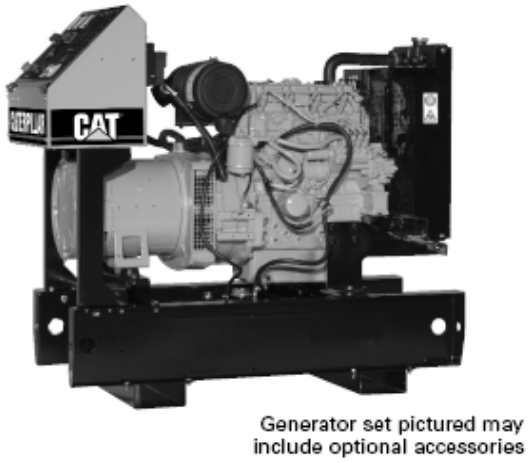

Figure 4.9: Model D13-2, 12-kW Diesel Engine Generator Set from Caterpillar (http://www.cat.com)

- Cummins, based in Columbus, Indiana, is a manufacturer of engines and power generators for many applications. Cummins products operate on a wide variety of fuels and have power outputs of 2 kW to 2 MW. Figure 4.10 pictures a Cummins model GNAA 60 Hz 6-kW spark-ignited generator set that can run off either natural gas or propane. Cummins also offers models that use gasoline and diesel as fuels.

Figure 4.10: Cummins Model GNAA 60 Hz 6-kW Spark-ignited Generator Set (http://www.cumminspower.com)

- Deutz Corporation, North American headquarters located in Norcross, Georgia, is an international supplier of reciprocating gas- and diesel-fueled engine/generator systems. Deutz offers generator sets ranging from 4 kW to 2 MW. The 4-19 kW Model 1008F water cooled diesel engine generator set is pictured in Figure 4.11.

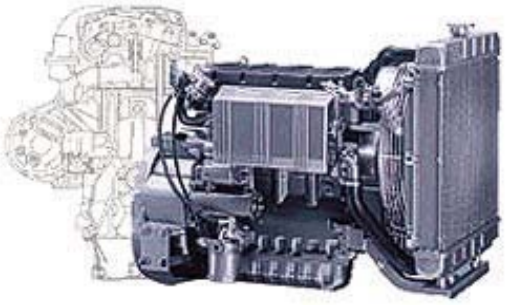

- Figure 4.11: Deutz Model 1008F Diesel Engine Generator Set (http://deutzusa.coml)

- Kohler, based in Kohler, Wisconsin, manufactures 6 kW to 20 kW engines and 8.5 kW to 2 MW on-site power generators. The model 6ROY, 6-kW diesel engine generator set is pictured in Figure 4.12.

Figure 4.12: Kohler Model 6ROY, 6-kW Diesel Engine Generator Set (www.kohler.com)

Microturbines

Technology Overview

Microturbines are small gas turbines used to generate electricity. Microturbines were derived from turbocharger technologies found in large trucks or the turbines in aircraft auxiliary power units (APUs). Most microturbines are single-stage, radial flow devices with rotating speeds of 90,000 to 120,000 rpm. Many microturbines occupy a space no larger than a telephone booth and have power outputs in the range of 25 – 300 kW. While the “micro” regime of CHP was earlier defined as less than fifteen kilowatts (<15 kW), microturbines are included here as they could possibly have commercial applications in small complexes. Most manufacturers use a single shaft design where the compressor, turbine, and a permanent magnet generator are mounted on the same shaft which is supported by lubrication-free air bearings. The microturbines can be fueled by natural gas, diesel, gasoline, or alcohol.

The operation of a microturbine is similar to that of an industrial turbine except that most microturbine designs incorporate a recuperator to recover part of the exhaust heat for preheating the combustion air. The schematic shown in Figure 4-13 shows the major components and operation of a microturbine.

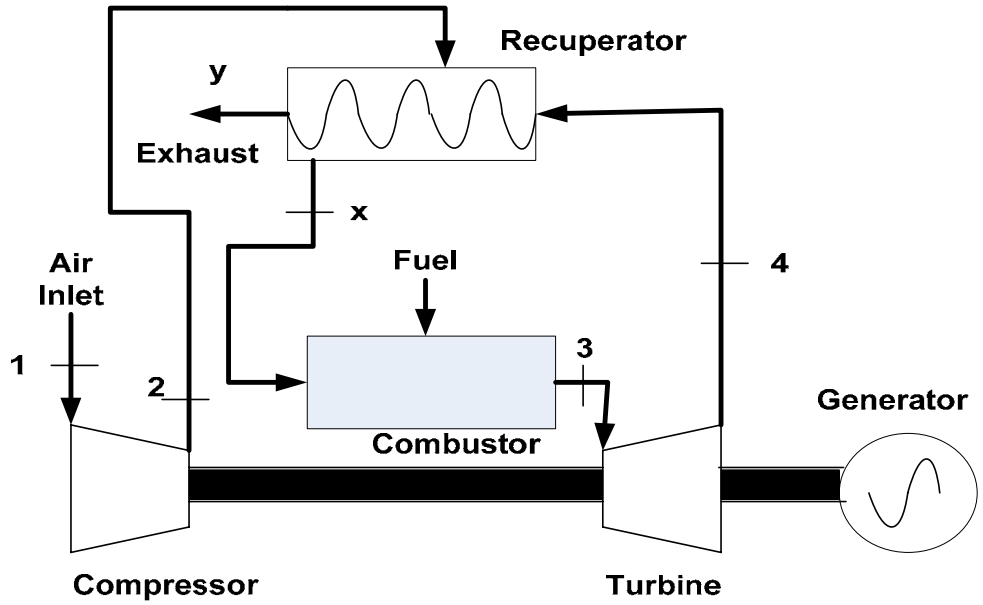

Figure 4.13: Microturbine Components and Operation

As can be seen in Figure 4.13, air enters the compressor and is pre-heated for combustion in the recuperator. The air mixes with the fuel in the combustor, and the combusted air/fuel mixture expands through the turbine. The rotation of the turbine drives the shaft which powers both the compressor and generator. The exhaust from the turbine is fed back through the recuperator to preheat the combustion air.

Unrecuperated microturbines produce electricity from natural gas at efficiencies around 15%. Microturbines equipped with recuperators obtain electrical efficiencies in the range of 20% - 30%. The difference in electrical efficiency is that the preheated combustion resulting from the recuperator reduces the amount of fuel required. Overall system efficiencies of 85% can be reached when microturbines are coupled with thermally-activated components for

heat recovery. As compared to industrial turbines, microturbines have very low emissions. Table 4.2 lists an overview of microturbine technology.

Table 4.2: Overview of Microturbine Technology (http://www.energy.ca.gov/distgen)

Microturbine Overview	
Commercially Available	Yes (Limited)
Size Range	25 – 500 kW
Fuel	Natural gas, hydrogen, propane, diesel
Efficiency	20 – 30% (Recuperated)
Environmental	Low (< 9 – 50 ppm) NOx
Other Features	Cogen (50 – 80°C water)
Commercial Status	Small volume production, commercial prototypes now.

The simplest model for gas turbines is the air-standard Brayton cycle. The air-standard model is comprised of isentropic compression and expansion processes and reversible, constant-pressure heat addition and rejection. Air is the working fluid and is modeled as an ideal gas with constant specific heat throughout the cycle. The pressure-specific volume (pv) and temperature-entropy (Ts) diagrams for the air-standard ideal Brayton cycle are shown in Figure 4.14.

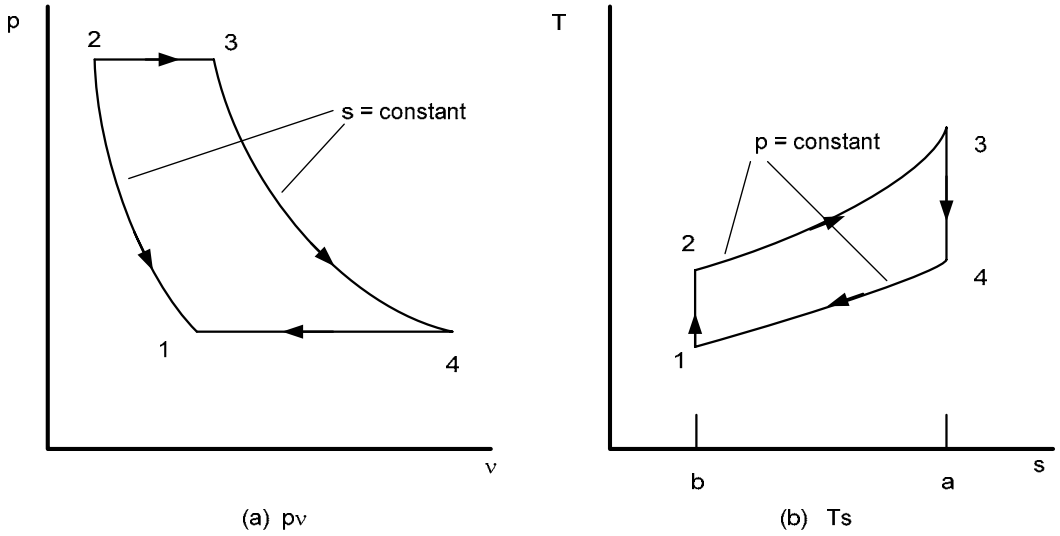

Figure 4.14: Pressure-Specific Volume and Temperature-Entropy Diagrams for the Ideal Brayton Cycle

On the T-s diagram, area 2-3-a-b-2 represents the heat added per unit of mass flowing and area 1-4-a-b-1 represents the heat rejected per unit mass flowing. On the p-v diagram, area 1-2-a-b-1 represents the compressor work input per unit mass flowing and area 3-4-b-a-3 represents the turbine work output per unit mass flowing. The enclosed area on each diagram of Figure 4-14 can be viewed as the net work output (pv) and net heat added (Ts).

Application of the first law of thermodynamics to the model determines the expression for turbine work (W_T), compressor work (W_C) net work (W_{net}), heat added (Q_{in}), and cycle efficiency (η).

$$W_C = \dot{m} \cdot \left(h_1 - h_2 \right) \tag{4-13a}$$

$$W_C = \dot{m} \cdot c_p \cdot (T_1 - T_2) \tag{4-13b}$$

$$W_T = \dot{m} \cdot \left(h_3 - h_4 \right) \tag{4-14a}$$

$$W_T = \dot{m} \cdot c_p \cdot (T_3 - T_4) \quad \text{(4-14b)}$$

$$Q_{in} = \dot{m} \cdot \left(h_3 - h_2\right) \quad \text{(4-15a)}$$

$$Q_{in} = \dot{m} \cdot c_p \cdot (T_3 - T_2) \quad \text{(4-15b)}$$

$$W_{net} = W_T + W_C \quad \text{(4-16a)}$$

$$W_{net} = \dot{m} \cdot c_p \cdot (T_3 - T_4) + c_p \cdot (T_1 - T_2) \quad \text{(4-16b)}$$

$$W_{net} = \dot{m} \cdot c_p \cdot (T_3 + T_1 - T_2 - T_4) \quad \text{(4-16c)}$$

$$\eta = \frac{W_{net}}{Q_{in}} \quad \text{(4-17a)}$$

$$\eta = \frac{T_3 + T_1 - T_2 - T_4}{T_3 - T_2} \quad \text{(4-17b)}$$

$$\eta = 1 - \frac{T_1 - T_4}{T_3 - T_2} \quad \text{(4-17c)}$$

Since the specific heats are constant, then

$$\frac{T_4}{T_1} = \frac{T_3}{T_2} \quad \text{(4-18)}$$

For an isentropic process,

$$\frac{T_2}{T_1} = \left(\frac{p_2}{p_1}\right)^{\frac{k-1}{k}} \quad \text{(4-19)}$$

where k is the ratio of specific heats (C_p/C_v). A similar relationship can be written for T_3 and T_4 with P_3 and P_4. The cycle efficiency becomes

$$\eta = 1 - \frac{1}{\left(\frac{p_2}{p_1}\right)^{\frac{k-1}{k}}} \qquad (4\text{-}20)$$

The thermal efficiency of the air-standard Brayton cycle is as function of the pressure ratio (P_2/P_1). The Brayton cycle is primarily described by the pressure ratio, the turbine inlet temperature, the compressor inlet temperature, the isentropic turbine efficiency, and the isentropic compressor efficiency. The effect of pressure ratio on the efficiency is shown in Figure 4.15.

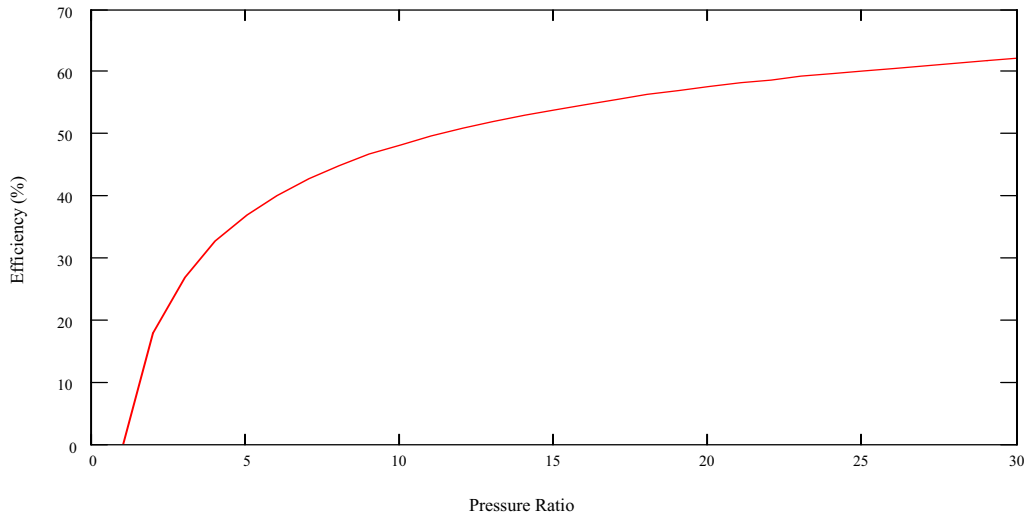

Figure 4.15: Air-standard Brayton Cycle Efficiency as a Function of Pressure Ratio

The air-standard Brayton cycle includes the assumptions that the compressor and turbine operate isentropically and that there is no pressure drop during heat addition and rejection. These assumptions are not realistic in a microturbine cycle. In a real gas turbine cycle, irreversibilities in all processes

cause the working fluid specific entropy to increase. However, the irreversibilities in the heat exchanger process are less significant than those in the compression and expansion processes and are often ignored. The Ts diagram in Figure 4.16 illustrates the effects of irreversibilities in a microturbine cycle.

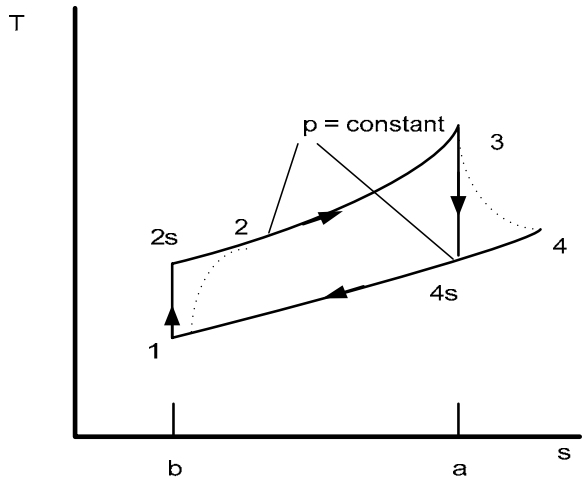

Figure 4.16: Temperature-Entropy Diagram of a Real Microturbine Cycle

The isentropic compressor efficiency is defined as the ratio of the isentropic compressor work to the actual compressor work, when both are compressed through the same pressure ratio. The isentropic turbine efficiency is defined as the ratio of actual work of expansion to the isentropic work of expansion, when both expand from the same initial state to the same final pressure. The expressions for the isentropic compressor efficiency and the isentropic turbine efficiency are

$$\eta_C = \frac{h_{2s} - h_1}{h_2 - h_1} \tag{4-21}$$

$$\eta_T = \frac{h_3 - h_4}{h_3 - h_{4s}} \tag{4-22}$$

For constant specific heats, the isentropic compressor and expansion efficiencies become

$$\eta_C = \frac{\left(\frac{P_2}{P_1}\right)^{\frac{k-1}{k}}}{\frac{T_2}{T_1} - 1} \tag{4-23}$$

$$\eta_T = \frac{1 - \frac{T_4}{T_3}}{1 - \left(\frac{P_4}{P_3}\right)^{\frac{k-1}{k}}} \tag{4-24}$$

The compressor work (W_{Comp}) and the turbine work (W_{Turb}) for a gas turbine cycle become

$$W_{Comp} = \dot{m} \cdot \frac{Cp}{\eta_C} \cdot T_1 \cdot \left[1 - \left(\frac{P_2}{P_1}\right)^{\frac{k-1}{k}}\right] \tag{4-25}$$

$$W_T = \dot{m} \cdot \eta_T \cdot Cp \cdot T_3 \cdot \left[1 - \left(\frac{P_4}{P_3}\right)^{\frac{k-1}{k}}\right] \tag{4-26}$$

where the constant pressure specific heat is that of air (1.004 kJ/kg-K) for the compressor and that of the combustion products (1.148 kJ/kg-K) for the turbine. The ratio of specific heats, k, is 1.4 for the compressor and for the combustion products in the turbine is 1.333. The constant pressure specific heat for the combustion products is generally taken as the average of the compressor and

turbine C_p values, and the constant pressure specific heat in the heat rejection process is generally assumed to be that of air.

As mentioned earlier, most microturbine designs incorporate a recuperator, as shown in Figure 4.13, to preheat the air exiting the compressor before the entering the combustor. The effect of the recuperator is to heat the air from state 2 to state x as indicated in Figure 4.17. Hence, energy from a fuel source is required only to increase the air temperature from state x to state 3, rather than from state 2 to state 3.

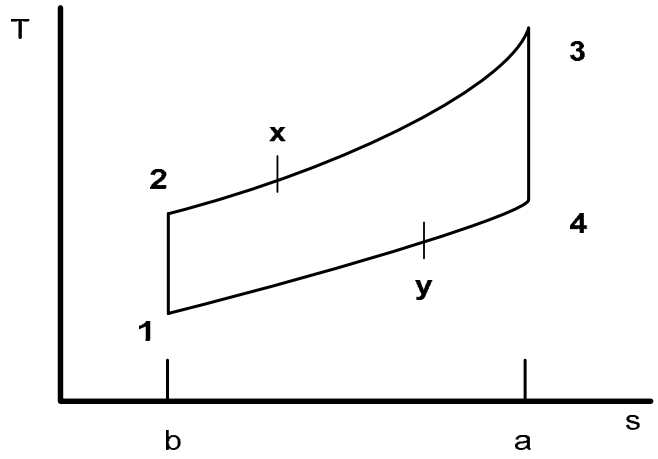

Figure 4.17: Temperature-Specific Entropy Diagram including Recuperator Effects

The heat added by the fuel per unit of mass flowing is then given by

$$Q_{in} = h_3 - h_x \tag{4-27}$$

The effectiveness of a recuperator depends upon its construction, but typical recuperator effectiveness values for microturbines range between 65% and 80%. The effectiveness of the recuperator (ξ_{rec}) is defined as the ratio of the actual

enthalpy increase of the air flowing through the compressor side of the recuperator to the maximum theoretical enthalpy increase.

$$\xi_{rec} = \frac{h_x - h_2}{h_4 - h_2} \tag{4-28}$$

For a microturbine with prescribed pressure ratios, the work required of the compressor is a function of the inlet temperature (T_1). As T_1 decreases, the work required of the compressor decreases and the net work accomplished by the power plant is enhanced. However, a decrease in T_1 will result in a lower inlet temperature to the combustor (T_2); hence, the fuel/air ratio in the combustor will have to increase to meet the prescribed turbine inlet temperature (T_3). An increase in T_3 will enhance both the turbine work and the net work. The turbine inlet temperature is limited by the thermal-mechanical properties of the materials used in construction of the turbine.

Example 4-2

A microturbine has a inlet temperature of 1500 F, a compression ratio of 14, and compressor and turbine efficiencies of 82% and 89%, respectively. The ambient conditions are 90 F and 1 atm. Sketch (a) the T-s diagram for this engine and determine (b) the net work for the cycle, (c) the engine thermal efficiency, and (d) the available waste heat rejected to the ambient air.

Solution:
Given Information:

$T_1 := (459.67 + 90)\text{R}$	Compressor inlet temperature
$T_3 := (459.67 + 1500)\text{R}$	Turbine inlet temperature
$\eta_c := 0.83$	Compressor efficiency
$\eta_t := 0.89$	Turbine efficiency
$PR := 14$	Pressure Ratio

Figure 4.18: Example 4-2

The following property values are used for the working fluid:

$c_{pc} := 1.004\frac{kJ}{kg\cdot K}$ Specific heat of air

$c_{pt} := 1.148\frac{kJ}{kg\cdot K}$ Specific heat of combustion products

$c_{pAve} := \frac{c_{pc} + c_{pt}}{2}$ Average specific heat

$k_c := 1.4$ c_p/c_v for air

$k_t := 1.333$ c_p/c_v of combustion products

(a) Sketch the T-s diagram for this engine.

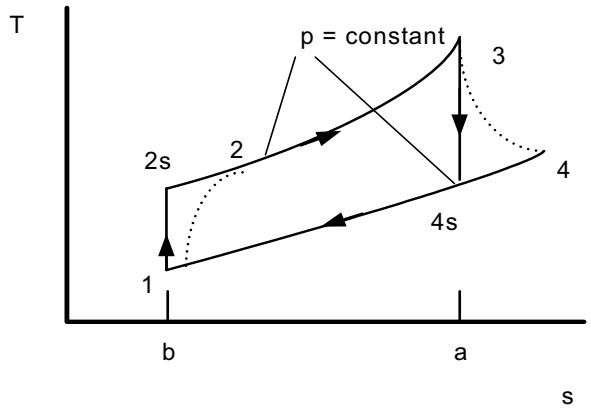

(b) Determine the net work of the engine.

The compressor and turbine exit temperatures:

$$T_2 := T_1\cdot\left[1 + \eta_c^{-1}\cdot\left(PR^{\frac{k_c-1}{k_c}} - 1\right)\right] \qquad T_2 = 1.295\times 10^3\,R$$

$$T_4 := T_3\cdot\left[1 - \eta_t\cdot\left[1 - \left(\frac{1}{PR}\right)^{\frac{k_t-1}{k_t}}\right]\right] \qquad T_4 = 1.118\times 10^3\,R$$

Compressor work and turbine work

$W_c := c_{pc}\cdot(T_1 - T_2)$ $W_c = -178.743\frac{BTU}{lb}$

$W_t := c_{pt}\cdot(T_3 - T_4)$ $W_t = 230.873\frac{BTU}{lb}$

Figure 4.18 (continued)

The net work of the turbine can be found as

$W_{net} := W_c + W_t$ $\quad W_{net} = 52.13 \frac{BTU}{lb}$ Net work

(c) Determine the thermal efficiency of the turbine.

$Q_s := c_{pAve} \cdot (T_3 - T_2)$ $\quad Q_s = 170.806 \frac{BTU}{lb}$

$\eta := \frac{W_{net}}{Q_s}$ $\quad \eta = 30.52\%$ Thermal efficiency

(d) What is the amount of waste heat available from the cycle?

$Q_{waste} := c_{pt} \cdot (T_1 - T_4)$ $\quad Q_{waste} = -155.742 \frac{BTU}{lb}$ Available waste heat

The negative sign on the waste heat results from the sign convention used applying the first law of thermodynamics. Heat added to the system is positive and heat rejected from the system is negative.

Figure 4.18 (continued)

Application

Markets for microturbines include commercial and light industrial facilities. Microturbines can be used for stand-by power, power quality and reliability, peak shaving, and cogeneration applications. In addition, because microturbines are being developed to utilize a variety of fuels, microturbines are used for resource recovery and landfill gas applications. Microturbines produce between 25 and 500 kW of power and are well-suited for small commercial establishments such as restaurants, hotels, motels, small offices, retail stores.

The development of the microturbine technology for transportation applications is also in progress. Automotive companies are interested in microturbines to provide a lightweight and efficient fossil-fuel-based energy source for hybrid electric vehicles, especially buses. Microturbines are also

being developed to utilize a variety of fuels and are being used for resource recovery and landfill gas applications.

Heat Recovery

The waste heat from a microturbine is primarily in the form of hot exhaust gases. This heat is suitable for powering a steam generator, heating of a building, allocation to thermal storage devices, or use in absorption cooling system. However, most designs incorporate a recuperator that limits the amount of heat available for m-CHP applications.

The manner in which the waste heat can be used depends upon the configuration of the turbine system. In a non-recuperated turbine, the exhaust gas typically exits at a temperature between 1000 – 1100 F (538 – 594 C). A recuperated turbine can provide waste heat for heating and operating an absorption cooling system at exhaust temperatures around 520 F (271 C). The recovered heat can also be used to drive a desiccant dehumidification device. The use of the recovered heat influences the selection of the microturbine with or without a recuperator.

Cost

The capital costs of microturbines range from $700 - $1,100/kW when mass produced. These costs include all hardware, associated manuals, software, and initial training. Adding heat recovery components increases the

cost by $75- $350/kW. Installation and site preparation can increase the capital costs by 30-50%. Manufacturers are striving for future capital costs of microturbines to be below $650/kW. This goal appears feasible if the market expands and sales volumes increase.

With fewer moving parts, vendors hope their microturbines can provide higher reliability and require less maintenance than conventional reciprocating engine generators. The single-shaft design with air bearings will not require lubricating oil or water. Microturbines that use lubricating oil should not require frequent oil changes as the oil is isolated from the combustion products.

Manufacturers expect microturbines to require maintenance once-a-year when the technology matures and are targeting maintenance intervals of 5,000 – 8,000 hours. Actual maintenance costs and intervals for mature microturbines are less well known since there is a limited base of empirical data from which to draw conclusions. Forecasted maintenance costs for microturbines range from $0.005 – $0.016 per kWh, slightly lower than the costs for small reciprocating engine systems.

Advantages and Disadvantages

The operation of a microturbine offers several advantages. Microturbines have fewer moving parts than IC engines. The limited number of moving parts and the low lubrication requirements allow microturbines long maintenance intervals. Accordingly, microturbines have lower operating costs in terms of cost

per kilowatt of power produced. Another advantage of microturbines is their relatively small size for the amount of power that is produced. Microturbines are also light weight and have relatively low emissions. Potentially, one of the greatest advantages of microturbines is their ability to utilize a number of fuels, including waste fuels or biofuels. Microturbines have great potential in cogeneration applications because microturbines produce a large quantity of clean, hot exhaust gases compared to other distributed generators.

The primary disadvantages of microturbines are that they have a low fuel to electrical efficiency. Also, with higher elevation and increased ambient temperatures, microturbines experience a loss of power output and efficiency. The ambient temperature directly affects the temperature of the air at the intake. A gas turbine will operate more effectively when colder air is available at the intake. A gas turbine cycle must compress the inlet air and the greater the compression, the greater efficiency. Another potential disadvantage is that microturbines experience more efficient operation and require less maintenance when operated continuously.

Exercises

1. A 25-kW microturbine meets all of the electricity requirements of an office building. The set point for the thermostat remains at 68°F. The turbine inlet temperature is 1,800°F and the compressor and turbine have efficiencies of 0.72 and 0.80, respectively. The shaft work produced by the turbine is completely converted into electrical power. If the compressor pressure ratio is 8, determine the compressor and turbine work in kJ/kg, the net work in kJ/kg, and the thermal efficiency of the microturbine.

2. The minimum and maximum temperatures of an ideal Brayton cycle are 290 K and 1300 K, respectively. The pressure ratio is that which maximizes the net work developed by the cycle per unit mass of air-flow. Using a cold air-standard analysis, determine per unit of mass of air flow (a) the compressor work, (b) the turbine work, and (c) the thermal efficiency of the cycle.
3. An ideal Brayton cycle is modeled on an air-standard basis. The compression ratio of the cycle is 9 with air entering the compressor at T_1 = 70 F, p_1 = 14.7 psi, with a mass flow rate of 35,000 lb/hr. If the turbine inlet temperature is 1,150 F, determine (a) the thermal efficiency, (b) the net power developed, and (c) the amount of waste heat available for recovery.

4. The net power developed by an ideal air-standard Brayton cycle is 2.5×10^4 Btu/hr. The pressure ratio for the cycle is 10, and the minimum and maximum temperatures are 520 R and 1800 R, respectively. Calculate (a) the thermal efficiency of the cycle, (b) the mass flow rate of the air, and (c) the amount of waste heat available for recovery.

5. A stationary gas turbine has compressor and turbine efficiencies of 0.85 and 0.90, respectively, and a pressure ratio of 12. Determine the work of the compressor and the turbine, the net work, the turbine exit temperature, and the thermal efficiency for 80 F ambient and 1000 F turbine inlet temperatures.

6. A simplified analysis is performed on a gas turbine engine cycle with a Compression ratio of 7 to 1. The compressor and turbine inlet temperatures are 320 K and 1100 K, respectively. The compressor has an efficiency of 0.84 and the turbine has an efficiency of 0.88. Calculate the thermal efficiency of (a) the ideal Brayton cycle, (b) the actual gas turbine cycle, and (c) the amount of waste heat available for recovery.

Manufacturers

- Capstone Turbine Corporation, based in Chatsworth, California, is a leader in the commercialization of low-emission, high-reliability microturbine power generators. The company offers 30-kW and 60-kW systems for distributed energy resource applications. The Capstone C30, a 30-kW microturbine, is pictured in Figure 4.19.

Figure 4.19: Capstone C30 Microturbine. (http://www.capstoneturbine.com/)

- Elliot Energy Systems, located in Stuart, Florida, develops and manufactures the 100-kW TA CHP unit shown in Figure 4.20.

Figure 4.20: Elliot Systems 100-kW TA CHP Unit
(www.elliottmicroturbines.com)

- Ingersoll-Rand Energy Systems of Portsmouth, New Hampshire develops the PowerWorks™ line of microturbine generators with output of 70 kW, pictured in Figure 4.21.

Figure 4.21: Ingersoll-Rand 70-kW PowerWorks™ Microturbine
(www.irpowerworks.com/)

- TURBEC, recently purchased by API Com, an Italian company, manufactures a 100-kW microturbine that is equipped for cogeneration. The 100-kW T100 CHP is shown in Figure 4.22.

Figure 4.22: TURBEC 100-kW T100 CHP Microturbine (www.turbec.com/)

- Bowman Power Systems is a U.K. company that develops 80-kW microturbine power generation systems for DER and mobile power applications. The system is pictured in Figure 4.23.

Figure 4.23: Bowman Power Systems 80-kW Microturbine System (www.bowman.com)

Stirling Engines

Technology Overview

The Stirling engine is a heat engine invented in 1816 by Robert Stirling, a Scottish clergyman. The Stirling engine is a type of external combustion piston engine which uses a temperature difference to create motion in the form of shaft work. The Stirling cycle uses an external heat source, which could be anything from petroleum based product, to solar energy, to the heat produced by decaying plants. No combustion takes place inside the cylinders of the engine. To date, there has not been a successful mass-market application for the Stirling engine. However, recently companies such as Microgen and WhisperTech have developed m-CHP systems based on the Stirling engine technology.

The operation of a Stirling engine is based upon the behavior of a fixed amount of air or gas such as helium or hydrogen enclosed in the cylinders of the engine. Two gas properties allow for the operation of a Stirling engine: (1) for a constant amount of gas in a fixed volume as the temperature is increased, the pressure will increase, and (2) when a fixed amount of gas is compressed, the temperature of that gas will increase.

Stirling engines use a displacer piston to move the enclosed gas back and forth between the hot and cold reservoirs. The gas expands at the hot reservoir and displaces a power piston, producing work while at the same time forcing the gas to move to the cold reservoir. At the cold reservoir, the gas contracts,

retrieving the power piston and closing the cycle. The operation of a Stirling engine can be best understood by examining the operation of a two-cylinder (or alpha) Stirling engine. A step-by-step diagram of a two-cylinder Stirling engine and further explanation on the operation of the Stirling engine are shown in Figure 4.24. In the two-cylinder Stirling engine, one cylinder is kept hot while the other is kept cool. In Figure 4.24, the lower-left cylinder is heated by burning fuel. The other cylinder is kept cool by an air cooled sink. In a two-cylinder Stirling engine each piston acts as both a power piston and displacer piston.

The pressure-specific volume (pv) and temperature-entropy (Ts) diagrams for the Stirling cycle are shown in Figure 4.25. The Stirling cycle consists of four internally reversible processes in series: an isothermal compression from state 1 to state 2 at temperature T_C, a constant-volume heating from state 2 to state 3, an isothermal expansion from state 3 to state 4 at temperature T_H, and a constant-volume cooling from state 4 to state 1 to complete the cycle. A regenerator can be used to utilize the heat rejected in Process 4-1 to be used to aid the heat input process during Process 2-3.

The thermal efficiency of the Stirling cycle is equal to that of the Carnot cycle when both constant volume heating and constant volume cooling are employed. The Stirling cycle is a reversible cycle.

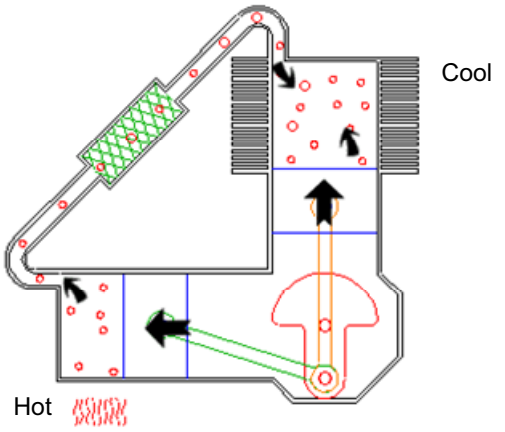

Step 1: Compression. At this point, the majority of the gas has been shifted to the cool cylinder. As the gas cools and contracts, both pistons are drawn outward.

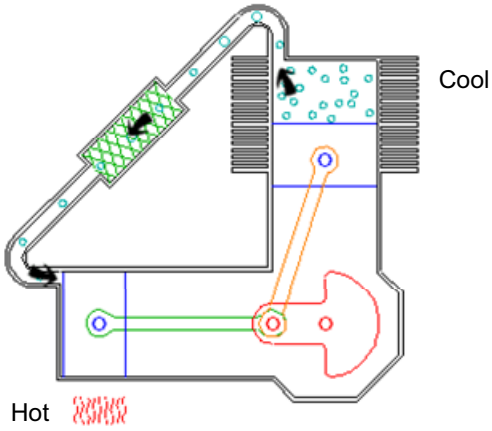

Step 2: Heat Transfer. The now contracted gas is still located in the cool cylinder. Flywheel momentum carries the crank another 90 degrees, transferring the gas to back to the hot cylinder.

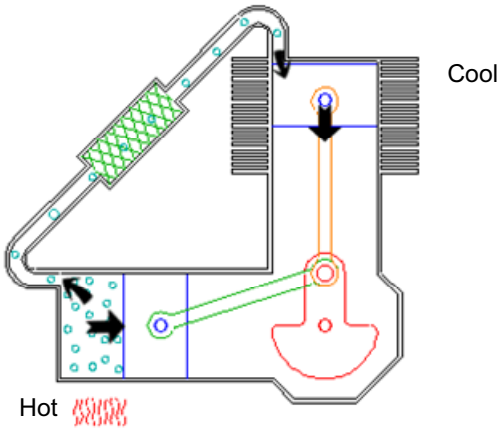

Step 3: Expansion. Now, most of the gas in the system has just been driven into the hot cylinder. The gas heats and expands driving both pistons inward.

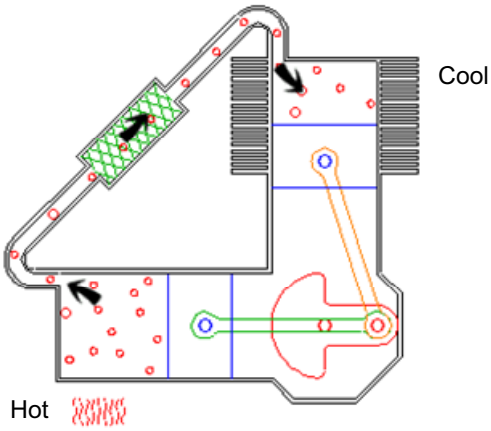

Step 4: Heat Transfer. At this point, the gas has expanded (about 3 times in this example). Most of the gas (about 2/3rds) is still located in the hot cylinder. Flywheel momentum carries the crankshaft the next 90 degrees, transferring the bulk of the gas to the cool cylinder to complete the cycle.

Figure 4.24: Two-cylinder Stirling Engine Diagram (www.keveny.com/vstirling.html)

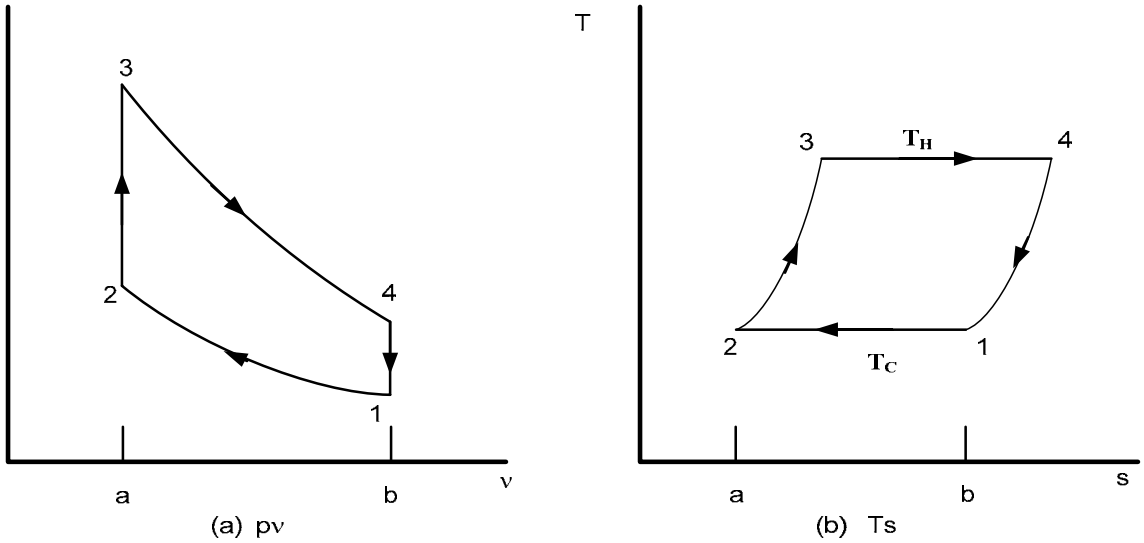

Figure 4.25: Pressure-Specific Volume and Temperature-Entropy Diagrams for the Stirling Cycle.

The expressions for the work accomplished by the cycle ($W_{Stirling}$), the heat added (Q_{in}), and the thermal efficiency ($\eta_{Stirling}$) can be determined through the application of the first law of thermodynamics. For an ideal monatomic gas C_v=3/2*R. For a thermally perfect gas

$$p \cdot V = n \cdot R \cdot T \tag{4-29a}$$

$$p = \frac{n \cdot R \cdot T}{V} \tag{4-29b}$$

Where p is pressure, V is volume, R is the ideal gas constant, n is the number of moles of the gas, and T is the respective temperature. The work of the cycle is expressed as:

$$W_{Stirling} = \oint p \cdot dV \tag{4-30}$$

From examination of the cycle and substituting the relationship from the ideal gas law, the work per unit mass becomes

$$W_{Stirling} = R \cdot T_H \cdot \int \frac{dV}{V} \tag{4-31a}$$

$$W_{34} = R \cdot T_H \cdot \ln\left(\frac{V_b}{V_a}\right) \tag{4-31b}$$

$$W_{14} = R \cdot T_C \cdot \ln\left(\frac{V_a}{V_b}\right) \tag{4-31c}$$

$$W_{Stirling} = R \cdot \left(T_H - T_C\right) \cdot \ln\left(\frac{V_b}{V_a}\right) \tag{4-31d}$$

$$W_{Stirling} = R \cdot \left(T_3 - T_2\right) \cdot \ln\left(\frac{V_b}{V_a}\right) \tag{4-31e}$$

Note that $T_H = T_3 = T_4$, and $T_C = T_1 = T_2$ due to the isothermal processes. The heat transfer into the system per unit mass can be expressed as:

$$Q_{in} = n \cdot c_v \cdot \Delta T \tag{4-32a}$$

$$Q_{in} = \frac{3}{2} \cdot R \cdot (T_H - T_C) + R \cdot T_H \cdot \ln\left(\frac{V_b}{V_a}\right) \tag{4-32b}$$

$$Q_{in} = \frac{3}{2} \cdot R \cdot (T_3 - T_2) + R \cdot T_H \cdot \ln\left(\frac{V_b}{V_a}\right) \tag{4-32c}$$

The expression for the cycle efficiency is:

$$\eta_{Stirling} = \frac{W_{Stirling}}{Q_{in}} \tag{4-33a}$$

$$\eta_{Stirling} = \frac{R \cdot \left(T_3 - T_2\right) \cdot \ln\left(\frac{V_b}{V_a}\right)}{\frac{3}{2} \cdot R \cdot (T_3 - T_2) + R \cdot T_3 \cdot \ln\left(\frac{V_b}{V_a}\right)} \tag{4-33b}$$

While the Stirling engine is always less efficient that the Carnot engine, the difference becomes small when V_b is much greater than V_a and T_H is much greater than T_C.

Example 4-3

A Stirling engine has a volume ratio of V_b/V_a = 2.0 and operates with helium as the working fluid. The operating conditions of the engine are T_H = 473 K and T_C = 298 K. Determine the (a) work per unit mass of the cycle, (b) the heat input per unit mass, and (c) the thermal efficiency of the cycle.

Input the given information.

$T_H := 473K$ $T_C := 298K$ $V_{ratio} := 2$ $V_{ratio} = \frac{V_b}{V_a}$

Input the gas constant for helium.

$R_{He} := 2.0769\frac{kJ}{kg \cdot K}$

(a) The work of the cycle (Equation 4-31d) is

$W_{Stirling} := R_{He} \cdot (T_H - T_C) \ln(V_{ratio})$ $W_{Stirling} = 251.93\frac{kJ}{kg}$

(b) The heat put into the cycle per unit mass (Equation 4-32b) is

$Q_{in} := \frac{3}{2} \cdot R_{He} \cdot (T_H - T_C) + R_{He} \cdot T_H \cdot \ln(V_{ratio})$ $Q_{in} = 1.226 \times 10^3 \frac{kJ}{kg}$

(c) The efficiency of the cycle is defined as

$\eta_{Stirling} := \frac{W_{Stirling}}{Q_{in}}$ $\eta_{Stirling} = 20.547\%$

or substituting for $W_{Stirling}$ and Q_{in}

$\eta_{Stirling} := \frac{R_{He} \cdot (T_H - T_C) \ln(V_{ratio})}{\frac{3}{2} \cdot R_{He} \cdot (T_H - T_C) + R_{He} \cdot T_H \cdot \ln(V_{ratio})}$ $\eta_{Stirling} = 20.547\%$

Figure 4.26: Example 4-3

Stirling engines come in three configurations, alpha, beta and gamma. An alpha Stirling engine contains two separate power pistons, one “hot” piston and one “cold” piston. The hot piston is placed in the heat exchanger with the higher temperature while the cold piston is in the heat exchanger with the lower temperature. While the alpha configuration has a high power-to-volume ratio, the high temperature used for the “hot” piston and its seals typically creates technical problems.

A beta Stirling engine uses a single power piston arranged coaxially on the same shaft as the displacer piston. The displacer piston moves the working gas from the hot heat exchanger to the cold heat exchanger, but does not extract any power from the working fluid. As the working gas is displaced to the hot end of the cylinder, the gas expands and moves the power piston, producing work. As the working fluid is moved to the cold side of the cylinder, the fluid contracts and the power piston is moved in the opposite direction due to the external atmospheric pressure. As the beta configuration does not require moving seals in the hot portion of the engine, higher compression ratios can be achieved.

A gamma Stirling engine is a beta Stirling engine in which the power piston is not mounted coaxially to the displacer piston. The advantage of the gamma Stirling engine is that it is often mechanically simpler and can be used in multi-cylinder Stirling engines. However, the gamma Stirling produces lower compression ratios.

Application

Stirling engines are an old technology; however their use became limited with the improvement of steam engines and the invention of the Otto cycle engine. Recent interest in distributed energy has revived interest in Stirling engines. Stirling engines can be used in a variety of applications due to their thermal output, simple operation, low production costs, and relatively small size. Applications for Stirling engines include power generation units for space crafts and vehicles, small aircraft, refrigeration, m-CHP, solar dish application, and small scale residential or portable power generation. An overview of Stirling engine characteristics is presented in Table 4.3.

Table 4.3: Overview for Stirling Engine Technology (http://www.energy.ca.gov/distgen)

Stirling Engine Overview	
Commercially Available	Yes, mostly in Europe
Size Range	<1 kW - 25 kW
Fuel	Natural gas primarily but broad fuel flexibility is possible
Efficiency	12 – 20% (Target: >30%)
Environmental	Potential for very low emissions
Other Features	Cogen (some models)

Commercially available Stirling engines can produce between 1 kW – 25 kW. Stirling engine technology has been widely used in England and Europe with great success, particularly in the m-CHP arena. However, a very small percentage of the world's electrical capacity is currently provided through the use of Stirling engines.

Heat Recovery

Traditional large-scale electric power generation is typically about 30% efficient, while combined cycle power plants are approximately 48% efficient. In either case, the reject heat is lost to the atmosphere with the exhaust gases. Stirling engines are typically in the range of 15 – 30% efficient, with many reporting efficiencies of 25 – 30%. The overall efficiencies of these systems can be greatly increased by recovering the waste heat.

A high percentage of the Stirling engine heat losses will go to the cooling fluid instead of into the exhausts, which makes the Stirling engine suitable for combined heat and power generation. Typical operating temperatures range from 1200 – 1470 F (650 – 800 C), resulting in electrical engine conversion efficiencies of around 30% to 40% when a recuperator is included in the engine system. These high operating temperatures can convert into high quality waste heat. The reject heat can be recaptured through piping the cooling fluid through a heat exchanger and by ducting the exhaust gases through a heat exchanger to produce hot water.

Cost

The capital costs of Stirling engines are comparably high and vary greatly depending upon manufacturer ($2,000 - $50,000). And, overall cost increases with size. However, several companies have targeted Stirling technology for m-CHP units and have achieved relative success. These companies include PowerGen, WhisperTech, Sunpower, and ENATEC.

Advantages and Disadvantages

Some advantages of Stirling engines are:

- The burning of the fuel air mixture can be more accurately controlled due to the external heat source.
- Emission of unburned fuel can be eliminated as a continuous combustion process can be used to supply heat.
- Less lubrication is required leading to greater periods between overhauls because the bearings and seals are placed on the cool side.
- Simplicity of design; no valves are needed, fuel and intake systems are very simple.
- Low noise and vibration free operation.
- Low maintenance and high reliability.
- Multi-fuel capability.
- Long service life.

Some disadvantages of Stirling engines are:

- High costs.
- Low efficiencies.
- Require both input and output heat exchangers which must withstand the working fluid pressure and resist corrosion effects.
- Relatively large for the amount of power they produce due to the heat exchangers.
- Cannot experience instantaneous start-up.
- Power output is relatively constant and rapid change to another level is difficult to achieve.

Exercises

1. Hydrogen is the working fluid of a Stirling engine operating at T_H = 400 K and T_C = 298 K. If the volume ratio is 2.0, calculate the work of the cycle and the heat input of the cycle.

2. A Stirling engine has a volume ratio of V_b/V_a = 3.0 and operates with hydrogen as the working fluid. The operating conditions of the engine are T_H = 500 K and T_C = 298 K. Determine the (a) work per unit mass of the cycle, (b) the heat input per unit mass, and (c) the thermal efficiency of the cycle.

3. The volume ratio of a Stirling engine is 2.0. Helium is the working fluid and 12 kW of heat is added to the system. If T_C = 298 K, determine (a) T_H, (b) the work of the cycle and (c) the thermal efficiency of the cycle.

4. Helium is the working fluid of a Stirling Engine. The operating conditions of the engine are T_H = 500 K and T_C = 298 K. If the engine produces 270 kg/kJ of work, calculate (a) the volume ratio, (b) the heat added to the cycle, and (c) the efficiency of the cycle.

5. For a Stirling engine operating between T_H = 450 K and T_C = 310 K, and using helium as the working fluid, plot the thermal efficiency as a function of volume ratio. Let the volume ratio (V_b/V_a) vary from 0.5 to 5. How does the volume ratio effect the thermal efficiency of the cycle?

Manufacturers

There are a relatively large number of companies that are developing and manufacturing Stirling engines and/or complete generator sets for m-CHP. Five of these companies are listed as follows:

- WhisperTech, located in Christchurch, New Zealand, manufactures the AC and DC WhisperGen generator sets illustrated in Figure 4.27. The AC WhisperGen (left) uses a four-cylinder Stirling cycle fuelled by hydrogen and natural gas to produce up to 1.2 kW of electrical power at 220 – 240V, as well as 8 kW of thermal energy via a sealed liquid circulation system. The DC WhisperGen (right) uses a four-cylinder Stirling engine fuelled by automotive grade diesel and produces up to 0.8 kW electric and 5.5 kW of thermal energy via a sealed liquid circulation system.

Figure 4.27: AC and DC WhisperGen Micro-CHP Units (www.whispergen.com)

- The BG Group has developed the BG Microgen, which uses a linear free piston Stirling engine. The output of this unit has not yet been specified. The BG Microgen is shown in Figure 4.28.

Figure 4.28: BG Microgen Micro-CHP Unit (www.microgen.com)

- The Stirling Technology Company headquartered in Kennewick, Washington, produces the ATAG/ENATEC 1-kW unit which is fueled by natural gas. The unit is shown in Figure 4.29.

Figure 4.29: 1-kW ENATEC Field Prototype CHP Unit – Full System (http://www.enatec.com)

- SOLO, out of Sindelfingen, Germany manufactures Stirling engines that produce from 2 – 9 kW of electrical power as well as 8 – 26 kW of thermal energy when fueled by natural gas or liquid gas. The company also produces models that are solar powered. The model used for m-CHP is shown in Figure 4.30.

Figure 4:30: SOLO 9-kW Stirling Engine (www.stirling-engine.de/engl/l)

- Stirling Engine, Inc. headquartered in Phoenix, Arizona manufactures the Stirling based ST – 5. Virtually any combustible material is a suitable fuel for the ST-5. Power outputs are not listed for the ST – 5. The ST – 5 is shown in Figure 4:31.

Figure 4:31: Stirling Engine, Inc. ST – 5.
(http://www.waoline.com/science/NewEnergy/Motors/StirlingCie.htm)

Rankine Cycle Engines

Technology Overview

Rankine cycle engines are a relative newcomer to the m-CHP arena. Originally, Rankine cycle engines were rejected as an applicable technology because of their relatively low electrical conversion efficiency. However, as electrical efficiency came to be considered a less important issue, Rankine cycle engines were again considered due to their relative simplicity (low production costs) and known durability and performance characteristics.

Rankine cycle systems are used by most commercial electric power plants. The Rankine cycle uses a liquid that evaporates when heated and expands to produce shaft work. The exhaust vapor is condensed and the liquid is pumped back to the boiler to repeat the cycle. The working fluid most commonly used is water, though other fluids can also be used. The Rankine engine itself can be either a piston engine or a turbine. Figure 4.32 illustrates the components and operation of a Rankine cycle system that utilizes a turbine.

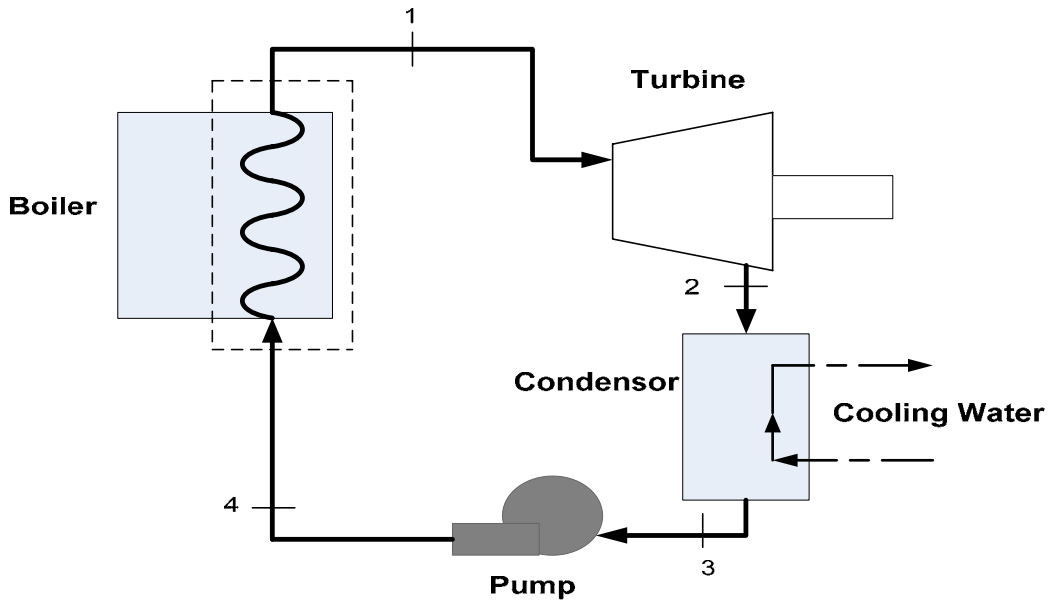

Figure 4.32: Rankine Cycle Engine Schematic

As can be seen from Figure 4.31, the Rankine cycle is a closed-loop cycle. The temperature-entropy diagram for the ideal Rankine cycle is shown in Figure 4.33.

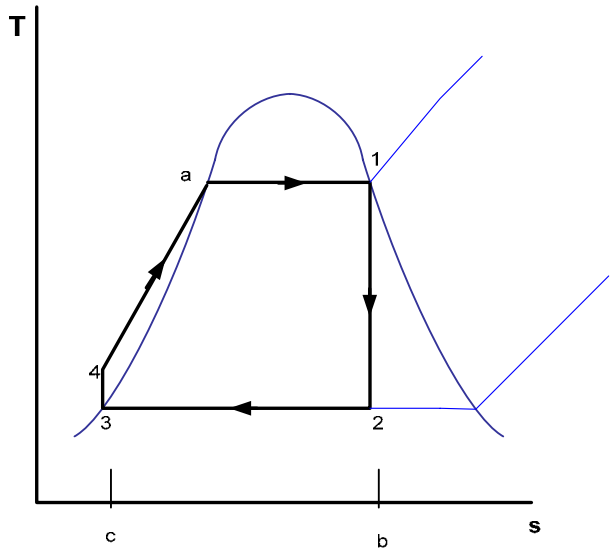

Figure 4.33: Ideal Rankine Cycle Temperature Entropy Diagram

Conservation of mass and application of the first law yield expressions for the work of the turbine (W_t), the work of the pump (W_p), the net work (W_{net}), the heat transfer into the system (Q_{in}), and the efficiency (η_{Rank}). The work of the turbine and work of the pump can be expressed as

$$W_t = \dot{m}\left(h_1 - h_2\right) \tag{4-34}$$

$$W_p = \dot{m}\left(h_4 - h_3\right) \tag{4-35}$$

The work input into the system is denoted as negative work; the net work of the cycle can be expressed as

$$W_{net} = W_t - W_p \tag{4-36a}$$

$$W_{net} = \dot{m}\left[(h_1 - h_2) - (h_4 - h_3)\right] \tag{4-36b}$$

The heat transfer supplied by the boiler is

$$Q_{in} = \dot{m}\left(h_1 - h_4\right) \tag{4-38}$$

The heat transfer leaving the system at the condenser is

$$Q_{out} = \dot{m}\left(h_2 - h_3\right) \tag{4-39}$$

The thermal efficiency of the Rankine cycle can be expressed as the net work of the system divided by the heat input into the system.

$$\eta_{Rank} = \frac{W_{net}}{Q_{in}} \tag{4-40a}$$

$$\eta_{Rank} = \frac{h_1 + h_3 - h_2 - h_4}{h_1 - h_4} \tag{4-40b}$$

$$\eta_{Rank} = 1 - \frac{h_2 - h_3}{h_1 - h_4} \tag{4-40c}$$

The net work output equals the net heat input for the ideal Rankine cycle. Thus, the thermal efficiency can also be expressed in terms of the heat transfer terms and finally in terms of temperatures in the following manner:

$$\eta_{Rank} = \frac{Q_{in} - Q_{out}}{Q_{in}} \tag{4-41a}$$

$$\eta_{Rank} = 1 - \frac{Q_{out}}{Q_{in}} \tag{4-41b}$$

$$\eta_{Rank} = 1 - \frac{T_{out}}{T_{in}} \tag{4-41c}$$

where T_{out} denotes the temperature on the steam side of the condenser of the ideal Rankine cycle and T_{in} denotes the average temperature of heat addition at the boiler.

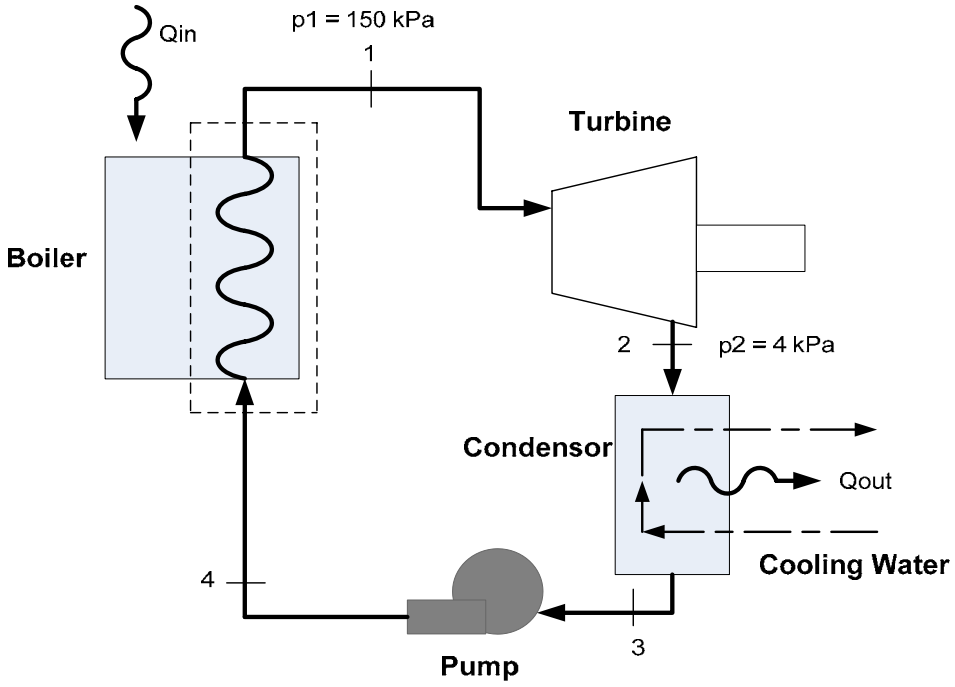

Figure 4.34: Rankine Cycle Engine Diagram for Example 4-4

Example 4-4

An ideal Rankine cycle operates with steam as the working fluid as shown in Figure 4.33. The net power output of the cycle is 10 kW. Saturated vapor enters the turbine at 70 kPa and saturated liquid exits the condenser at a pressure of 4 kPa.

Determine for the cycle (a) the thermal efficiency, (b) the mass flow rate of the steam in kg/h, (c) the rate of heat transfer into the working fluid as it passes through the boiler in kW, (d) the work of the turbine, (e) the heat lost through the condenser, and (f) the work of the pump.

Assumptions:
1. All the processes of the working fluid are internally reversible,
2. The turbine and pump operate adiabatically.
3. Each component of the cycle is analyzed as a control volume at steady state.
4. Kinetic and potential energy efects are negligible.
5. Saturated vapor enters the turbine. Condensate exits the condenser as saturated liquid.

Solution:

Starting at the inlet to the turbine, the pressure is 150 kPa and the steam is a saturated vapor, from the thermodynamic properties for water are (steam tables)

$$h_1 := 2693.6\frac{kJ}{kg} \qquad s_1 := 7.2233\frac{kJ}{kg\cdot K}$$

State 2 is fixed by p_2 = 4 kPa and the fact that the specific entropy is constant for adiabatic, internally reversible expansion through the turbine ($s_1 = s_2$) . The specific entropy for saturated liquid at 4 kPa is s_f = 0.4226 kJ/kg-K and the specific entropy for saturated vapor data at 4 kPa is s_g = 8.4746 kJ/kg-K. The quality at State 2 is

$$x_2 := \frac{s_2 - s_f}{s_g - s_f} \qquad x_2 = 0.845$$

The specific enthalpy for saturated liquid at 4 kPa is h_f = 121.46 kJ/kg and the specific enthalpy for saturated vapor data at 4 kPa is h_g = 2554.4 kJ/kg. The enthalpy at State 2 is

$$h_2 := x_2\cdot\left(h_g - h_f\right) + h_f \qquad h_2 = 2.176\times 10^3\ \frac{kJ}{kg}$$

State 3 is saturated liquid at 4 kPa, so h_3 = 121.46 kJ/kg, ν_3 = 1.0040x10^{-3} m^3/kg, and s_3 = 0.4226 kJ/kg-K.

State 4 is fixed by the boiler pressure p_4 = 100 kPa and the specific entropy, $s_4 = s_3$ = 0.4226 kJ/kg-K. However, the enthalpy at State 4 can be found using Equation 4-35. The work of the pump per unit of mass flowing can be approximated as

$$\frac{W_p}{m} = \nu_3\cdot\left(p_4 - p_3\right) = 1.0040\,10^{-3}\,\frac{m^3}{kg}\cdot(100kPa - 4kPa) = 0.147\frac{kJ}{kg}$$

Figure 4.35: Example 4-4

From the first law of thermodynamics, the work of the pump is

$$\frac{W_p}{m} = \left(h_4 - h_3\right)$$

$$0.147\frac{kJ}{kg} = h_4 - 121.46\frac{kJ}{kg} \qquad h_4 = 121.607\frac{kJ}{kg}$$

(a) Determine the thermal efficiency of the system.

The efficiency of the system can be determined as

$$\eta_{Rank} := 1 - \frac{h_2 - h_3}{h_1 - h_4} \qquad \eta_{Rank} = 20.107\%$$

(b) Determine the mass flow rate of the fluid through the system.

The net work of the system is given as 10 kW. The mass flow rate through the system can be determined using from the first law of thermodynamics.

$$W_{net} = m\cdot\left[\left(h_1 - h_2\right) - \left(h_4 - h_3\right)\right]$$

so that

$$m := \frac{W_{net}}{\left(h_1 - h_2\right) - \left(h_4 - h_3\right)} \qquad m = 0.019\,\frac{kg}{s}$$

(c) Determine the rate of heat transfer into the fluid passing through the boiler.

The heat transfer into the fluid passing through the boiler can be determined using either Equation 4-40a because both the net work of the cycle and efficiency are known, or Equation 4-38 can be used since both the flow rate and enthalpies at States 1 and 4 are known. Both methods will be demonstrated here.

Using Equation 4-40a

$$\eta_{Rank} = \frac{W_{net}}{Q_{in}}$$

$$Q_{in} := \frac{W_{net}}{\eta_{Rank}} \qquad Q_{in} = 49.735\text{kW}$$

Using Equation 4-38

$$Q_{in} := m\cdot\left(h_1 - h_4\right) \qquad Q_{in} = 49.735\text{kW}$$

(d) Determine the work of the turbine.

The work of the turbine can be determined as

$$W_t := m\cdot\left(h_1 - h_2\right) \qquad W_t = 10.003\text{kW}$$

Figure 4.35 (continued)

(e) Determine the heat loss through the condenser.

From the first law of thermodynamics, the heat loss through the condenser is

$Q_{out} := m \cdot (h_2 - h_3)$ $\quad Q_{out} = 39.735\,kW$

(f) Determine the work of the pump.

The work of the pump can be found applying the first law of thermodynamics to the pump

$W_p := m \cdot (h_4 - h_3)$ $\quad W_p = 2.835\,W$

Figure 4.35 (continued)

Generally speaking, as compared to other technologies, the Rankine cycle engines have one of the lowest electrical conversion efficiencies. The thermal efficiencies of most other competing technologies are also higher than that of the Rankine cycle engines.

Application

The advantage of the Rankine cycle for power plants is that the working fluid is a liquid. Many times this liquid is water, which is a cheap and readily available resource. Currently, companies such as the Baxi Group, Enginion, and Cogen Microsystems are exploring the possibility of using Rankine Cycle engines for m-CHP.

Heat Recovery

As the Rankine cycle is a closed-loop, which incorporates a condenser, heat recovery can be achieved easily at the condenser. However, as most of the

Rankine cycle engine technologies for m-CHP are still under development, the quality and quantity of heat that can be recaptured is currently not well defined.

Cost

Unfortunately, little is known about potential costs of small-scale Rankine cycle units for m-CHP. As more of these technologies complete the field trial stage of development, more information concerning capital and maintenance costs will be available.

Exercises

1. The turbine of an ideal Rankine cycle generates 12 kW of power while the pump requires 2.2 kW of power. If the heat input to the cycle is 20 kW, determine the net work of the cycle and the thermal efficiency of the cycle.

2. In an ideal Rankine cycle, the pump increases the pressure of water from 10 psia to 22 psia. The turbine produces 15 hp. If the mass flow rate through the system is 15 lb/min, determine the net work of the cycle and the heat added to the cycle if the plant has an efficiency of 40%.

3. A steam plant receives heat from a source at a rate of 10 kW. The plant operates with a boiler pressure of 80 kPa and a condenser pressure of 6 kPa. If the plant operates as an ideal Rankine cycle, calculate (a) the cycle efficiency, (b) the net work of the cycle, (c) the required mass flow rate of the working fluid, and (d) the heat rejected at the condenser.

4. An ideal Rankine cycle operates with steam as the working fluid. The net power of the plant is 8 kW. The pumping power requirement is 1.4 kW. The boiler pressure is 70 kPa and the condenser pressure is 10 kPa. Determine (a) the work of the turbine, (b) the mass flow rate of the working fluid, (c) the heat input into the cycle, (d) the cycle efficiency, and (e) the waste heat rejected through the condenser.

5. The efficiency of an ideal Rankine cycle is 45%. Steam exits the boiler at 25 psia and the condenser operates at 12 psia. If the flow rate of water exiting the condenser is 20 lbm/min, determine (a) the heat input to the cycle, (b) the

net work of the cycle, (c) the work of the turbine, (d) the work of the pump, and (e) the heat rejected through the condenser.

6. An ideal Rankine cycle operates with steam as the working fluid. The net power output of the cycle is 10 kW. Saturated vapor enter s the turbine at 80 kPa and 210 C. Saturated liquid exits the condenser at a pressure of 4 kPa. Find (a) the heat input into the cycle, (b) the thermal efficiency of the cycle, (c) the mass flow rate of the working fluid, and (d) the heat rejected by the cycle.

Manufacturers

- Enginion, based in Berlin, Germany is the developer of the SteamCell. The SteamCell pictured in Figure 4.36 has an output of 4.6-kW electrical and 25-kW of thermal energy. A trial installation is scheduled for 2005.

Figure 4.36: Enginion 4.6-kW SteamCell Unit (www.enginion.com)

- Cogen Microsystems, based in Australia manufacture 2.5-kW and 10-kW units based on Rankine cycle engines. Market release is expected in 2007. A 2.5-kW unit is pictured in Figure 4.37.

Figure 4.37: Cogen Microsystems 2.5-kW Rankine Cycle m-CHP Unit (www.cogenmicro.com)

Fuel Cells

Technology Overview

A fuel cell is an electrochemical energy conversion device, comprised of three major components, a cathode, an anode, and electrolyte. Fuel cells are similar to batteries in that they both produce direct current (DC) through an electrochemical process without direct combustion of a fuel source. Unlike batteries, which deliver power from a finite amount of stored energy, fuel cells can operate indefinitely provided that a fuel source is continuously supplied.

Typically, a fuel cell electrochemically reacts hydrogen and oxygen to form water and in the process produces electricity. The process consists of a hydrogen-based input fuel passing over an anode where a catalytic reaction occurs, splitting the fuel into ions and electrons. Consider the reactions at the anode and cathode of an acid electrolyte fuel cell. At the anode, the hydrogen gas ionizes, releasing electrons and creating H^+ ions in an exothermic reaction. The reaction is

$$2H_2 \rightarrow 4H^+ + 4e^-$$

Ions pass from the anode, through the electrolyte, to an oxygen-rich cathode. At the cathode, oxygen reacts with the electrons taken from the electrode and the H^+ ions that have traveled through the electrolyte to form water according to the following reaction:

$$O_2 + 4H^+ + 4e^- \rightarrow 2H_2O$$

For the reactions to occur simultaneously, electrons produced at the anode must pass through an electric circuit to the cathode while the H^+ ions pass through the electrolyte. A schematic diagram of the reaction occurring in a phosphoric acid fuel cell (PAFC) is illustrated in Figure 4.38.

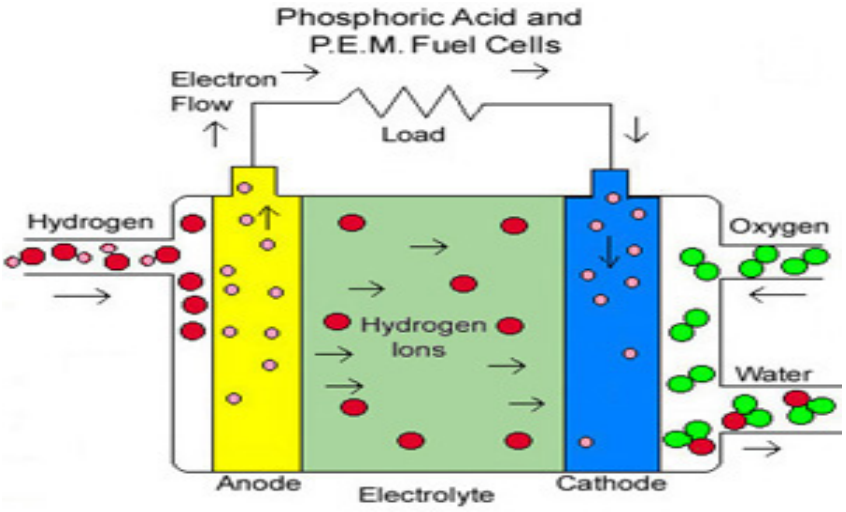

Figure 4.38: PAFC Electrochemistry (http://www.fctec.com/fctec)

The performance of a fuel cell can be analyzed by using the Gibbs function or Gibbs free energy of reaction. The Gibbs free energy of reaction is an indication of the maximum work that can be achieved from combining two substances in a chemical reaction.

The maximum theoretical work (W_{MAX}) is the difference in the Gibbs free energy (G) of the reactants and the products of the chemical reaction.

$$W_{MAX} = G_{react} - G_{prod} \tag{4-42}$$

The Gibbs free energy is a function of the enthalpy (h), entropy (s), and temperature (T) associated with the chemical compound of interest at a specific state of matter and is defined as

$$G = h - T \cdot s \tag{4-43}$$

The temperature-entropy product represents the loss due to changes in entropy. The maximum work that can be achieved by a fuel cell is

$$W_{MAX} = \left(h_{react} - h_{prod}\right) - T \cdot \left(s_{react} - s_{prod}\right) \tag{4-44}$$

And the thermal efficiency (η_{th}) is defined as

$$\eta_{th} = \frac{G_{react} - G_{prod}}{h_{react} - h_{prod}} \tag{4-45}$$

The thermal efficiency of a fuel cell typically ranges from 82 – 94% in ideal cases. The thermal efficiency of a fuel cell as defined in Equation 4-45 is not the actual electrical conversion efficiency achieved by the fuel cell. Due to ohmic losses resulting from concentration polarization and activation polarization the electrical conversion efficiency of a fuel cell (η_{fc}) generally falls between 40 – 60%. The ohmic losses are accounted for using a voltage efficiency (η_v) and a current efficiency (η_i). The electrical conversion efficiency of a fuel cell is defined as the product of the thermal, voltage, and current efficiencies.

$$\eta_{fc} = \eta_{th} \cdot \eta_v \cdot \eta_i \tag{4-46}$$

Example 4-5

A PEMFC (hydrogen-oxygen) fuel cell has liquid water as a product when it operates at 363 K. What is the maximum work that the fuel cell can achieve per mole of reactant and what is the thermal efficiency?

The overall reaction for a PEMFC is: $2H_2 + O_2 \Leftrightarrow 2H_2O$

The thermodynamic properties needed are obtained from the JANAF thermodynamic tables:

$h_{O2} := 0\frac{kcal}{mole}$ $s_{O2} := 41.395\frac{cal}{mole \cdot K}$

$h_{H2} := 0\frac{kcal}{mole}$ $s_{H2} := 24.387\frac{cal}{mole \cdot K}$

$h_{H2O} := -57.433\frac{kcal}{mole}$ $s_{H2O} := 36.396\frac{cal}{mole \cdot K}$

The enthalpy of formation for the products and reactants are

$h_{prod} := 2mole \cdot h_{H2O}$ $h_{prod} = -114.866kcal$

$h_{react} := 2mole \cdot h_{H2} + 1mole \cdot h_{O2}$ $h_{react} = 0kcal$

The entropy of the products and reactants are

$s_{prod} := 2mole \cdot s_{H2O}$ $s_{prod} = 0.073\frac{1}{K}kcal$

$s_{react} := 2mole \cdot s_{H2} + 1mole \cdot s_{O2}$ $s_{react} = 0.09\frac{1}{K}kcal$

The maximum work the PEMFC can achieve is determined using Equation 4-44

$W_{MAX} := (h_{react} - h_{prod}) - T_{oper} \cdot (s_{react} - s_{prod})$

$W_{MAX} = 4.545 \times 10^5 J$ per 2 moles of reactant

Combining Equations 4-42 and 4-45, the thermal efficiency of the fuel cell becomes

$\eta_{th} := \frac{W_{MAX}}{h_{react} - h_{prod}}$ $\eta_{th} = 94.51\%$

Figure 4.39: Example 4-5

The components needed for the operation of a fuel cell system vary depending on the type of fuel cell used and the fuel. Common major

components for a fuel cell system include a fuel reformer (processor), the fuel cell “stack,” and a power conditioner. The fuel reformer, also known as a fuel processor, generates hydrogen-rich gas from the supply fuel and removes poisons from the fuel stream. Poisoning and fuel flexibility are two major considerations when selecting a fuel cell. Nitrogen, phosphorous, arsenic, antimony, oxygen (in specific instances), sulfur, selenium and tellurium (Group VA and VI A on the Periodic Table) are typical poisons for fuel cells. Table 4.4 displays the fuel requirements of each fuel cell type.

Table 4.4: Fuel Requirements for Fuel Cells (Laramie, et al., 2003)

Gas Species	PEMFC	PAFC	MCFC	SOFC
H_2	Fuel	Fuel	Fuel	Fuel
CO	Poison (>10 ppm)	Poison (>0.5%)	Fuel	Fuel
CH_4	Diluent	Diluent	Diluent	Diluent
CO_2 and H_2O	Diluent	Diluent	Diluent	Diluent
S (as H_2S and COS)	Few studies, to date	Poison (>50 ppm)	Poison (>0.5 ppm)	Poison (>1.0 ppm)

Fuel reformers are needed because the fuel is often in the form of hydrocarbons, such as methane, and the hydrogen concentration is not at a level suitable for operation. The fuel cell “stack” consists of layers of the cathode, anode, and electrolyte mentioned earlier. A power conditioner converts the direct current (DC) electricity generated by the fuel cell into alternating current (AC) electricity at the appropriate voltage and frequency.

Fuel cells are categorized by the electrolyte used to transport ions between the cathode and the anode (or vise versa). Fuel cell technologies include molten carbonate (MCFC), alkaline (AFC), proton exchange membrane (PEMFC), solid oxide (SOFC), direct methanol (DMFC), and phosphoric acid (PAFC). While PEMFC are arguably the most advanced of the fuel cell technologies, the low operating temperatures are not ideal for CHP applications, particularly if the waste heat is required to drive thermally activated components. Because high temperature or high quality waste is heat needed for m-CHP applications, the solid oxide (SOFC) and the molten carbonate (MCFC) configurations are two likely candidates. Direct methanol fuel cells also hold some potential because a hydrogen reformer is not required, thereby reducing the system costs. Currently, the PEMFC and the SOFC are regarded as having the most potential for m-CHP. Table 4.5 shows the characteristics of the five major types of fuel cell technologies.

Table 4.5: Characteristics of Fuel Cells (http://www.oit.doe.gov)

	Alkaline (AFC)	Proton Exchange Membrane (PEM)	Phosphoric Acid (PAFC)	Molten Carbonate (MCFC)	Solid Oxide (SOFC)
Electrolyte	Alkaline lye	Perfluorated sulphonated polymer	Stabilized phosphoric acid	Molten carbonate solution	Ceramic solid electrolyte
Typical Unit Sizes (kW)	<<100	0.1-500	5-200 (plants up to 5,000)	800-2000 (plants up to 100,000)	2.5-100,000
Electric Efficiency	Up to 70%	Up to 50%	40-45%	50-57%	45-50%
Installed Cost ($/kW)		4,000	3,000-3,500	800-2,000	1,300-2,000
Commercial Availability	Not for CHP	R&D	Yes	R&D	R&D
Power Density lbs/kW ft^3/kW		8-10 ~0.2	~25 0.4	~60 ~1	~40 ~1
Heat Rejection (Btu/kWhr)		1640 @ 0.8 V	1880 @0.74V	850 @0.8V	1780 @0.6V
Electric/ Thermal Energy		~ 1	~ 1	Up to 1.5	Up to 1.5
Oxidation Media	Oxygen	Oxygen from Air	Oxygen from Air	Oxygen from Air	Oxygen from Air
Cooling Medium		Water	Boiling Water	Excess Air	Excess Air
Fuel	H_2	H_2 and reformed H_2	H_2 reformed from natural gas	H_2 and CO reformed from natural gas or coal gas	H_2 and CO reformed from natural gas or coal gas
Operating Temp (F)	160-210	120-210	320-410	1250	1500-1800
Operating Pressure (psig)		14.7-74	14.7-118	14.7-44	14.7->150
Applications	Space and military (today)	Stationary power (1997-2000) Bus, railroad, automotive propulsion (2000-2010)	Stationary power (1998) Railroad propulsion (1999)	Stationary power (2000->2005)	Stationary power and railroad propulsion (1998->2005)

PEMFC

Proton exchange membrane fuel cells (PEMFC) use an ion-conducting polymer as the electrolyte. The electrolyte works well at low temperatures, typically around 175 – 212 F (80 – 100 C), which allows for fast start-up. The

polymer membrane construction varies depending on manufacturer; however a standard practice uses a modified polymer known as polytetrafluoroehtylene (PTFE), or as it is commonly know, Teflon®. Because the electrolyte is a solid polymer, electrolyte loss is not an issue with regard to stack life. Most PEMFC's use platinum as the catalyst for both the anode and the cathode. Hydrogen is used as the fuel at the anode, and air or oxygen is supplied to the cathode. The reactions that occur within a generic PEMFC are as follows:

$$\text{Anode Reaction:} \quad H_2 \Leftrightarrow 2H^+ + 2e^-$$
$$\text{CathodeReaction:} \quad O_2 + 4H^+ + 4e^- \Leftrightarrow 2H_2O$$
$$\text{Overall Reaction:} \quad 2H_2 + O_2 \Leftrightarrow 2H_2O$$

The electrode reactions are shown in Figure 4.37. Hydrogen ions and electrons are produced from the fuel gas at the anode. The hydrogen ions travel through the electrolyte to the cathode. Electrons pass through an outside circuit to join the hydrogen ions and oxygen atoms at the cathode to produce water and product gases. The solid electrolyte does not absorb the water. The operation of a PEMFC requires a certain level of water be maintained in the stack; however, too much water, or a "flood" of water, will shut the fuel cell down. The optimum water level creates water management issues in that the amount of water remaining in the fuel cell stacks and the amount of water rejected must be carefully controlled.

The primary advantage of the PEMFC is that extensive development has resulted in increased electrical efficiency and decreased size and material requirements. However, there are several disadvantages of using a PEMFC for

m-CHP applications. The operating temperature is too low to drive the thermally activated components of the m-CHP system. Water management and humidity control are critical issues in the operation of a PEMFC. There must be sufficient water content in the polymer electrolyte as the proton conductivity is directly proportional to the water content. However, there must not be so much water that the electrodes are bonded to the electrolyte, blocking the pores in the electrodes or the gas diffusion layer. Also, due to poisoning issues, relatively pure hydrogen is needed at the anode and a hydrogen reformer is necessary, which increases the overall costs of the system.

The American Council for an Energy Efficient Economy (ACEEE) Emerging Technologies & Practices (2004) performed a theoretical study on a residential CHP system using a 2-kW PEMFC as the power generation device. The economics indicated that with the estimated costs of the PEMFC unit and maintenance cost, the cost of the electricity generated would be $0.18/kWh. Therefore the installation of the 2-kW PEMFC unit would only be advantageous in an area that has an electrical cost higher than $0.18/kWh, or in an area where grid electricity is unavailable.

Thermally activated components were included only implicitly in the study, and the systems were not sized large enough to have excess power either to store or sell to the electricity grid. The study listed several major market barriers: dwindling natural gas supplies, introducing and integrating a new technology and

overcoming the inertia of the established market, and uncertain system reliability. Also to be considered is how and who will provide system maintenance.

The Entergy Centre of the Netherlands (ECN) experimented with a 2 kW PEMFC m-CHP system. The system uses natural gas, and the fuel cell operates at approximately 65 C. For system operation, natural gas is desulphurised and converted to hydrogen rich gas in the reformer. The study showed that a start-up time of 2.5 hours was needed when starting from cold conditions to steady operating conditions where the rejected heat could be used to aid the reforming process. This start-up time was reduced to 45 minutes when transitioning from hot stand-by conditions. Characteristics demonstrated by the system include:

- Gross (electrical + thermal) efficiency of fuel processor varies from 70% at 1 kW to 78% at full load (10 kW)
- Stack electrical conversion efficiency of 40% at 2 kW and 42% at 1 kW
- Recovered 53% of the waste heat (LHV basis)

The results of this study predicted a payback period of five years for a 1 kW m-CHP system costing 1000 – 1500 EUR ($1300 - $2000), taking into account the market value of Dutch natural gas, electric rates in the Netherlands, and local energy tariffs. *Note that system costs of $1300-$2000 is a theoretical value the manufacturers hope to achieve*.

SOFC

Solid oxide fuel cells use an oxide ion-conducting ceramic material as the electrolyte. The anode of a SOFC is usually a cermet composed of nickel and

yttria-stabilised zirconia. A cermet is a mixture of ceramic and metal. The cathode is a porous structure typically made of lanthanum manganite. All of the materials used to construct a SOFC are solid state. SOFC's operate in the temperature range of 800 – 1100 C. Either hydrogen or methane can be supplied at the anode, and a SOFC can accommodate both oxygen and air at the cathode. The reactions that occur within a generic SOFC are illustrated in Figure 4.40.

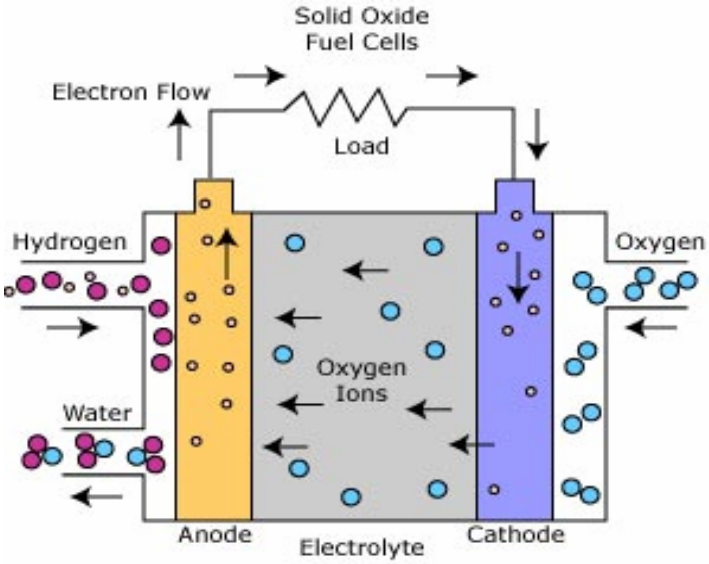

Figure 4.40: SOFC Reactions (http://www.fctec.com/fctec)

The reactions that occur within a generic SOFC are as follows:

Anode Reaction: $H_2 + O^{2-} \Leftrightarrow H_2O + 2e^-$

$CO + O^{2-} \Leftrightarrow CO_2 + 2e^-$

$CH_4 + 4O^{2-} \Leftrightarrow 2H_2O + CO_2 + 8e^-$

Cathode Reaction: $O_2 + 4e^- \Leftrightarrow 2O^{2-}$

Overall Reaction: $2H_2 + O_2 \Leftrightarrow 2H_2O$

In the SOFC reactions, hydrogen or carbon monoxide in the fuel stream reacts with oxide ions traveling through the electrolyte. These reactions produce water and carbon dioxide and disperse electrons to the anode. The electrons pass through the exterior load and return to the cathode. At the cathode, the electrons are used to ionize the oxygen molecules from the air. The oxide ions then enter the electrolyte and the process begins again.

Solid oxide fuel cells have several advantages from an m-CHP point of view. First, the high operating temperatures are attractive for driving thermally activated components and for heating domestic hot water. The construction negates any electrolyte management issues or water management difficulties. The presence of nickel at the cathode can be used as an internal reforming catalyst, eliminating the need for a reformer and reducing system cost.

The SOFC has challenges and disadvantages. The high temperatures result in construction and material difficulties. The elevated temperatures also decrease the open-circuit voltage achieved by a SOFC because the Gibbs free energy of formation of the products (water) tends to be less negative. The reduced open-circuit voltage leads to a decrease in electrical efficiency. However, the advantage of the quality of the waste heat overcomes the small decrease in the system efficiency.

Solid oxide fuel cells hold perhaps the most promise for m-CHP applications. The European Commission has recognized the natural gas powered, high-temperature fuel cell as being among the most efficient and

environmentally friendly means of achieving distributed cogeneration. Several m-CHP systems using SOFC technology have been developed and tested. Ceramic Fuel Cells Limited (CFCL) has been developing flat plate SOFC technology for thirteen years. In 2004 CFCL announced an all-ceramic stack design capable of volume fabrication for a 1-kW m-CHP fuel cell system targeting the residential market. The SOFC stack developed by CFCL has been designed with commercial requirements in mind. The stack has the ability to reform fuel at the anode without the use of an external reformer and operates at temperatures of 1470 – 1600 F (800 – 870 C). The SOFC stack utilizes a modular design that allows stacks to be arranged in parallel to generate power in a range of 1 – 10 kW.

An example of an SOFC installed for residential m-CHP use is at the Canadian Centre for Housing Technology in Ottawa. The unit is a 5-kW system that operates on natural gas, using a tubular arrangement developed by Siemens Westinghouse Power Corporation. The unit has the ability to use low fuel pressures which decreases operational costs. The system also includes an inverter that meets residential standards and output control that allows the system to output/receive electricity to the grid. The SOFC unit has been placed in a research house that incorporates simulated occupancy and an “intensively monitored real world environment.” Researchers intend to monitor heating, ventilation, and air-conditioning conditions to develop methods for better controls systems and grid connections.

The Energy Research Centre of the Netherlands (ENC) has also experimented with the use of a 1-kW SOFC m-CHP unit. The system operates with an HXS 1000 Premiere fuel cell system installed in September 2002. The unit has a thermal output of 2.5 kW and is equipped with an auxiliary heater. The unit is fueled by natural gas, and the operating temperature is approximately 900 C. The SOFC cells are manufactured by InDEC and are arranged in a stack assembly. The system is pictured in Figure 4.41.

A.Thermal insulation
B.SOFC stack
C.Heat Exchanger
D.Heat storage tank (200 l)
E.Process control unit
F.Auxiliary burner
G.DC/AC inverter
H.Desulphurisation unit
I. Exhaust line

Figure 4.41: SOFC Stack Assembly (one cell shown) (Oosterkamp, et. al)

The operation of the system begins with the desulphurization of the natural gas which is mixed with de-ionized water vapor. The mixture is internally reformed at the anode, and carbon monoxide and hydrogen are consumed at the anode. Waste heat is recovered by the combustion of the mixture of anode “off

gas" (water vapor and carbon dioxide) and cathode exhaust. The combustion provides sensible heat to the storage vessel. (Oosterkamp, et. al)

The SOFC m-CHP system operates in a heat following mode and has demonstrated the following performance:

- Electrical efficiency of 25-32% at full load
- Thermal efficiency of 53-60% on LHV basis
- Total efficiency of approximately 85%

However, the study also found that the electrical efficiency does decrease over time. The efficiency decrease is rather fast for strongly dynamic system operation, but is also noticeable for a more stable and steady operation.

PAFC

Phosphoric acid fuel cells are generally considered the "first generation" technology. PAFC fuel cells typically operate at a temperature of 390 F (200 C) and can achieve 40 % to 50 % fuel to electrical efficiencies on a lower heating value basis (LHV). The PAFC operates similar to the PEMFC. The PAFC uses a proton-conducting electrolyte (phosphoric acid), and the reactions occur on highly-dispersed electrocatalyst particles supported on carbon black. Phosphoric acid (H_3PO_4) is the only common inorganic acid that has enough thermal, chemical, and electrochemical stability and low volatility to be considered as an electrolyte for fuel cells. Typically, platinum is used as the catalyst at both the anode and cathode. The reactions that occur within a generic PAFC are as follows:

Anode Reaction: $H_2 \Leftrightarrow 2H^+ + 2e^-$

Cathode Reaction: $O_2(g) + 4H^+ + 4e^- \Leftrightarrow 2H_2O$

Overall Reaction: $2H_2 + O_2 \Leftrightarrow 2H_2O$

In the PAFC reactions, hydrogen is ionized at the anode to produce two hydrogen ions and two electrons. The hydrogen ions pass through the electrolyte to the cathode while the electrons travel through a load in an external circuit. At the cathode, the hydrogen ions, electrons, and oxygen react to form water. The reactions that occur in the PAFC are shown in Figure 4.42.

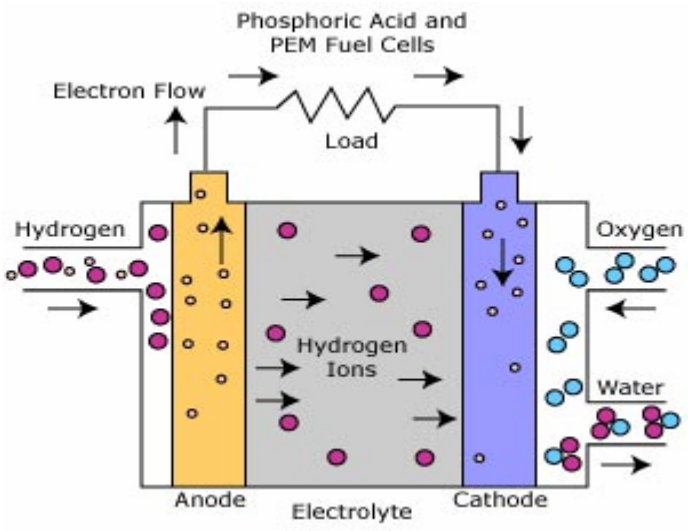

Figure 4.42: PAFC Reactions (http://www.fctec.com/fctec)

The PAFC has experienced success in the large-scale CHP arena and holds potential for the m-CHP market. However, currently few manufacturers are pursuing development of PAFC m-CHP based system but have expressed more interest in the SOFC and PEMFC fuel cells. One reason for manufacturers' lack of interest in PAFC fuel cells is that the PAFC fuel cell uses only pure hydrogen

as fuel and other fuel cell types have the capability to utilize a fuel other than a pure hydrogen stream. This selection could also result from potential hazards the electrolyte (phosphoric acid) could pose to inhabitants in the event of a leak. The PAFC requires an external fuel reformer, increasing the production cost.

MCFC

Molten Carbonate Fuel Cells (MCFC) are high-temperature fuel cells and promise the highest fuel-to-electricity efficiencies for carbon based fuels. The higher operating temperature allows the MCFC's to use natural gas directly without the need for a fuel reformer. MCFC have also been used with low-Btu fuel gas from industrial processes and other fuel sources. Developed in the mid 1960s, improvements have been made in fabrication methods, performance and endurance.

The MCFC operates differently than the fuel cells previously discussed. MCFC's use an electrolyte composed of a molten mixture of alkali metal carbonate salts, which is retained in a ceramic matrix of $LiAlO_2$. Two mixtures are currently used: lithium carbonate and potassium carbonate or lithium carbonate and sodium carbonate. To melt the carbonate salts and achieve high ion mobility through the electrolyte, MCFC's operate at temperatures of 600-700 C. When heated to a temperature of around 650 C, the salts melt and become conductive to carbonate ions (CO_3^{2-}). These ions flow from the cathode to the anode where they combine with hydrogen to give water, carbon dioxide and

electrons. Electrons are routed through an external circuit back to the cathode, generating electricity and by-product heat.

Unlike other fuel cells, carbon dioxide as well as oxygen needs to be delivered to the cathode. The carbon dioxide and oxygen react to form carbonate ions, which provide the means of ion transfer between the cathode and anode. At the anode, the carbonate ions are converted back into carbon dioxide. There is a net transfer of CO_2 from the cathode to the anode; one mole of CO_2 is transferred for every two moles of electrons. The operation of a MCFC is illustrated in Figure 4.43. The reactions occurring in the MCFC are

$$\text{Anode Reaction:} \quad CO_3^{2-} + H_2 \Leftrightarrow H_2O + CO_2 + 2e^-$$

$$\text{Cathode Reaction:} \quad CO_2(g) + \tfrac{1}{2} O_2 + 2e^- \Leftrightarrow CO_3^{2-}$$

$$\text{Overall Reaction:} \quad H_2 + \tfrac{1}{2} O_2 + CO_2(cathode) \Leftrightarrow 2H_2O + CO_2(anode)$$

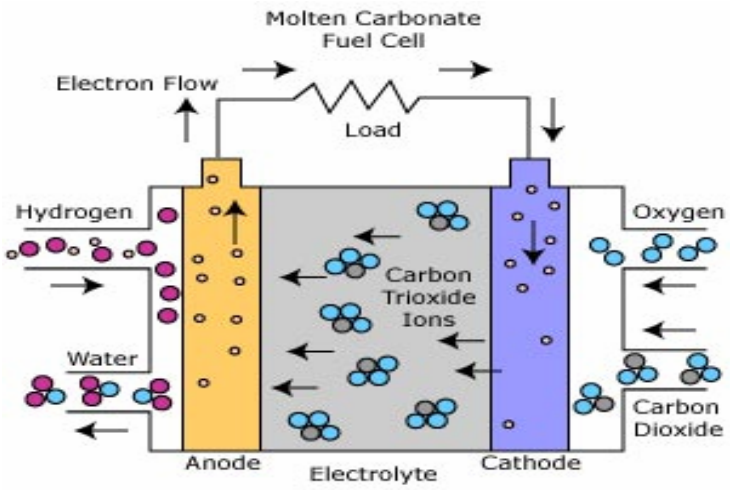

Figure 4.43: MCFC Reactions (http://www.fctec.com/fctec)

The higher operating temperature of the MCFC creates both advantages and disadvantages compared to fuel cells such as the PAFC and PEMFC with lower operating temperatures. The higher operating temperature allows fuel reforming of natural gas to occur internally, eliminating the need for a fuel reformer. The MCFC can also utilize standard materials for construction, such as stainless steel and nickel-based catalysts. The by-product heat from an MCFC can be used to generate domestic hot water, space heating and cooling, and even high-pressure steam.

The high operating temperatures and the electrolyte chemistry of the MCFC also lead to disadvantages. The high temperature requires significant time to reach operating conditions and correspondingly slow response time to changing power demands. These characteristics make the MCFC less attractive for dynamic power applications and restrict it to constant-power supply applications. The carbonate electrolyte can also cause electrode corrosion problems. Due to the use of the carbonate ions as the charge carrier, the supply of carbon dioxide to the cathode must be carefully controlled in order to achieve optimum performance.

Each fuel cell type has both advantages and disadvantages over its counterparts. The selection of the “best” fuel cell will depend upon the details of the application. An overview of fuel cell characteristics is given in Table 4.6.

Table 4.6: Overview of Fuel Cell Characteristics (www.energy.ca.gov/distgen/)

Fuel Cells Overview				
	PAFC	**SOFC**	**MCFC**	**PEMFC**
Commercially Available	Yes	Yes	Yes	Yes
Size Range	100-200 kW	1 kW - 10 MW	250 kW - 10 MW	3-250 kW
Fuel	Natural gas, landfill gas, digester gas, propane	Natural gas, hydrogen, landfill gas, fuel oil	Natural gas, hydrogen	Natural gas, hydrogen, propane, diesel
Efficiency	36-42%	45-60%	45-55%	25-40%
Environmental	Nearly zero emissions	Nearly zero emissions	Nearly zero emissions	Nearly zero emissions
Other Features	Cogen (hot water)	Cogen (hot water, LP or HP steam)	Cogen (hot water, LP or HP steam)	Cogen (80°C water)
Commercial Status	Some commercially available	Commercialization likely in 2004	Some commercially available	Some commercially available

Application

Fuel cells are being developed for stationary power in small commercial and residential markets and as peak shaving units for commercial and industrial uses. Some fuel cells, such as PEMFC, are currently undergoing development for use in automobiles and portable power applications.

Phosphoric acid fuel cells have been installed at medical, industrial, and commercial facilities throughout the country, and the 200-kW size is a good match for distributed generation applications. The operating temperature is about 400 F, which is suitable for co-generation applications. Developers are targeting commercial and light industrial applications in the 100-200 kW power range, for both electric-only and cogeneration applications.

The high efficiency and high operating temperature of MCFC units makes them most attractive for base-loaded power generation, either in electric-only or

cogeneration modes. Potential applications for the MCFC are industrial, government facilities, universities, and hospitals.

Solid oxide fuel cells are being considered for a wide variety of applications, especially in the 5 – 250 kW size range. These applications include small commercial buildings, industrial facilities, m-CHP, and base load utility applications.

Proton exchange membrane fuel cells are currently undergoing the most rapid development of any fuel cell type. Part of this development has been driven by the desire of automotive manufacturers to develop a fuel cell powered automobile. This surge in development has led to breakthroughs for stationary power applications as well. Research is aimed at commercial-sized power generation (e.g., Ballard's 250 kW unit) and residential power generation (e.g., Plug Power's 3-5 kW units). For the units to achieve market potential, natural gas is selected as the fuel of choice. Reject system heat in the form of hot water makes them particularly attractive for cogeneration, which is included in almost all products currently under development.

Heat Recovery

The type of fuel cell determines the temperature of the heat rejected during operation and directly influences the fuel cell type’s suitability for m-CHP applications. Low temperature fuel cells create waste heat suitable for producing hot water and in some cases, low pressure steam. Lower temperature fuel cells such as the PAFC and PEMFC produce lower quality waste heat and are

suitable for small commercial and industrial cogeneration applications. The MCFC and the SOFC operate at high temperatures and are capable of producing waste heat that can be used to generate steam for use in a steam turbine, or combined cycle microturbine. If space cooling is considered and an absorption chiller is to be used, the recaptured heat should be at a temperature of at least 185 F (85 C).

Cost

The initial cost of fuel cells is higher than those of other electricity generation technologies. The only product available commercially today is the PureCell 200 (formerly PC-25)™ built by UTC Power. The cost of the unit is approximately $4,000/kW. The installed cost of the unit approaches $1.1 million. At a rated output of 200 kW, this translates to about $5,500/kW, installed. However, on January 3, 2005, Delphi Corp., in partnership with the DOE's advanced fuel cell development program, reported that researchers have exceeded the government's $400/kW power cost goal for fuel cells. At this price, fuel cells could compete with traditional gas turbine and diesel electric generators and become viable power suppliers for the transportation sector. Table 4.7 shows the uninstalled projected long-term costs of fuel cell technologies. The price of $400/kW is not included in Table 4-7 as the information was only recently released and currently, the development has not been proven for production costs in a fuel cell of substantial size.

Table 4.7: Projected Long-Term Costs of Fuel Cell Technologies (www.energy.ca.gov/distgen/)

Emerging Fuel Cell Technologies	
Technology	**Projected Cost (Long-term, Uninstalled)**
MCFC	$1,200-1,500/kW
SOFC	$1,000-1,500/kW
PEMFC	Initially $5,000/kW Long term $1,000/kW

As no combustion is occurring, and there are no moving parts, fuel cells are expected to have minimal maintenance requirements. The primary maintenance will be focused on preventing poisoning of the catalyst and periodic inspection and maintenance to the fuel supply system and fuel reformers. The cell stack itself will not require maintenance until the end of its service life. The maintenance and reliability of the system still needs to be proven in a long-term demonstration. Maintenance costs of a fuel cell are expected to be comparable to that of a microturbine, ranging from $0.005-$0.010/kWh (based on an annual inspection visit to the unit). (http://www.energy.ca.gov/distgen/)

Advantages and Disadvantages

Each fuel cell type will have advantages and disadvantages in certain areas, both as compared to other fuel cell technologies and other DER equipment. Table 4.8 displays some of the advantages of the four primary types of fuel cells.

Fuel cells convert chemical energy directly into electricity without the combustion process. As a result, a fuel cell does not incur losses resulting from mechanical inefficiencies. Fuel cells can achieve high efficiencies in energy conversion terms, especially where the waste heat from the cell is utilized in cogeneration. A high power density allows fuel cells to be a relatively compact source of electric power, a benefit in applications with space constraints. In a fuel cell system, the fuel cell itself is often smaller than the other components of the system such as the fuel reformer and power inverter.

Fuel cells, due to their nature of operation, are extremely quiet in operation. This allows fuel cells to be used in residential or built-up areas where the noise pollution is undesirable. Unfortunately, the primary disadvantage of the fuel cells is the cost. The two basic reasons are high component costs compared to other energy systems technology and fuel cell operation requires a continuous, highly selective, expensive fuel supply.

Table 4.8: Advantages and Disadvantages of Fuel Cell Types (www.energy.ca.gov/distgen/)

PAFC	
Advantages	**Disadvantages**
Quiet	High Costs
Low emissions	
High efficiency	Low energy density
Proven reliability	
PEMFC	
Advantages	**Disadvantages**
Quiet	High Costs
Low emissions	
High efficiency	Limited field test experience
Synergy with Automotive R&D	Low temperature waste heat may limit cogeneration potential
SOFC	
Advantages	**Disadvantages**
Quiet	High Costs
Low emissions	
High efficiency	Planar SOFC's are still in the R&D stage but recent developments in low temperature operation show promise
High energy density	
Self reforming	
MCFC	
Advantages	**Disadvantages**
Quiet	High Costs
Low emissions	
High efficiency	Need to demonstrate long term reliability
Self reforming	

Exercises

1. A SOFC fuel cell has liquid water as a product when it operates at 700 K. What is the maximum work that the fuel cell can achieve per mole of reactant?

2. For the SOFC of problem 1, what is the thermal efficiency?

3. If the PEMFC of Example 4-5 has current and voltages efficiencies of 80%, what is the electrical conversion efficiency of the fuel cell?

3. A MCFC has liquid water and carbon dioxide as the products when is operates at 400 K. What is the maximum work that the fuel cell can achieve and what is the thermal efficiency?

4. What is the thermal efficiency and the maximum work that a PAFC can achieve when operating at 373 K and liquid water is the product?

6. A PEMFC operating at 298 K produces liquid water. If the current efficiency and voltage efficiencies are 75% and 85%, respectively, determine the electrical conversion efficiency of the fuel cell.

Manufacturers

- Ceramic Fuel Cells Limited (CFCL) of Victoria, Australia, develops and manufactures SOFC based m-CHP units. Figures 4.44 and 4.45 show a 1-kW m-CHP demonstration unit and CFCL's 5-kW concept unit, respectively.

Figure 4.44: CFCL 1-kW Technology Demonstrator System (http://www.cfcl.com.au/html/)

Figure 4.45: CFCL's 5-kW m-CHP Concept Unit (http://www.cfcl.com.au/html/)

- Plug Power of Latham, New York manufactures fuel cell units for continuous, standby, and emergency applications with two lines of fuel cells, GenSys and GenCore. GenSys systems provide continuous power supply. GenCore systems provide standby power for buildings.

Figure 4.46: Plug Power Fuel Cell Unit (www.plugpower.com)

- Baxi Technologies, of the Baxi Group produces a m-CHP fuel cell unit. Baxi's networkable fuel cell produces 1.5 kW of electrical output, 3 kW of thermal output, and includes a 15-kW integral boiler. The beta unit shown in Figure 4.47 is 1.7 m high.

Figure 4.47: Baxi Technology 1.5-kW m-CHP Fuel Cell Unit (www.baxitech.co.uk)

CHAPTER V:

HEAT RECOVERY

Electrical power generation devices do not convert 100% of an energy source potential into usable energy. Electrical efficiencies of reciprocating engines, microturbines, Stirling engines, and fuel cells are about 50%, 30%, 30%, and 60%, respectively. This means that the electrical power generation devices fail to utilize 40% - 70% of the available energy. Energy that is not converted to electrical or shaft power is rejected from the process in the form of waste heat. In order to utilize more of the energy stored in a given fuel and increase the overall thermal efficiency of a system, heat recovery must be incorporated into a system. Heat recovery converts waste heat to useful energy and is primarily accomplished through the use of heat exchangers.

Distributed energy generation prime movers possess waste heat that can be recovered as useful energy. The type of prime mover determines the characteristics of the waste heat and the effectiveness with which useful energy can be recovered. Waste heat is typically released in the form of hot exhaust gases, process steam, or process liquids/solids. The usable temperature for heat recovery is listed for various prime movers in Table 5.1. Potential uses for the waste heat are hot water, space heating and cooling, and process steam.

Table 5.1: Waste Heat Characteristics of Prime Mover Technologies

	Usable Temp. for m-CHP (°F)
Diesel Engine	180 - 900
Natural Gas Engine	300 - 500
Stirling Engine	800 - 1000
Fuel Cell	140 - 750
Microturbine	400 - 650

Recovered heat that is utilized in the power generation process is internal heat recovery, and recovered heat that is used for other processes is external heat recovery. Recuperators, turbochargers, and combustion pre-heaters are examples of internal heat recovery. Absorption chillers, desiccant dehumidification devices, and heat recovery steam generators are examples of external heat recovery components. Recovered heat is classified as low-temperature when less than 445 F (<230 C), medium-temperature 445 F – 1202 F (230 C – 650 C), or high-temperature when greater than 1202 F (>650 C). The majority of heat exchangers used in m-CHP are used for external heat recovery.

Technology Overview

Because combustion exhaust gases or process liquids cannot be used directly in many applications, heat exchangers are used to facilitate the transfer of waste heat thermal energy to heat recovery applications. Devices that transfer energy between fluids at different temperatures by heat transfer modes are known as heat exchangers. Heat exchangers come in a wide variety of sizes, shapes, and types and utilize a wide range of fluids. Applications for heat exchangers are vast, ranging from heating and air-conditioning systems, to

chemical processing and power production in large plants. Heat exchanger classification is based upon component and fluid characteristics. Several classification schemes have been proposed for heat exchangers. Hewitt et al. suggests the following four-tiered system:

1. Recuperator/Regenerator
2. Direct-contact/Transmural heat transfer
3. Single phase/Two-phase
4. Geometry

A recuperator is based on a continuous transfer of heat between two fluid streams. A regenerator is a device which uses a heat-absorbing material, alternately cooled and heated in a batch mode, to transfer heat between two streams; these are often rotary devices. Direct-contact heat exchangers, such as a feedwater heater used in a power plant, allow the two fluids to come into contact with each other. Transmural heat exchangers separate the two fluid streams using a wall or series of walls. Single phase/two-phase refers to the physical state of the fluids flowing in the heat exchanger. Single-phase flow implies that both fluids are either completely gaseous or liquid. If evaporation or condensation is taking place, the device involves two phases. Geometry refers to the basic shape of the heat-exchanger passages that contain the fluid.

This section will focus on transmural recuperators with fluids in single-phase; however, other arrangements will also be discussed. Transmural

recuperators with single-phase flow can be divided further by flow arrangement into the following categories:

- Counterflow
- Cross-flow
- Parallel flow

Counterflow and parallel flow tube-within-a-tube and cross-flow configurations are shown in Figure 5.1.

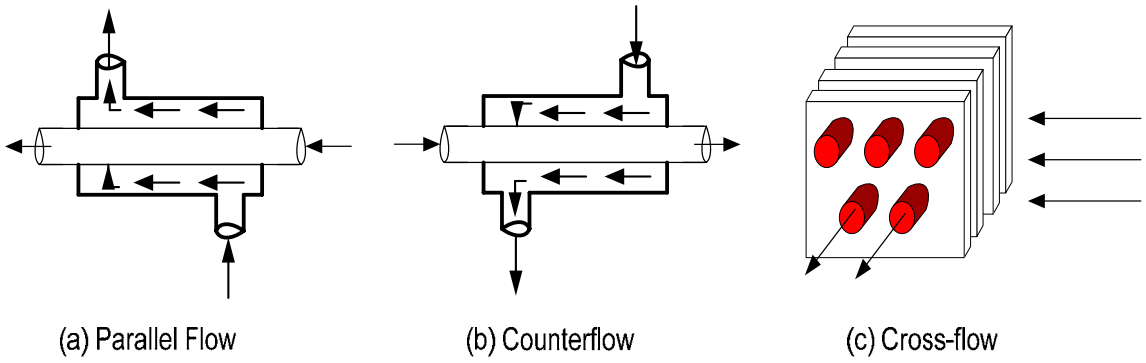

Figure 5.1: Main Types of Transmural Recuperators with Fluids in Single-phase

The temperature versus area diagrams for the parallel flow and counterflow arrangements are shown in Figure 5.2. In the parallel arrangement, the fluid temperatures approach each other so that the temperature difference ΔT_1 is much greater in magnitude than ΔT_2. If the length of the heat exchanger were extended long enough in parallel flow, the exit temperatures of each of the fluids would be approximately equal. The counterflow average ΔT will be larger than the parallel flow average ΔT.

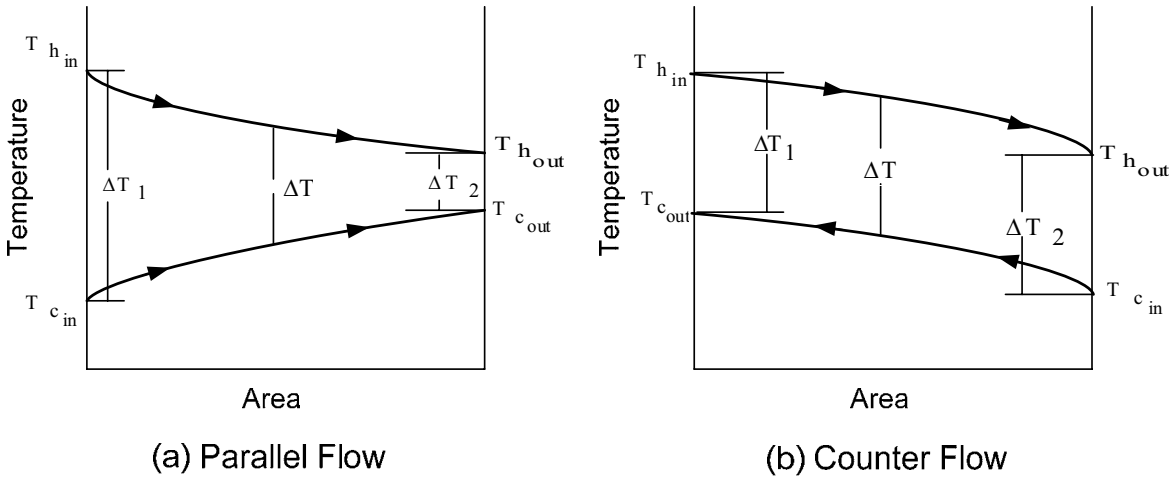

Figure 5.2: Temperature-area Diagram of Parallel and Counterflow Arrangements

Cross-flow heat exchangers are arranged so that the two fluids flow perpendicular to each other as shown in Figure 5.3. An important concept when discussing cross-flow heat exchangers is *mixing*. A fluid is said to be *unmixed* if the passageway contains the same discrete portion of fluid throughout its traverse of the exchanger. If the fluid passageways are such that fluid from one passageway can mix with fluid from others, the fluid is *mixed*. In Figure 5.3, mixed and unmixed arrangements are illustrated. Cross-flow heat exchangers are classified as both fluids unmixed, both fluids mixed, or one fluid mixed and one fluid unmixed.

When several tubes are placed inside a shell, the classical single-pass shell-and-tube heat arrangement results. A schematic of a shell-and-tube heat exchanger with one shell pass and one tube pass is illustrated in Figure 5.4.

Baffles are often placed inside a shell-and-tube heat exchanger to promote higher heat transfer rates and increase the effectiveness of the heat exchanger.

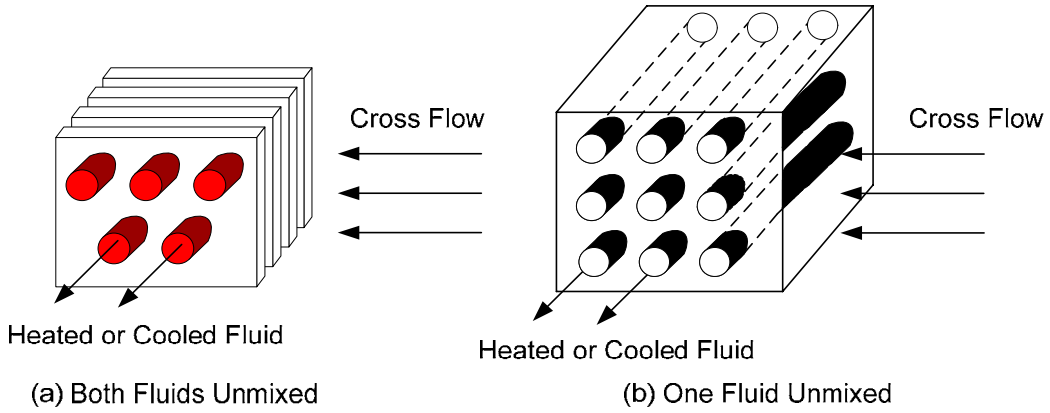

Figure 5.3: Cross-flow Heat Exchangers

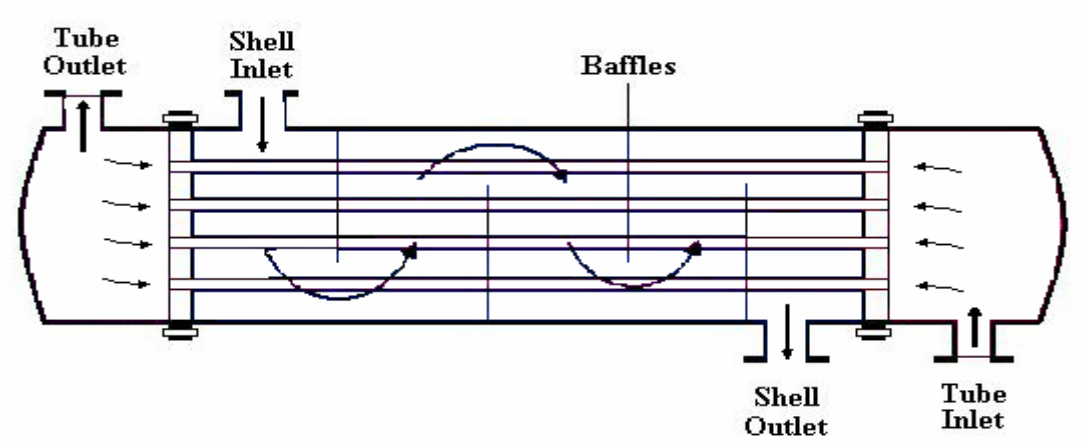

Figure 5.4: Shell-and-tube Heat Exchanger

Heat Exchanger Analysis

Heat transfer in a heat exchanger usually involves *convection* in each fluid and *conduction* through the walls separating the two fluid streams. The two methods used to design or analyze heat exchangers are the Log-Mean

Temperature Difference (LMTD) method and the Number of Transfer Units (NTU) method.

The LMTD method utilizes a log mean temperature, the effective average temperature across the length of the heat exchanger. The heat transfer rate between two fluids separated by a surface is

$$\dot{q} = UA \cdot (\overline{T_h - T_c}) = UA \cdot \overline{\Delta T} \tag{5-1}$$

where the log mean temperature difference ($\overline{\Delta T}$) is

$$\overline{\Delta T} = \frac{\Delta T_2 - \Delta T_1}{\ln\left(\Delta T_2 / \Delta T_1\right)} \tag{5-2}$$

The temperature differences ΔT_1 and ΔT_2 are the same temperature differences represented in Figure 5.2. The UA in Equation (5-1) is known as the *conductance* and is the product of the overall heat transfer coefficient (U) and the area (A) on which U is based.

The NTU method is derived around the formal definition of *effectiveness*. The heat exchanger effectiveness is defined as the ratio of the actual rate of heat transfer to the maximum possible rate of heat exchange.

$$\xi = \frac{\text{Actual Rate of Heat Transfer}}{\text{Maximum Possible Rate of Heat Transfer}} \tag{5-3}$$

The maximum possible rate of heat transfer would be obtained in a counterflow heat exchanger of infinite heat transfer area. In such a unit, the outlet temperature of the warmer fluid equals the inlet temperature of the colder fluid when $\dot{m}_h c_{p_h} < \dot{m}_c c_{p_c}$, and the outlet temperature of the colder fluid equals the

inlet temperature of the warmer fluid when $\dot{m}_c c_{p_c} < \dot{m}_h c_{p_h}$. $\dot{m}$ is the mass flow rate of each of the respective fluid, and c_p is the constant pressure specific volume of the respective fluids. The subscripts c and h are used to denote the cold and hot streams, respectively. The product $\dot{m} \cdot c_p$ is the capacity of the fluid.

The NTU method introduces the following definitions

$$C_h = \dot{m}_h c_{p_h} \tag{5-4}$$

$$C_c = \dot{m}_c c_{p_c} \tag{5-5}$$

$$C = \frac{C_{\min}}{C_{\max}} \tag{5-6}$$

with C_{min} being the smaller capacity and C_{max} the larger. Next, the number of transfer units (NTU) is defined as

$$NTU = \frac{UA}{C_{\min}} \tag{5-7}$$

The effectiveness is defined as

$$\xi = \frac{\dot{q}}{C_{\min}(T_{h_{in}} - T_{c_{in}})} \tag{5-8}$$

The effectiveness becomes

$$\xi = \frac{C_h(T_{h_{in}} - T_{h_{out}})}{C_{\min}(T_{h_{in}} - T_{c_{in}})} \tag{5-9}$$

$$\xi = \frac{C_c(T_{c_{out}} - T_{c_{in}})}{C_{\min}(T_{h_{in}} - T_{c_{in}})} \tag{5-10}$$

The rate of heat transfer is given by

$$\dot{q} = \xi \cdot C_{\min} (T_{h_{in}} - T_{c_{in}}) \quad (5\text{-}11)$$

The relationship between the effectiveness and NTU of different heat exchanger configurations can be derived analytically. Table 5.2 presents these relationships.

Another important issue when selecting heat exchangers is the effect of pressure drops. The pressure drop in a heat exchanger determines how much pumping power must be supplied to achieve the effective heat transfer. Excessive pressure drop can negate energy savings from thermal energy recovery. Also, many thermally activated components require a specific temperature and pressure at the inlet to perform their desired function. Performance data are available for heat exchangers that fit a wide variety of scenarios, but the scale and uniqueness of m-CHP present many new heat recovery scenarios.

Table 5.2: Summary of Effectiveness-NTU Relationships for Heat Exchangers

Exchanger Type	Effectiveness	NTU
Parallel Flow: single pass	$\xi = \frac{1-\exp[-NTU(1+C)]}{1+C}$	$NTU = -\frac{\ln[1-\xi(1+C)]}{1+C}$
Counterflow: single pass	$\xi = \frac{1-\exp[-NTU(1-C)]}{1-C\cdot\exp[-NTU(1-C)]}$	$NTU = \frac{1}{C-1}\ln\left(\frac{\xi-1}{\xi\cdot C-1}\right)$
Shell and tube (one shell pass, 2,4,6,etc., tube passes)	$\xi_1 = 2\left[1+C+\frac{1+\exp\left[-NTU(1+C^2)^{1/2}\right]}{1-\exp\left[-NTU(1+C^2)^{1/2}\right]}(1+C^2)^{1/2}\right]^{-1}$	$NTU = -(1+C^2)^{-1/2}\ln\left(\frac{E-1}{E+1}\right)$ $E = \frac{2/\xi_1 - (1+C)}{(1+C^2)^{1/2}}$
Cross flow (both streams unmixed)	$\xi \approx 1-\exp\left[\frac{1}{C}NTU^{0.22}\left[\exp(-C(NTU)^{0.78})\right]-1\right]$	
Cross flow (stream C_{min} unmixed)	$\xi = \frac{1}{C}\left\{1-\exp\left[-C\left[1-\exp(-NTU)\right]\right]\right\}$	$NTU = -\ln\left[1+\frac{1}{C}\ln(1-\xi\cdot C)\right]$
Cross flow (stream C_{max} unmixed)	$\xi = 1-\exp\left\{-\frac{1}{C}\left[1-\exp\left[-(NTU)(C)\right]\right]\right\}$	$NTU = -\frac{1}{C}\ln\left[C\ln(1-\xi)+1\right]$

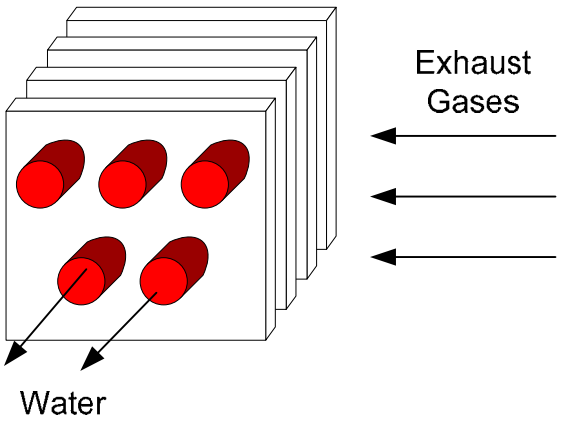

Figure 5.5: Cross-flow Heat Exchanger for Example 5-1

Example 5-1

A diesel engine driven generator is to be installed in an m-CHP system. In order to produce hot water, the hot exhaust gases are passed through a cross-flow heat exchanger with both fluids unmixed. The operating conditions are :

	Engine Exhaust	
Temperature (F)	300.0	65.0
Pressure (psia)	16.1	30.0
Flow rates (lbm/hr)	760.0	193.0
Density (lbm/ft^3)	0.0316	62.43
Specific Heat (Btu/lbm F)	0.251	1.003

If the conductance of the heat echanger is 2.0×10^3 Btu/lb*F, determine the effectiness of the heat exchanger and the exit temperature of the water.

The subscripts E and W will be used to denote the exhaust and water streams, respectively, and the subscripts 1 and 2 will be used to denote the entrance and exit conditions, respectively.

Input the given operating conditions

$T_{E1} := 300F \qquad T_{W1} := 65F \qquad m_E := 760\frac{lb}{hr} \qquad m_W := 193\frac{lb}{hr} \qquad UA := 2 \cdot 10^3 \frac{BTU}{hr \cdot F}$

The constant pressure specific heats of the respective streams are

$c_{pW} := 1.003\frac{BTU}{lb \cdot F} \qquad c_{pE} := 0.251\frac{BTU}{lb \cdot F}$

The thermal capacity of each fluid stream is calculated as

$C_E := m_E \cdot c_{pE} \qquad C_E = 190.76\frac{BTU}{hr \cdot F}$

$C_W := m_W \cdot c_{pW} \qquad C_W = 193.579\frac{BTU}{hr \cdot F}$

The maximum and minimum capacities are defined as

$C_{min} = 190.76\frac{BTU}{hr \cdot F} \qquad C_{max} = 193.579\frac{BTU}{hr \cdot F}$

Determine the capacity ratio.

$C := \frac{C_{min}}{C_{max}} \qquad C = 0.985$

Determine the number of transfer units (NTU) using the definition of NTU

$NTU := \frac{UA}{C_{min}} \qquad NTU = 10.484$

Determine the effectiveness of the heat exchanger using the effectiveness equation for a cross-flow heat echanger with both fluids unmixed found in Table 5-2.

$\xi := 1 - \exp\left[\frac{1}{C} \cdot NTU^{0.22} \cdot \left(\exp\left(-C \cdot NTU^{0.78}\right) - 1\right)\right] \qquad \xi = 0.817$

Figure 5.6: Example 5-1

Solving equation 5-9 for the exit temperature of the water,

$$T_{W2} := \frac{\xi \cdot C_{min} \cdot (T_{E1} - T_{W1})}{C_W} + T_{W1} \qquad T_{W2} = 254.194F$$

Figure 5.6 (continued)

Application

Waste heat recovery heat exchangers may be classified as gas-to-gas, gas-to-liquid, and liquid-to-liquid. The various types of these classifications are displayed in Figure 5.7.

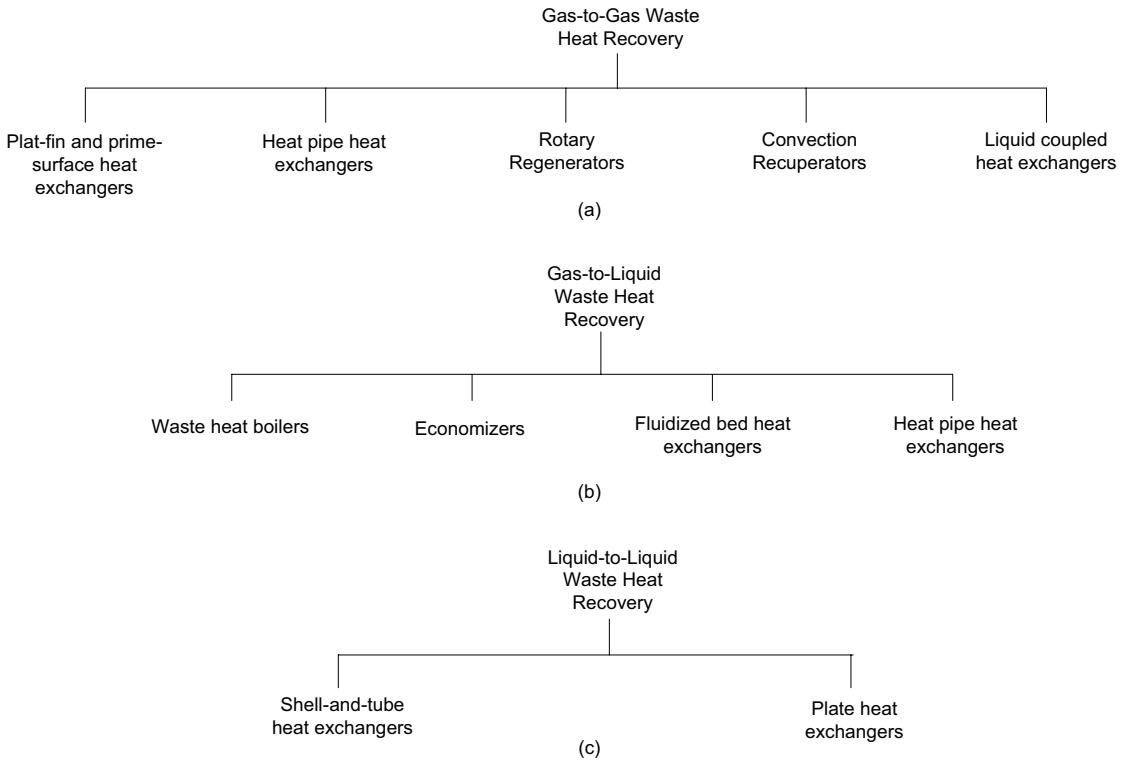

Figure 5.7: Classification of Waste Heat Recovery Heat Exchangers. (Recreated from the *CRC Handbook of Energy Efficiency*).

Gas-to-Gas Heat Exchangers

Gas-to-gas waste heat recovery exchangers can be used as recuperators to preheat combustion air in IC engines and microturbines. Rotary regenerators are often used in Stirling engines to recover and store heat. Gas-to-gas heat exchangers find many applications in m-CHP systems.

Metallic radiation recuperators, convection recuperators, and a runaround coil are the three primary types of gas-to-gas heat exchangers. A metallic radiation recuperator is a tube-in-tube heat exchanger that consists of two concentric metal tubes. Hot exhaust (flue) gas flows through the inner tube, and the air to be preheated flows through the outer tube or annulus. This type of recuperator can act as a part of a chimney, flue, or exhaust line. The majority of the heat is transferred from the hot gas to the inner wall through radiation. The heat transfer in the outer tube then takes place through convection. Air and gas flowing in counterflow is the most desirable arrangement because this arrangement has a high performance. Metallic radiation recuperators typically achieve an effectiveness of 40% or lower. Though metallic radiation recuperators could be used in m-CHP applications, their use will likely be limited by the relatively low effectiveness which would result in large heat exchangers.

Convection recuperators are cross-flow heat exchangers with flue gases flowing normal to a tube bundle with air to be preheated flowing in the tubes. Convection recuperators can be used in low-temperature applications such as

space heating, direct-fired absorption chillers, or return air heating in a desiccant dehumidification system.

A runaround coil consists of two connected heat exchangers that circulate a working fluid. The working fluid is heated by the waste gas with one heat exchanger and then circulated to the other heat exchanger where the fluid heats a stream of cool air. Runaround coils are used in HVAC applications and can be coupled with distributed generation components to produce warm air for district heating, to heat return air for desiccant dehumidification devices, or to fire an absorption chiller (Shah, 1997).

Gas-to-Liquid Heat Exchangers

Gas-to-liquid heat exchangers include economizers, waste heat boilers, heat-pipe heat exchangers, fluidized-bed, and thermal fluid heaters. Economizers and thermal fluid heaters are used for low- to medium-temperature waste heat recovery while waste heat boilers, heat-pipe heat exchangers, and fluidized bed heat exchangers are used for medium- to high-temperature heat recovery. Economizers are most often used with boilers to preheat the boiler feedwater. In other applications, economizers are referred to as a process fluid or water heaters. An economizer is an individually finned-tube bundle, with gas flowing outside normal to the finned tubes and water flowing inside the tubes.

Thermal fluid heaters are double-pipe heat exchangers that use waste heat gases to heat a high-temperature organic heat transfer fluid. Thermal fluid heaters operate on the same principle as a domestic warm-water system, except

that the water is replaced by a high-temperature organic heat transfer fluid. The heat transfer fluid can be circulated and used for heating and heat-driven absorption chillers.

Fluidized-bed heat exchangers utilize water, steam, or another heat transfer fluid heated by waste heat gases that flow over a bed of finely divided solid particles. As the waste heat fluid reaches a critical velocity, the particles begin to float, and the resulting mixture acts as a fluid.

Economizers and thermal fluid heaters are more likely to be used in m-CHP systems than either boilers or fluidized-bed heat exchangers due to the amount of thermal energy available for heat recovery and the size requirements of fluidized-bed heat exchangers. Process steam is also less likely to be needed for m-CHP applications, eliminating the need for waste heat boilers.

Liquid-to-Liquid Heat Exchangers

Liquid-to-liquid waste heat recovery heat exchangers are typically used in industrial applications. Shell-and-tube heat exchangers and plate heat exchangers are typically used for liquid-to-liquid heat recovery. Liquid coolant systems in reciprocating engines offer liquid-to-liquid heat recovery opportunities from hot oil and other liquid coolants. However, liquid-to-liquid heat recovery will not be as significant a contributor in m-CHP applications as are gas-to-gas and gas-to-liquid waste heat recovery exchangers. (Shah, 1997)

Exercises

1. Water flowing at 4 kg/s is cooled by air flowing at 10 kg/s in a cross flow heat exchanger. The conductance of the heat exchanger is 700 W/K and the entrance temperature of the water is 373 K. Determine the NTU and effectiveness of the heat exchanger.

2. A counterflow tube-within-a-tube heat exchanger is used to heat water from 20 C to 95 C at a rate of 1.2 kg/s. The heating is accomplished by engine coolant water circulating at 160 C and 2 kg/s. The overall heat transfer coefficient is 640 W/C. Determine the effectiveness of the heat exchanger.

3. A cross-flow heat exchanger with an effectiveness of 0.8 is used to heat water at 75 F and 100 lb/ min to a temperature of 110 F. Heat is supplied by exhaust gases flowing at 150 F and 200 lb/min. What is the conductance of the heat exchanger?

4. Hot oil is to be cooled by water in a 1-shell-pass and 8-tube-passes heat exchanger. The overall heat transfer coefficient is 545 W/K. Water flows through the tubes at a rate o 0.2 kg/s and the oil through the shell at a rate of 0.3 kg/s. The water and oil enter at temperatures of 20 C and 150 C, respectively. Determine the rate of heat transfer of the in the heat exchanger and the outlet temperatures of the water and oil.

5. A counterflow tube-within-a-tube heat exchanger is used to heat water from 80 F to 150 F at a rate of 120 lb/min. The heating is accomplished by engine coolant water circulating at 200 F and 150 lb/min. If the conductance of a heat exchanger is varied from 200 Btu/hr*R to 1000 Btu/hr* R, what is the effect on the effectiveness of the heat exchanger?

CHAPTER VI:

ABSORPTION CHILLERS

Technology Overview

Absorption chiller technologies are one of a group of technologies classified as heat pumps. Heat pumps may be either heat driven or work driven. Absorption technologies are heat driven, transferring heat from a low temperature to a high temperature using heat as the driving energy. Heat pumps operate on the principle of the absorption refrigeration cycle, which is similar to the vapor-compression cycle. Both the absorption refrigeration cycle and the vapor-compression cycle will be examined to draw analogies between the two.

Vapor-compression refrigeration systems are the most common refrigeration systems in use today. The vapor-compression cycle is a work-driven cycle that is illustrated in Figure 6.1. In the vapor-compression cycle, work is input to compress the refrigerant to a high pressure and temperature at State 2. At State 2, the refrigerant condensation temperature is below the ambient temperature. As the high-pressure and high-temperature refrigerant vapor passes through the condenser, heat is rejected to the ambient air and the refrigerant vapor condenses to a liquid to achieve State 3. The high-pressure liquid at State 3 passes through an expansion valve. As the liquid passes

through the expansion valve, the refrigerant experiences a reduction in both temperature and pressure to reach State 4. At State 4, the boiling temperature of the refrigerant is lower than that of the surroundings. The low-pressure liquid refrigerant passes through the evaporator, absorbing heat from the ambient environment when boiling occurs in the evaporator and creating a low-pressure refrigerant vapor at State 1. The low-pressure refrigerant vapor at State 1 enters the compressor completing the cycle.

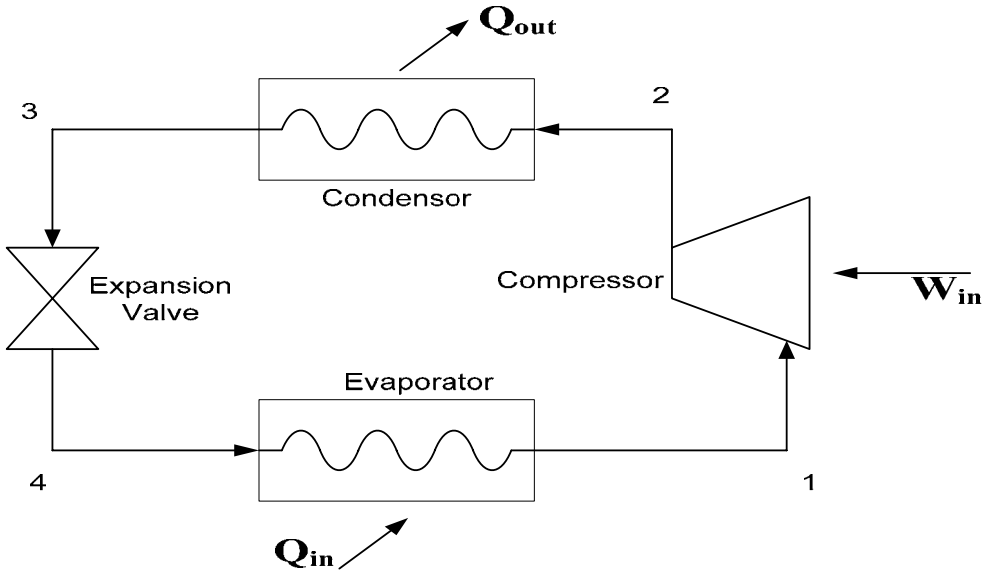

Figure 6.1: Vapor-Compression Cycle Schematic

The absorption cycle has some features in common with the vapor compression cycle. For example, the absorption cycle has a condenser, an evaporator, and an expansion valve. However, the absorption cycle and the vapor-compression cycle differ in two very important aspects. The absorption

cycle uses a different compression process and different refrigerants than the vapor-compression cycle.

The absorption cycle operates on the principle that some substances (absorbents) have an affinity for other liquids or vapors and will absorb them under certain conditions. Instead of compressing a vapor between the evaporator and condenser as in Figure 6.1, the refrigerant of an absorption system is absorbed by an absorbent to form a liquid solution. The liquid solution is then pumped to a higher pressure. Because the average specific volume of a liquid is much smaller than that of the refrigerant vapor, significantly less work is required to raise the pressure of the refrigerant to the condenser pressure. This corresponds to less work input for an absorption system as compared to a vapor-compression system.

Because the absorbent used in the absorption cycle forms a liquid solution, some means must also be introduced to retrieve the refrigerant vapor from the liquid solution before the refrigerant enters the condenser. This process involves heat transfer from a relatively high-temperature source. Because the thermal energy input into the system is much higher than the work input through the pump, absorption chillers are considered to be heat driven. The components used to achieve the pressure increase in an absorption chiller are viewed as a “thermal compressor” and replace the compressor in the vapor-compression cycle shown in Figure 6.1. The components of the absorption cycle are shown schematically in Figure 6.2. The components of the thermal compressor are a

pump, an absorber, and a (heat) generator and are shown to the right of the dashed Z-Z line. The components to the left of the dashed Z-Z line are the same as the ones used in the vapor-compression system.

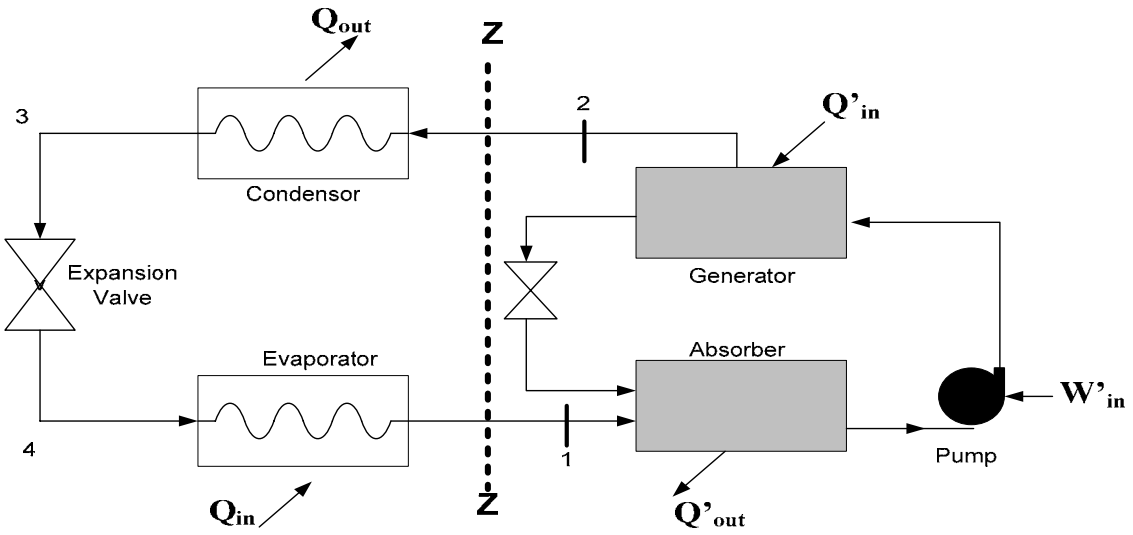

Figure 6.2: Basic Absorption Cycle Schematic

The operation of the absorption cycle shown in Figure 6-2 is as follows: At State 1, the low-pressure refrigerant vapor exits the evaporator and enters the absorber. In the absorber, the refrigerant vapor is dissolved in an absorbent and rejects the heat of condensation and the heat of mixing to form a liquid solution. The refrigerant/absorbent solution is then pumped to the condenser pressure and passed to the generator. In the generator, heat is added to the refrigerant/absorbent solution to vaporize the refrigerant, removing the refrigerant from the solution. The liquid absorbent has a higher boiling temperature than the refrigerant and, therefore, stays in the liquid form. There are two streams exiting

the generator. The refrigerant exits to the condenser at a high temperature and pressure (State 2) while the absorbent passes through an expansion valve, decreasing the pressure of the absorbent to the evaporator pressure before entering the absorber again.

The remainder of the operation is much the same as the vapor compression cycle. The high-temperature, high-pressure refrigerant vapor at State 2 enters the condenser with a pressure such that the ambient temperature is higher than the condensation temperature of the refrigerant. The refrigerant vapor condenses as it passes through the condenser, rejecting heat to the ambient environment to achieve State 3. At State 3, the high-pressure, low-temperature liquid refrigerant enters the expansion valve where the refrigerant experiences a decrease in pressure to the evaporator pressure. The low-pressure, low-temperature liquid refrigerant that results at State 4 is at a pressure such that the boiling temperature of the refrigerant is lower than the ambient temperature of the environment. As the liquid refrigerant passes through the evaporator, the refrigerant boils, absorbing heat from the ambient air. The refrigerant exits the evaporator as a high-temperature, low-pressure vapor to complete the cycle.

Refrigerant-Absorbent Selection

Though all absorption chillers operate on the basic cycle presented in Figure 6.2, each chiller design is dependent on the refrigerant-absorbent selection. Current refrigerant/ absorber media for absorption chillers are either

water/lithium bromide or ammonia/water. Water/lithium bromide absorption chillers utilize water as the refrigerant and lithium bromide as the absorbent. Because water is used as the refrigerant, applications for the water/lithium bromide absorption chillers are limited to refrigeration temperatures above 0 C. This combination of refrigerant and absorbent is advantageous in areas where toxicity is a concern because lithium bromide is relatively non-volatile. Absorption machines based on water/lithium bromide are typically configured as water chillers for air-conditioning systems in large buildings. Water/lithium bromide chillers are available in sizes ranging from 10 to 1500 tons. The coefficient of performance (COP) of these machines typically falls in the range of 0.7 to 1.2 (Herold, Radermacher, and Klein, 1996).

The ammonia/water combination utilizes ammonia as the refrigerant and water and the absorbent. The use of the ammonia as the refrigerant allows much lower refrigerant temperatures (the freezing temperature of ammonia is -77.7 C); however, the toxicity of ammonia is a factor that has limited the use of ammonia/water chillers to well-ventilated areas. In commercial and residential building applications where there is insufficient ventilation, emissions from an ammonia/water absorption chiller could be harmful to occupants.

The primary selling point of ammonia/water absorption chillers is their ability to provide direct gas-fired and air-cooled air conditioning. Ammonia/water absorption chillers are commonly sold as a single component in an air-conditioning system; however, use is restricted in some densely populated areas.

Ammonia/waster chillers are available in capacities ranging from 3 to 25 tons with COPs generally around 0.5 (Herold, Radermacher, and Klein, 1996).

A schematic of an absorption cycle of ammonia/water is shown in Figure 6.3. The addition of a heat exchanger is common in all absorption chillers to increase the efficiency of the thermal compressor. The hot solution leaving the generator is used to preheat the refrigerant/absorbent solution entering the generator. A rectifier is also included in the system of an ammonia/water chiller. This is because the ammonia vapor leaving the generator often includes a low concentration of water vapor. This water vapor will freeze in the expansion valve, negating the operation of the system.

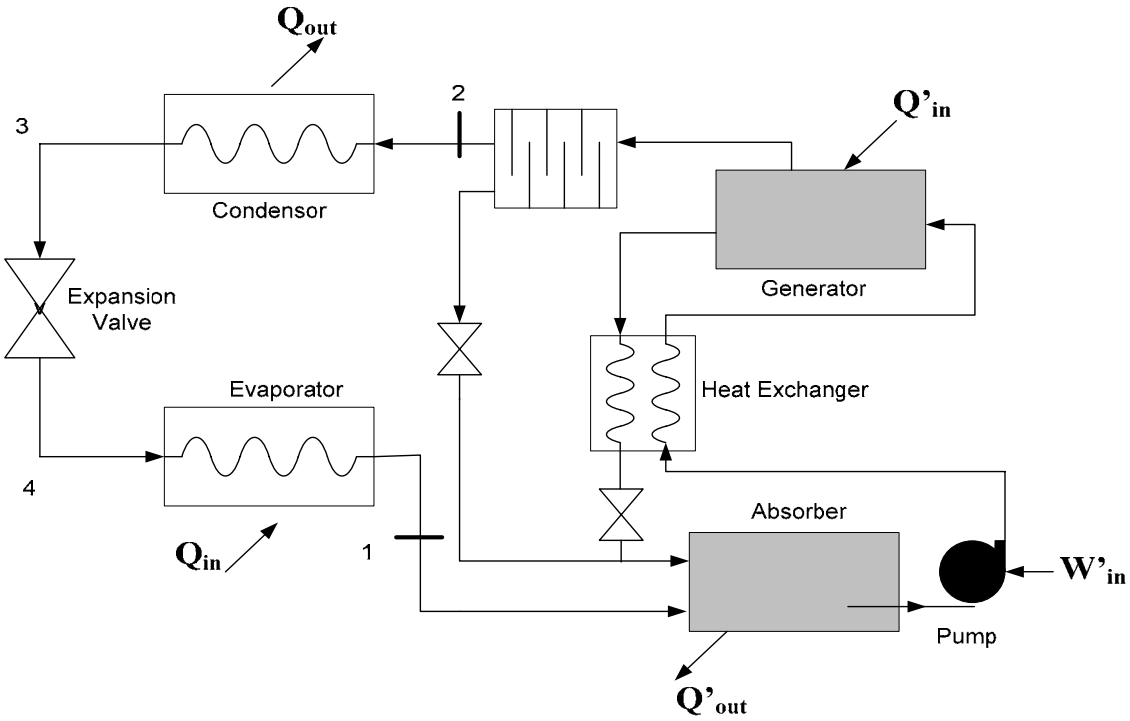

Figure 6.3: Ammonia/Water Absorption Cycle

Types of Absorption Chillers

Absorption chillers are classified as single-effect, double-effect, or triple effect. Single-effect absorption chillers contain one stage of generation, such as the systems shown in Figures 6.2 and 6.3. Single-effect absorption chillers use low-pressure steam or hot water as the energy source. Typical temperature requirements range from 200 to 270 F (93 to 132 C). Steam-powered systems operate at pressures between 9 and 15 psig. When the supplied temperatures are below the design specifications, the chiller capacity is reduced.

Double-effect absorption systems use a second generator, condenser, and heat exchanger that operate at higher temperature. A double-effect water/lithium bromide absorption system is shown schematically in Figure 6.4. Refrigerant vapor is recovered from the first-stage generator in the high-temperature condenser. The refrigerant/absorbent in the second-stage generator is at a lower temperature than the solution in the first-stage generator. The refrigerant vapor from the first stage generator flows through the second-stage generator where a portion of the refrigerant condenses back into liquid while the remainder remains in the vapor phase. Additional refrigerant is vaporized in the second-stage generator by the high temperature and the heat of vaporization supplied by the refrigerant from the first-stage generator. The refrigerant vapor from both generator stages flows to the condenser while the absorbent solution flows back to the absorber.

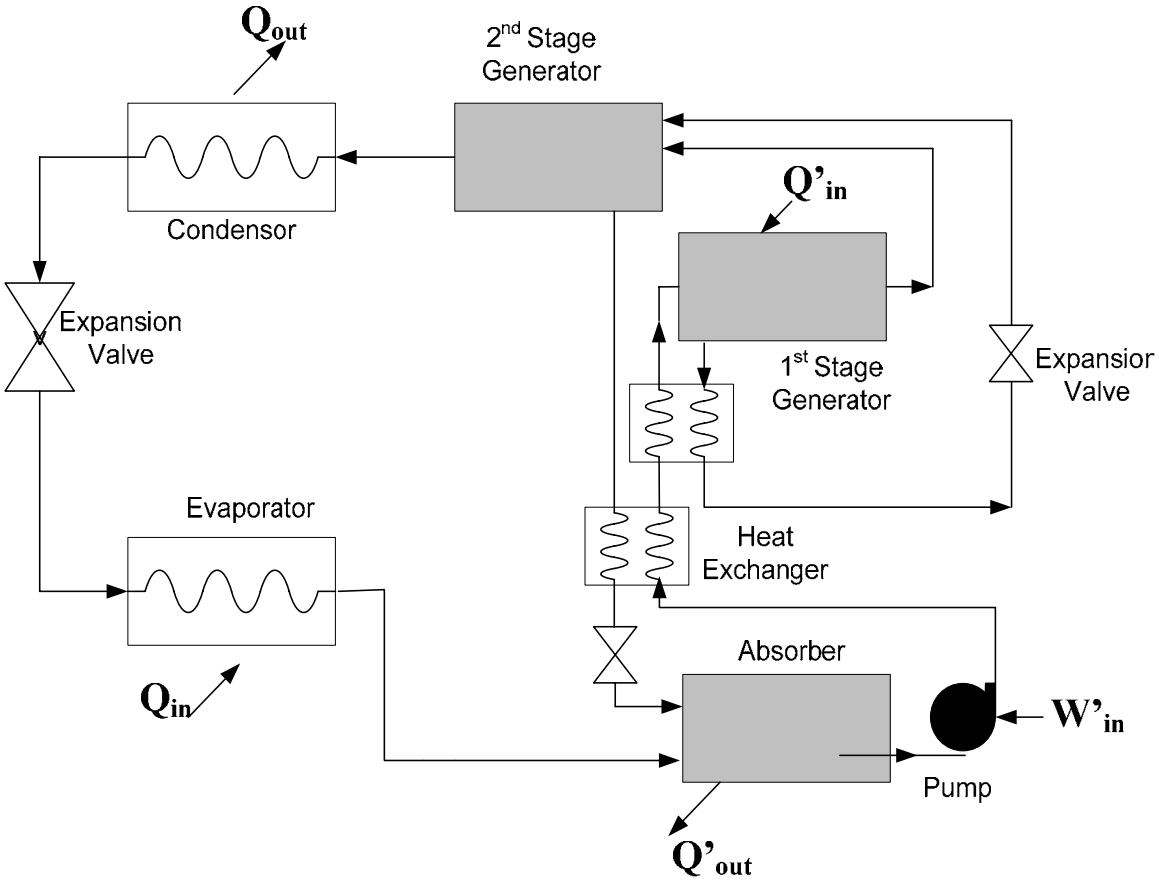

Figure 6.4: Double-Effect Water/Lithium Bromide Absorption Chiller Schematic

The purpose of the two stages that make up the double-effect absorption cycle is to increase the COP of the cycle. This is made possible through the use of the recuperative heat exchangers used in the system. Double-effect chillers yield higher COPs than single-effect chillers. The COP for double-effect absorption chillers varies from 1.0 to 1.2 for water/lithium bromide chillers (Herold, Radermacher, and Klein, 1996).

Triple-effect absorption chillers have been in prototype development for several years. These chillers will be direct-fired and are expected to provide a 50% thermal efficiency improvement over double-effect absorption chillers.

Triple-effect absorption chillers do not feature a distinct third generator stage; rather they use internally-recovered heat to achieve high efficiencies. Triple-effect water/lithium bromide chillers can achieve COPs of 1.6 and greater (Petchers, 2003).

One of the most promising absorption technologies is the generator-absorber heat exchange (GAX) cycle. GAX chillers use an ammonia/water working fluid. GAX-cycle systems hold great potential for residential and light-commercial applications and provide capacities as low as 3 tons. GAX absorption chillers have obtained COPs of approximately 0.7 (DeVault, et al., 2002).

System Analysis

An absorption refrigeration system consists of a working fluid undergoing a series of thermodynamic processes. Refrigerant and absorbent flow in a closed-loop system that includes adiabatic and non-adiabatic mixing, heating and cooling, pumping, and throttling. Each of these processes can be analyzed by energy and mass balances. The thermodynamic properties of the working fluid are essential for applying conservation of mass and energy relationships to a system.

Absorption systems use homogenous binary mixtures as working fluids. A homogenous mixture is a uniform composition that cannot be separated into its constituents by pure mechanical means. The thermodynamic properties of the working fluid will change throughout the cycle as the fluid flows through

components such as the generator, the evaporator, the expansion valves, and the heat exchangers.

Unlike pure substances, the thermodynamic state of a mixture cannot be determined by two independent properties. The concentration of a mixture (x) must be known along with two independent properties of the mixture to determine the thermodynamic state. The concentration of a mixture is defined as the ratio of the mass of one constituent to the mass of the mixture. For example, an ammonia/water mixture with a concentration of 0.3 contains 0.3 lbm of ammonia for every 10 lbm of ammonia/water mixture.

The properties of binary mixtures can be represented using an enthalpy-concentration (i-x) diagram. The liquid and vapor regions of the enthalpy-concentration diagram are of the interest for the working fluids used in absorption chillers. An example of an enthalpy-concentration diagram for an ammonia/water system is given in Figure 6.5. In the i-x diagram, the enthalpy is plotted in the vertical axis, and the concentration is plotted on the horizontal axis. Lines of constant temperature as well as condensing and boiling lines are plotted to aid in determining the thermodynamic properties at any point.

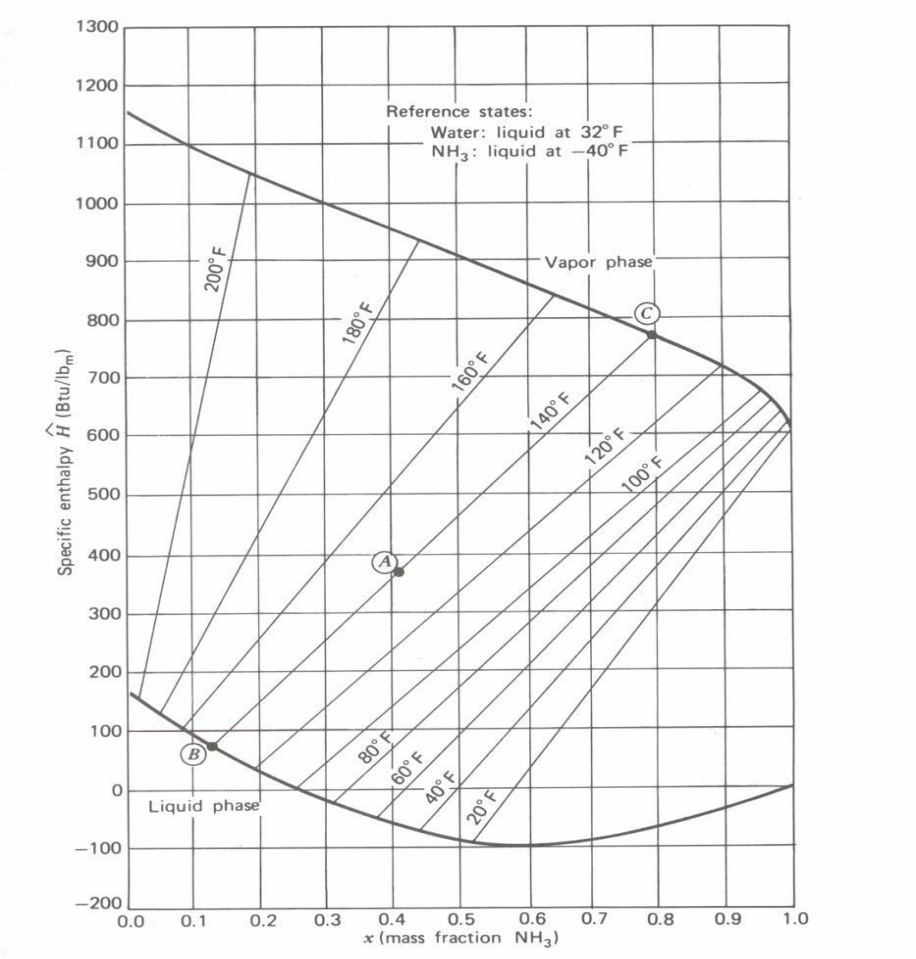

Figure 6.5: Enthaply-Concentration Diagram for Ammonia/water System. (Felder, et al., 1986)

An analysis of the thermodynamic processes in the absorption cycle is possible once all the thermodynamic properties are determined. The generator, evaporator, condenser, absorber, and rectifier all have refrigerant flowing through them and heat transfer and mass transfer occurring. Figure 6.6 presents a schematic of the thermodynamic processes that occur within the absorber.

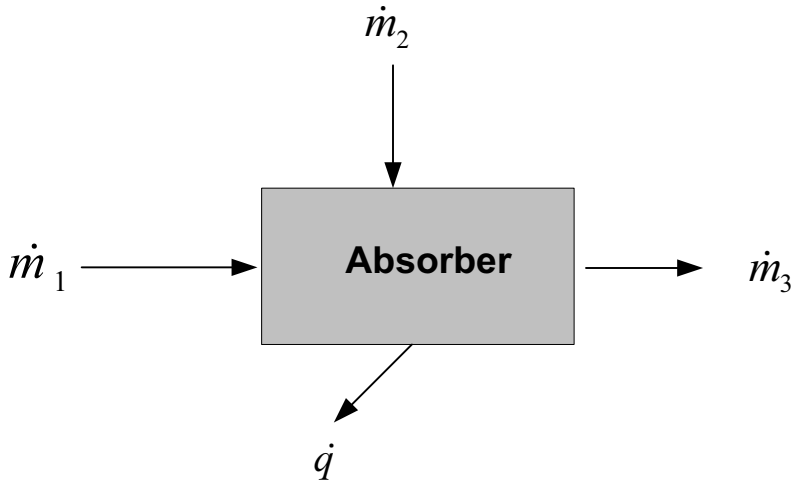

Figure 6.6: Absorber

Mass balance and energy equations for the absorber are

$$\dot{m}_1 + \dot{m}_2 = \dot{m}_3 \tag{6-1}$$

$$\dot{m}_1 x_1 + \dot{m}_2 x_2 = \dot{m}_3 x_3 \tag{6-2}$$

$$\dot{m}_1 i_1 + \dot{m}_2 i_2 = \dot{m}_3 i_3 + \dot{q} \tag{6-3}$$

Substitution and simplification of equations 6-1, 6-2, and 6-3 yields expressions for the enthalpy and concentration of the stream exiting the absorber (stream 3)

$$x_3 = x_1 + \frac{\dot{m}_2}{\dot{m}_3}(x_2 - x_1) \tag{6-4}$$

$$i_3 = i_1 + \frac{\dot{m}_2}{\dot{m}_3}(i_2 - i_1) + \frac{\dot{q}}{\dot{m}_3} \tag{6-5}$$

The last term in Equation 6-5 represents the loss of enthalpy through heat rejection during the process. Equations 6-4 and 6-5 can be used to identify the concentration and enthalpy of the fluid stream exiting the absorber.

The mass and energy balance equations for a first-stage or single-effect generator can be determined in the same manner as for the absorber. A schematic of the thermodynamic processes occurring within the first-stage generator is shown in Figure 6.7.

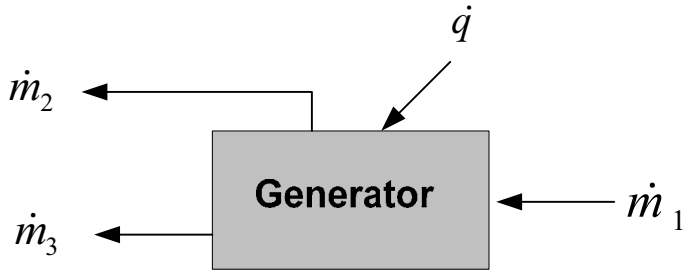

Figure 6.7: First-Stage Generator Schematic

Mass balance and energy equations for the first-stage generator are

$$\dot{m}_1 = \dot{m}_2 + \dot{m}_3 \tag{6-6}$$

$$\dot{m}_1 x_1 = \dot{m}_2 x_2 + \dot{m}_3 x_3 \tag{6-7}$$

$$\dot{m}_1 i_1 + \dot{q} = \dot{m}_3 i_3 + \dot{m}_2 i_2 \tag{6-8}$$

Substitution and simplification of Equations 6-6, 6-7, and 6-8 yields expressions for the enthalpy and concentration of the refrigerant vapor stream exiting the absorber (stream 2)

$$x_2 = \frac{\dot{m}_1 x_1 - \dot{m}_3 x_3}{\dot{m}_1 - \dot{m}_3} \tag{6-9}$$

$$i_2 = \frac{\dot{m}_1 i_1 + \dot{q} - \dot{m}_3 i_3}{\dot{m}_1 - \dot{m}_3} \tag{6-10}$$

Heat exchange also occurs in the heat exchangers shown in Figures 6.3 and 6.4. Figure 6.7 illustrates the fluid flow occurring in a heat exchanger in an absorption system and the heat transfer occurring within the heat exchanger.

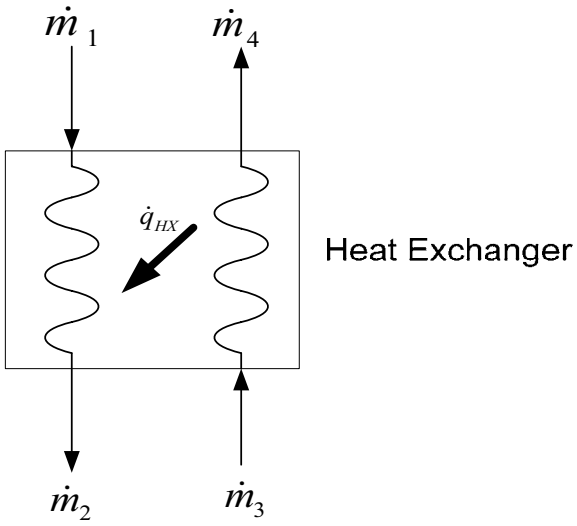

Figure 6.8: Heat Exchanger Schematic

The energy and mass balance relationships for the heat exchangers are

$$\dot{m}_1(i_2 - i_1) = \dot{q}_{HX} = \dot{m}_3(i_3 - i_4) \tag{6-11}$$

$$\dot{m}_1 = \dot{m}_2 \quad \text{and} \quad \dot{m}_3 = \dot{m}_4 \tag{6-12}$$

$$x_1 = x_2 \quad \text{and} \quad x_3 = x_4 \tag{6-13}$$

where

$$\dot{q}_{HX} = \xi \cdot \dot{q}_{Max} \tag{6-14}$$

The effectiveness (ξ) and maximum heat transfer ($\dot{q}_{Max}$) in Equation 6-14 are as discussed for heat exchangers in Chapter 5.

Another thermodynamic process encountered in the absorption refrigeration cycle is throttling. Throttling is achieved through the use of an expansion valve as illustrated in Figures 6.1 – 6.4. In an expansion valve, the fluid experiences a decrease in pressure and temperature as it exits the valve. Because only one stream enters and exits the valve and the process has no external heat source or sink, the mass and energy balance for a throttling device yields $m_1=m_2$, $i_1=i_2$, and $x_1=x_2$.

At least one pump is required in an absorption system to pump the low-pressure refrigerant/vapor solution from the evaporator pressure to the condenser pressure. Figure 6.9 schematically represents the energy transfer required for the fluid.

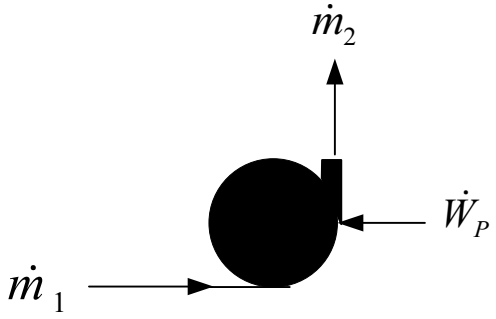

Figure 6.9: Pump Schematic

The power requirement of the pump in an absorption system is minimal and is often neglected in an overall performance analysis. The pumping power can be calculated as

$$\dot{W}_P = (p_2 - p_1)\frac{v \cdot \dot{m}_1}{\eta_P} \qquad (6\text{-}15)$$

where ν is the specific volume of the solution, p_1 and p_2 are the pressures entering and leaving the pump, respectively, and η_P is the pump efficiency.

The coefficient of performance for the absorption cycle can be obtained by applying the first and second laws of thermodynamics. Neglecting pump work, the actual COP of an absorption cycle is defined as

$$(COP)_{Actual} = \frac{\dot{q}_{evaporator}}{\dot{q}_{generator}} \tag{6-16}$$

A first law expression when all processes in the absorption cycle are irreversible is given in Equation 6-17. Equation 6-17 is based on the Carnot cycle and yields unrealistic results. This equation demonstrates that increasing the generator or evaporator temperatures will produce higher efficiencies in the absorption cycle.

$$(COP)_{Max} = \frac{T_e(T_g - T_o)}{T_g(T_o - T_e)} \tag{6-17}$$

where T_e is the temperature of the refrigerated region associated with the vapor, T_g is the temperature associated with the heat supplied to the generator, and T_o is the temperature of the ambient air associated with heat rejected at the absorber and condenser.

Increasing the evaporator temperature may not always be a practical means to increase the COP. Increasing the generator temperature is often a more feasible and desirable method to increase the COP of the absorption cycle. Multiple-effect absorption systems offer more cooling than single-effect chillers because more heat can be added to the refrigerant through additional generator

stages. Because the additional heat that is added is often recovered from the first stage generator, this option is very desirable because the heat supplied to the generator is not increasing. The quality of waste heat available to an absorption chiller in an m-CHP system is vital to the success of the overall system performance, especially in areas where the cooling load is high.

The following example is derived from an example in *Absorption Chillers and Heat Pumps* (Herold, et al., 1996) and provides and analysis of an ammonia/water absorption system. Graphical methods, energy balances and mass balance equations, and COP relationships are implemented to determine the system performance.

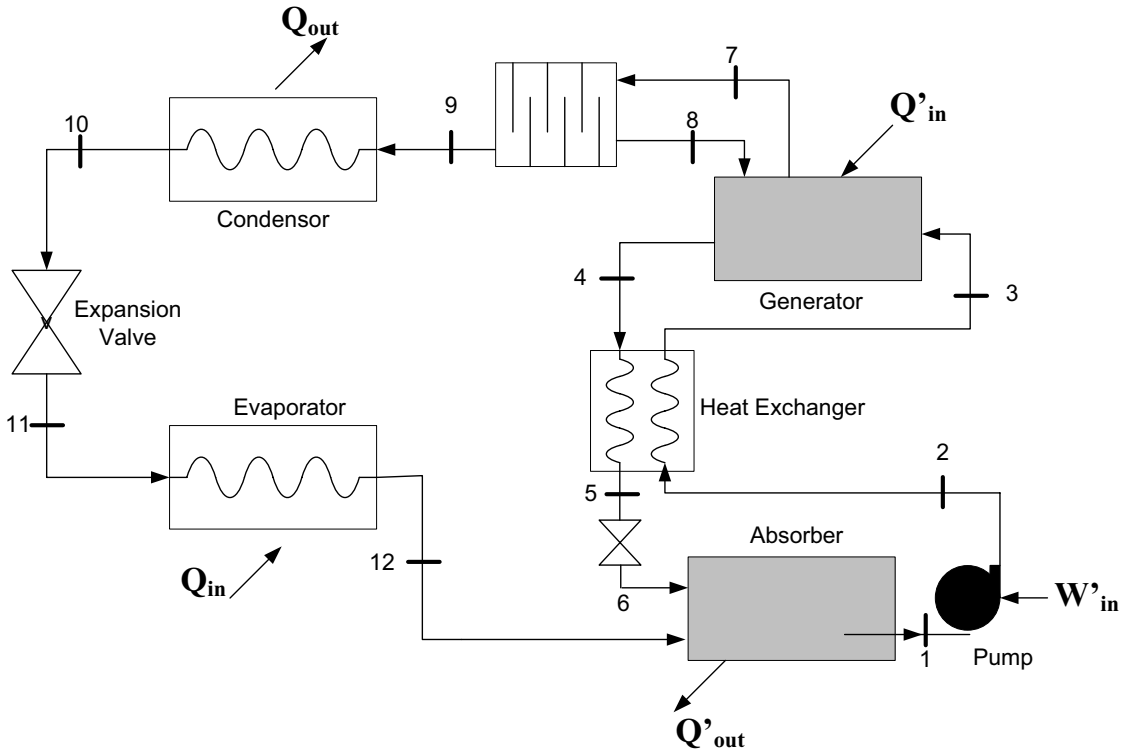

Figure 6.10: Single-stage Ammonia/water Absorption Chiller for Example 6-1

Table 6.1: State Points for the Ammonia/water System in Figure 6.10

State	i (J/kg)	m (kg/s)	p (kPa)	Vapor Quality	T (C)	x (kg/kg)
1	42.30	0.100	240.20	-	40.00	0.37
2	39.20	0.100	1555.00	-	40.50	0.37
3	306.80	0.100	1555.00	0.02	110.70	0.37
4	401.60	0.086	1555.00	-	131.00	0.27
5	0.90	0.086	1555.00	-	40.50	0.27
6	0.90	0.086	240.20	-	40.70	0.27
7	1547.00	0.015	1555.00	1.00	108.00	0.94
8	246.70	0.001	1555.00	-	108.00	0.37
9	1294.00	0.014	1555.00	1.00	44.00	1.00
10	190.10	0.014	1555.00	0.00	40.00	1.00
11	190.10	0.014	240.20	0.20	14.50	1.00
12	1246.00	0.014	240.20	0.99	10.00	1.00

Example 6-1

An ideal single-stage ammonia/water absorption system is given as shown in Figure 6-10. The evaporator saturation temperature at the outlet is assumed to be -10 C with saturated vapor leaving. The mass flow rate of solution through the solution pump is 0.10 kg/sec. The temperature of the saturated liquid leaving the absorber and the condensor is 40 C. The difference in mass fraction of the two solution streams is given to be 0.10. The rectifier prodeuces a vapor with a mass fraction of 0.999634 ammonia. The pump efficiency is taken to be 100% and the effectiveness of the solution heat exchanger is taken as 1.0. Find the COP, the amounts of heat exchanged, and the work performed by the pump. (Note: "Q" and "m" are heat rate and mass flow rate, respectively.)

Solution:
Using binary mixture analysis methods along with an enthalpy-concentration chart for ammonia-water (or using suitable software) the state points can be found for all conditions as shown in Table 6-1.

Based on the values in Table 6-1, and the equations specified in this chapter, the following detailed results are obtained.

The pump power, W_P is

$$W_p := \left(p_2 - p_1\right)\cdot\frac{\nu\cdot m_1}{\eta_P} \qquad W_p = 0.158\text{kW} \qquad W_p = 0.212\text{hp}$$

with ν = 0.0012 m^3/kg, the specific volume of the rich solution, and a pump efficiency of 1.0. Assuming a heat exchanger effectiveness of 1.0, the amount of heat exchanged in the solution heat exchanger can be found by writing an energy balance on either side.

$$Q_{shx} := m_2\cdot\left(i_3 - i_2\right) \qquad Q_{shx} = 9.979\text{tons}$$

Figure 6.11: Example 6-1

The heat losses and gains of the remaining components can be found by their respective energy balance equations.

$Q_{absorber} := \left(m_{12} \cdot i_{12} + m_6 \cdot i_6 - m_1 \cdot i_1\right)$ $\quad Q_{absorber} = 3.906\text{tons}$

$Q_{rectifier} := \left(m_7 \cdot i_7 - m_9 \cdot i_9 - m_8 \cdot i_8\right)$ $\quad Q_{rectifier} = 1.397\text{tons}$

$Q_{generator} := \left(m_7 \cdot i_7 + m_4 \cdot i_4 - m_8 \cdot i_8 - m_3 \cdot i_3\right)$ $\quad Q_{generator} = 7.734\text{tons}$

$Q_{condensor} := m_9 \cdot \left(i_9 - i_{10}\right)$ $\quad Q_{condensor} = 4.457\text{tons}$

$Q_{evaporator} := m_9 \cdot \left(i_{12} - i_{11}\right)$ $\quad Q_{evaporator} = 4.336\text{tons}$

The actual COP of this absorption system is evaluated as

$$COP_{actual} := \frac{Q_{evaporator}}{Q_{generator}} \qquad COP_{actual} = 0.561$$

Figure 6.11: Example 6-1 (continued)

Application

Absorption chillers can be directly fired or indirectly fired. Direct-fired absorption chillers utilize a natural gas burner and can supply waste heat for a desiccant dehumidification device or hot water. Direct-fired chillers are often used in areas where electric rates are high and gas utilities offer lower rates or rebate programs to replace vapor-compression chillers.

Indirect-fired fired absorption chillers are utilized where there is an existing source of heat that can be recovered. The supplied heat can be in the form of hot water, steam, or exhaust gases. All of the prime mover technologies that are applicable to m-CHP can produce waste heat sufficient to drive an absorption chiller. This coupling ability makes absorption cycle chiller systems very desirable for m-CHP applications. An absorption chiller in an m-CHP system

may not utilize all of the waste heat that is input into the chiller. Just as with direct-fired chillers, this remaining heat may be used in a desiccant dehumidification device or to produce hot water.

The temperature of the waste heat available from a power source determines the appropriate absorption configuration. Table 6.2 matches the waste heat temperatures typical of various prime movers with appropriate absorption configurations. The match is based on the temperature of the waste heat that could be obtained to drive the generator in an absorption chiller cycle.

Table 6.2. Matching of Power Generation and Absorption Technology. (Devault, Garland, Berry, and Fiskum, 2002)

Power Generation and Absorption Technology		
Power Source	**Temperature (F)**	**Matching Technology**
Microturbine	~600	Triple-, double-, or single-effect
Reciprocating Engine	~180	Single-effect
SOFC	~900	Triple-, double-, or single-effect
PAFC	~250	Double-effect or single effect
PEMFC	~140	Single-effect

Absorption chillers offer many advantages over electric chillers, especially when there is a source of waste heat available. As compared to electric chillers, absorption chillers have lower operating costs, shorter payback periods, quiet operation, low maintenance, and high reliability. Absorption systems also operate at lower pressures and offer safer operation. However, absorption chillers have higher initial costs and are not as widely available as electric chillers.

Vapor-compression systems are much more widely manufactured and more available than absorption chillers. Still, the fact that absorption chillers do not have mechanical compressors and have fewer moving parts gives absorption technologies an advantage over vapor-compression systems in terms of lower maintenance, higher reliability and quieter operation.

Cost

The capital cost of installing an absorption chiller is generally more than installing an equivalent electric or engine-driven chiller. The RS Means Mechanical Cost Data for a 100 ton steam or water-fired absorption chiller is presented in Table 6.3.

Table 6.3: RS Means Cost Data for a 100 Ton Absorption Chiller Installation

Cost Source	Cost ($)
Material	110,500
Labor	7,975
Total	118,475

Exercises

1. Two solution streams are adiabatically mixed at the same temperature. Assuming the process occurs at a constant pressure, determine the mass flow rate, quality, and enthalpy of the outlet state. Table 7.6 gives the properties of the inlet streams.

Table 6.4: Table for Problem 1

	m (kg/s)	x (%LiBr)	i (J/kg)
1	0.23	50	107.32
2	0.81	60	145.67

2. Consider a generator in an ammonia/water absorption cycle operating at steady state with the operating conditions specified in Table 7.7, where streams 1 and 2 are the inlet streams and stream 3 is the outlet stream. Find the required heat input that is to be supplied by a waste heat source assuming negligible pressure losses and a constant pressure throughout the system.

Table 6.5: Table for Problem 2

	m (kg/s)	x (%NH_3)	i (J/kg)
1	0.54	50	107.32
2			145.67
3	0.81	60	210.36

3. A double-effect water/lithium bromide absorption chiller has the operating conditions specified in Table 7.8, determine the enthalpy of the solution leaving the absorber and entering the pump. 87.5 kJ/s of energy is rejected during the absorption process. Assume negligible pressure losses and isobaric conditions.

Table 6.6: Table for Problem 3

	m (kg/s)	x (%LiBr)	i (J/kg)
From Evaporator	0.32	35	90.5
From Generator/HX to Pump	0.16	40	75.3

4. A microturbine supplies waste heat to a water/LiBr absorption chiller at 400 F. The ambient temperature is 75 F, and the chiller produces chilled water at 45 F. What is the maximum coefficient of performance this system can attain?

5. The mass flow rate of refrigerant vapor entering the absorber from the evaporator is 0.35 kg/s. The enthalpies of the streams on the inlet and outlet sides of the evaporator are 100 kJ/kg and 150 kJ/kg respectively. If an internal combustion engine provides 27.5 kJ/s of energy to the generator, determine the actual coefficient of performance of the absorption chiller.

6. The absorption system above removes heat from the refrigerant in the condenser at a rate of 25 kJ/s. Determine (a) the rate of heat transfer in the evaporator, the absorber, and the generator, (b) the power required of the pump, and (c) the coefficient of performance.

7. Table 6.7 refers to an absorption system like the one analyzed in Example 1. Determine the mass flow rate, the pressure, and the concentration of all the streams in the system.

Table 6.7: Table for Problem 6

	i (kJ/kg)	m (kg/s)	p (kPa)	T (C)	x (kg/kg)
1	-80.0	0.10	150.0	50.00	
2	-22.3			52.00	
3	256.30			125.00	
4			1450.0	145.00	
5	5.60			52.00	0.25
6	5.60	0.08		55.00	
7	1360.20			115.00	0.92
8		0.003		115.00	0.40
9				60.00	
10	1150			50.00	
11				10.00	1.00
12	1095.4	0.02		25.00	

8. Assuming that T_o = 55 C, T_g = 145 C, and T_e = 10 C, determine the maximum possible COP. What is the refrigerating efficiency of this chiller?

Manufacturers

- Yazaki Energy Systems, Inc. in Dallas, TX manufacture water fired chillers in 10-, 20-, and 30-ton capacities in the WFC-S Series. The WFC-S series water-fired chiller is pictured in Figure 6.12.

Figure 6.12: Yazaki Energy Systems WFCS Series 10-ton Absorption Chiller. (www.yazakienergy.com)

- Robur Corporation, located in Evansville, Indiana, utilizes GAX technology in the production of ammonia/water chillers. Robur manufacturers 3- and 5-ton units that can be packaged together to meet capacity requirements. The model ACF 60-00 is shown in Figure 6.13.

Figure 6.13: Robur Model ACF 60-00 Gas-fired Absorption Chiller. (www.robur.com)

- Carrier Corporation located in, Syracuse, New York manufactures the model 16NK double-effect, steam-fired absorption chiller which offers capacities from 98- to 1323-tons. The unit is pictured in Figure 6.14.

Figure 6.14: Carrier Model 16NK Absorption Chiller. (www.global.carrier.com)

- Trane, founded in La Crosse, Wisconsin, manufactures both single-effect and double-effect chillers that are direct-, steam-, and water-fired, Figure 6.15 illustrates the Trane Classic ® single-effect steam- or water-fired absorption chiller with capacities of 112-465 tons.

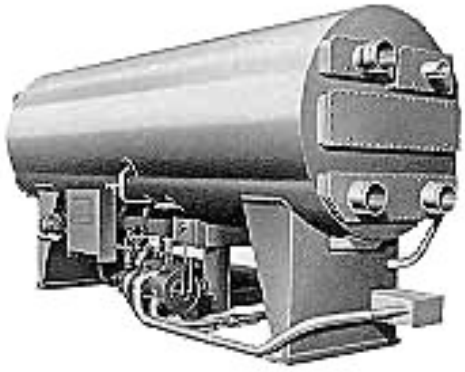

Figure 6.15: Trane Classic ® Absorption Chiller (www.trane.com)

- York International, based in York, Pennsylvania, manufactures single- and double-effect absorption chillers that can be driven by natural gas, propane, oil, high-pressure steam, or waste heat sources. Figure 6.16 pictures a single-effect absorption chiller available in capacities from 100 tons to 1,500 tons.

Figure 6.16: Single-effect Absorption Chiller by York International. (www.york.com)

CHAPTER VII:

DESICCANT DEHUMIDIFICATION TECHNOLOGIES

Introduction

Controlling humidity in a conditioned space can be important for a number of reasons. Concerns include humidity damage to moisture sensitive items, product protection from moisture degradation (foods, grains, and seeds), mildew growth, corrosion, and health issues. In the last thirty years, applications have expanded for desiccant technologies to include supermarkets, hospitals, refrigerated warehouses, ice rinks, hotels, and retail establishments. Recently, development has turned to applying desiccant dehumidification to commercial and residential buildings.

Desiccants are materials that attract and hold moisture. A desiccant dehumidifier is a device that employs a desiccant material to produce a dehumidification effect. The process involves exposing the desiccant material to a high relative humidity air stream, allowing the desiccant to extract and retain a portion of the water vapor, and then exposing the same desiccant to a lower relative humidity air stream where the retained moisture is drawn from the desiccant.

This chapter presents an overview of desiccant dehumidification. The principles of the sub-cooling system are introduced to contrast the differences between desiccant and conventional air dehumidification and to highlight the advantages of desiccant dehumidification. Also discussed are the principles of desiccant systems, types of desiccant systems, and cost considerations for choosing desiccant systems. Desiccant dehumidification technologies are an attractive component of an m-CHP system because desiccant regeneration provides an excellent use for waste heat.

Sub-cooling Systems vs. Desiccant Systems

In traditional air-conditioning systems, such as the units installed in most U.S. homes, dehumidification is achieved by cooling a moist air stream to a temperature below the dewpoint so that water (liquid) condenses out of the air. This process is familiar to anyone who has seen moisture condense on the exterior of a glass of ice water on a humid day. An example of the sub-cooling process is illustrated on a psychometric chart in Figure 7.1. The processes shown are for air being cooled and dehumidified from conditions of 95 F dry bulb (db) and 75 F wet bulb (wb) to 77 F db and 58 grains/lbm_{da}. The resulting air lies approximately in the center of the ASHRAE Summer Comfort Zone shown in Figure 7.2. Initially, the dry bulb temperature of the air decreases, while the moisture content remains constant. The dry bulb temperature continues to decrease as moisture begins to condense out of the air onto the cooling coil, resulting in a decrease in the moisture content. In order to deliver air at the

desired drier condition of approximately 45% relative humidity, some form of reheating must be used. The reheat process path is also illustrated in Figure 7.1. In this example, the total net cooling load is 10.8 Btu/lbm_{da}, and of this, 6.4 Btu/lbm_{da}, or about 59%, is latent load.

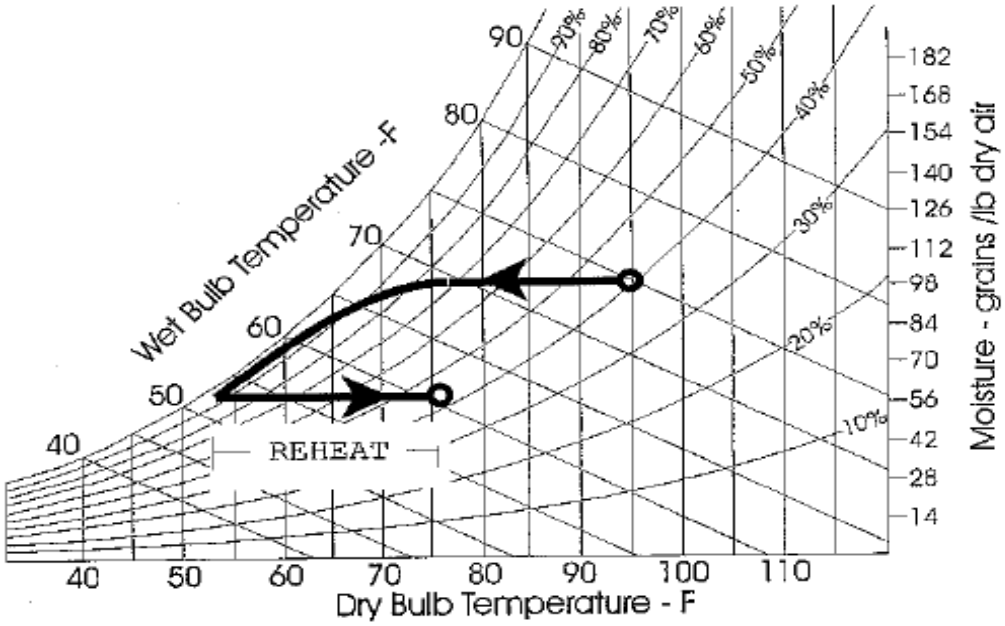

Figure 7.1: Sub-cooling Dehumidification Process (Chamra, et al., 2000)

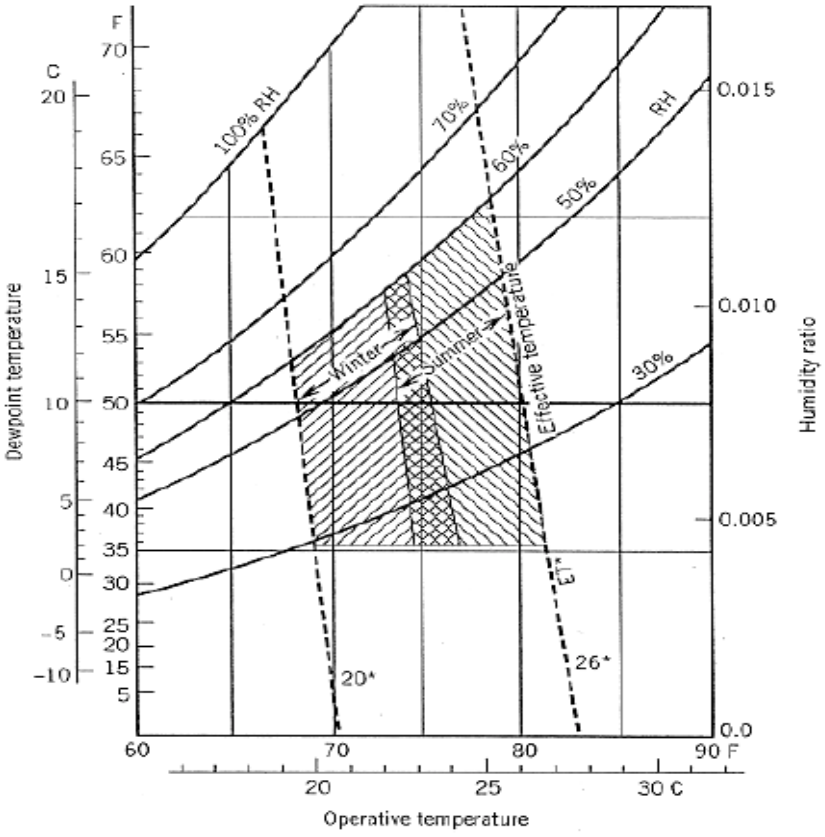

Figure 7.2: ASHRAE Comfort Zones (ASHRAE *Fundamentals*, 2001)

Summary of the Principles of Sub-cooling Systems

The same equipment is used for both the sensible cooling and dehumidification in the conventional system. If independent humidity and temperature control are required in a system, a provision for reheat of the cooled air must be included. In the example above, the net cooling load is 10.8 Btu/lbm_{da}, but the load on the cooling coil is 16 Btu/lbm_{da} with the difference (5.3 Btu/lbm_{da}) being added back in during the reheat process. Thus, energy is used both for the extra cooling and for reheat.

Another disadvantage of this approach is that the air leaving the evaporator coil is nearly saturated, with relative humidity typically above 90%. This moist air travels through duct work until the air is either mixed with dryer air or reaches the reheat unit. The damp ducts, along with the wet evaporator coils and standing water in a condensate pan (Figure 7.3), can generate problems with microbial growth and the associated health and odor problems.

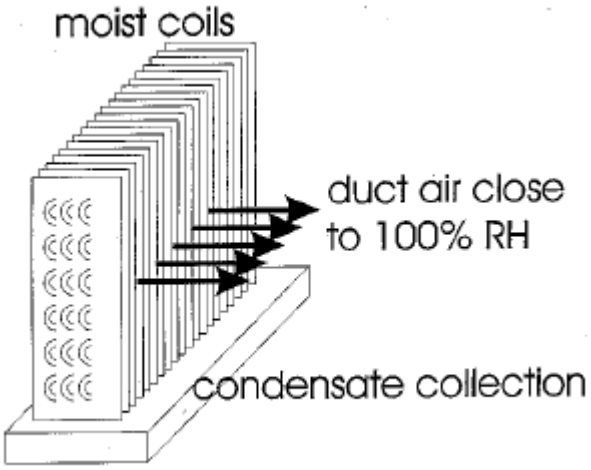

Figure 7.3: Damp Duct Symptoms (Chamra, et al., 2000)

Summary of Principles of Desiccant Systems

Desiccant dehumidification systems remove moisture from the air by forcing the water vapor directly into a desiccant material. The moisture from the air is attracted to desiccants since an area of low vapor pressure is created at the surface of the desiccant. The pressure exerted by the water in the air is higher, so the water molecules move from the air to the desiccant and the air is dehumidified.

The functioning of desiccant material might be compared to the action of a sponge in collecting a liquid. When the sponge is dry, it soaks up the liquid effectively. Once it becomes saturated, the sponge is taken to a different spot, the liquid is expelled by squeezing the sponge, and the sponge is ready to absorb more liquid. In a desiccant system, if the desiccant material is cool and dry, its surface vapor pressure is low, and moisture is attracted and absorbed from the air, which has a higher vapor pressure. After the desiccant material becomes wet and hot, it is moved to another air stream and the water vapor is expelled by raising the temperature (this step is called "regeneration"). After regeneration, the desiccant material is ready to be brought back to absorb more water vapor. Unlike the conventional cooling coil, the water vapor does not condense, but rather remains a vapor throughout all processes.

Desiccants can be either solids or liquids. The difference between solid and liquid desiccants is their reaction to moisture. Some simply collect moisture like a sponge collects water. These desiccants are called adsorbents and are mostly solid materials. Silica gel is an example of a solid adsorbent. Other desiccants undergo a chemical or physiological change as they collect moisture. These are called absorbents and are usually liquids or solids, which become liquid as they absorb moisture. Lithium chloride collects water vapor by absorption. Sodium chloride, common table salt, is another example of an absorbent.

Types of Desiccant Systems

General Classifications

Most commercial desiccant dehumidification systems use as their working material either a solid adsorbent or a liquid absorbent. Briefly, absorption is a process in which the nature of the absorbent is changed, either physically, chemically, or both. The change may include formation of a hydrate or phase change. An adsorbent, on the other hand, does not change either physically or chemically during the sorption process.

A variety of factors dictate whether an adsorbent will be commercially useful. These include cost, long-term stability, moisture removal characteristics (rate, capacity, saturation conditions, suitable temperatures), regeneration requirements (rate of moisture surrender as a function of temperature and humidity), availability, and manufacturing considerations.

Solid Adsorbents

Silica gels and zeolites are used in commercial desiccant equipment. Other solid desiccant materials include activated aluminas and activated bauxites. The desiccant material choice for a particular application depends on factors such as the regeneration temperature, the level of dehumidification, and the operating temperature.

Solid desiccant materials are arranged in a variety of ways in desiccant dehumidification systems. A large desiccant surface area in contact with the air

stream is desirable. A way to bring regeneration air to the desiccant material is necessary.

The most common configuration for commercial space conditioning is the desiccant wheel shown in Figure 7.4a. The desiccant wheel rotates continuously between the process and regeneration air streams. The wheel is constructed by placing a thin layer of desiccant material on a plastic or metal support structure. The support structure, or core, is formed so that the wheel consists of many small parallel channels coated with desiccant. Both "corrugated" and hexagonal (Figure 7.4b) channel shapes are currently in use. The channels are small enough to ensure laminar flow through the wheel. Some kind of sliding seal must be used on the face of the wheel to separate the two streams. Typical rotation speeds are between 6 and 20 revolutions per hour. Wheel diameters vary from one foot to over twelve feet. Air filters are an important component of solid desiccant systems. Dust or other contaminants can interfere with the adsorption of water vapor and quickly degrade the system performance. All commercial systems include filters and maintenance directions for keeping the filters functioning properly.

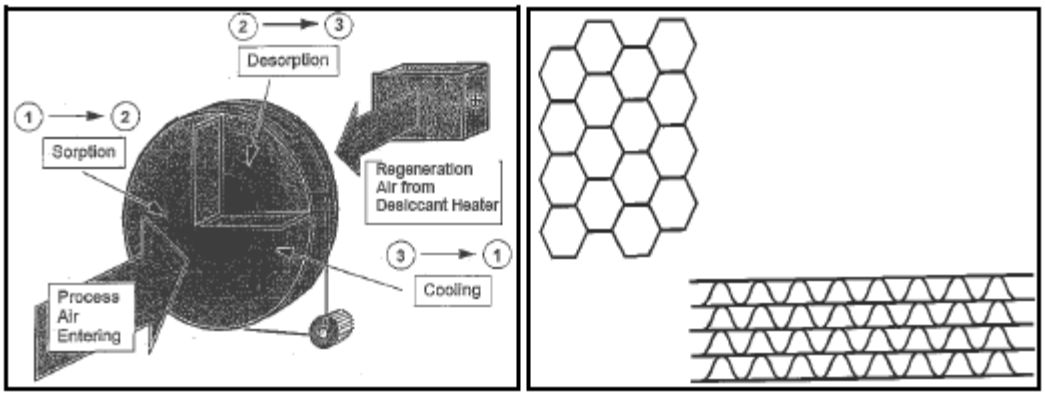

Figure 7.4: (a) Desiccant Wheel (Meckler, et al., 1995) (b) Corrugated and Hexagonal Channel Shapes (Chamra, et al., 2000)

Liquid Absorbents

Some materials that function as liquid absorbents are ethylene glycol, sulfuric acid, and solutions of the halogen group such as lithium chloride, calcium chloride, and lithium bromide (ASHRAE Fundamentals Handbook, 2001). A generic configuration for a liquid desiccant system is illustrated in Figure 7.5. The process air is exposed to a concentrated desiccant solution in an absorber, usually by spraying the solution through the air stream. As the solution absorbs water vapor from the air stream, the solution concentration drops, and the weak solution is taken to a regenerator where heat is used to drive off the water (which is carried away by a regeneration air stream) and the concentrated solution is returned to the absorber.

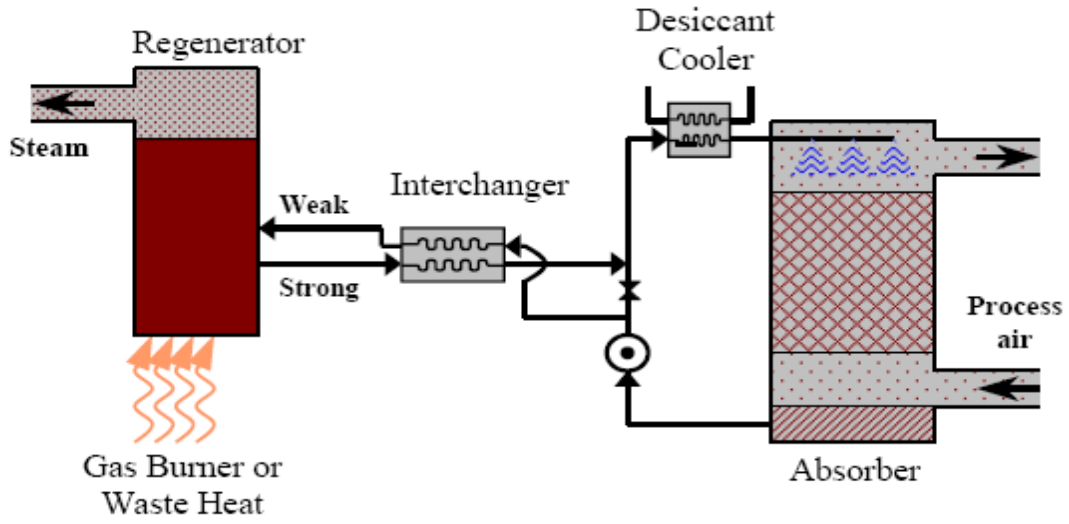

Figure 7.5: Liquid Desiccant System (Chamra, et al., 2000)

Regeneration

For solid or liquid systems, regeneration energy can be drawn from a variety of sources. In an m-CHP system, regeneration energy is drawn from the waste heat of a power-generation component. Due to the relatively low temperature requirements of regeneration (< 250 F or < 120 C), waste heat provided by combustion turbines, IC engines, and any of the fuel cell technologies is capable of supplying heat at regeneration temperatures. The thermal energy produced in many m-CHP systems is sufficient to meet the input requirements for absorption refrigeration as well as desiccant regeneration.

Solid Desiccant Systems

Figure 7-6 illustrates the components of a generic solid desiccant dehumidification system. At a minimum, the system will include separated

process and regeneration air-streams for the desiccant device and some kind of heater to raise the temperature of the regeneration air.

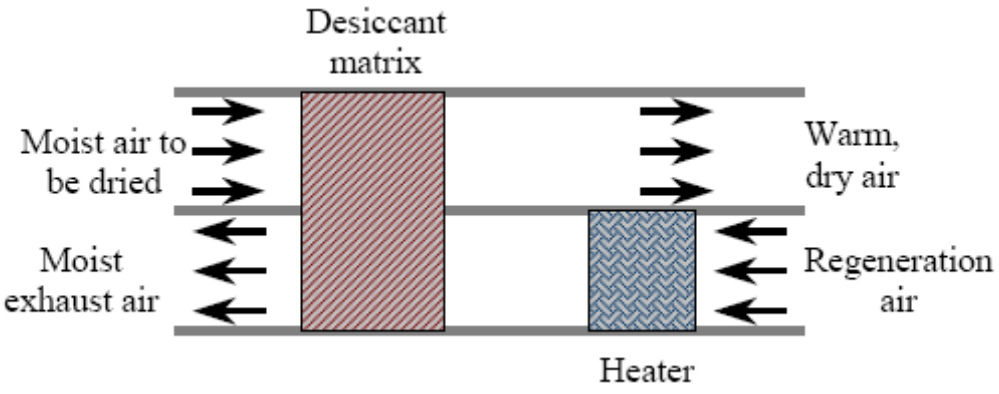

Figure 7.6: Solid Desiccant Dehumidification System (Chamra, et al., 2000)

The approximate path of the process air through a desiccant device is shown in Figure 7.7 for the same inlet and outlet conditions as were shown for the sub-cooling system (Figure 7.1). Note that, as indicated by the path from point 1 to point 2 in Figure 7.7, the desiccant process increases the dry bulb temperature of the process air. For solid desiccant materials, this increase is a result of the "heat of adsorption" which consists of the latent heat of vaporization of the adsorbed liquid plus an additional "heat of wetting." Heat of wetting is the energy released during dehumidification, in excess of the latent heat of vaporization. The path from point 1 to point 2 is close to a line of constant enthalpy. After the dehumidification process, the process air must undergo a sensible cooling process to reach the end point.

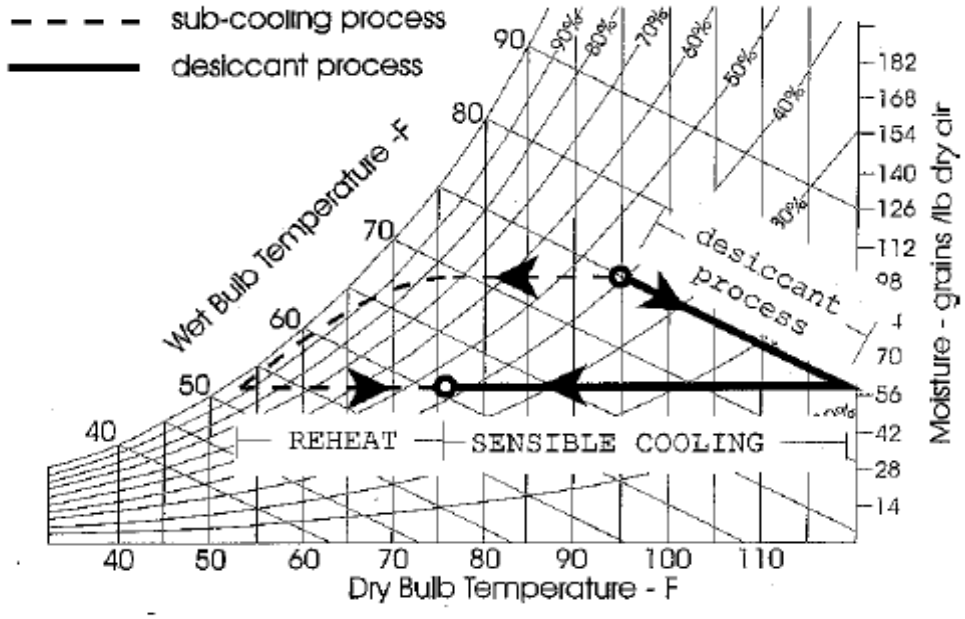

Figure 7.7: Dry Desiccant Dehumidification Process (Chamra, et al., 2000)

There are a wide variety of desiccant dehumidification system configurations available. The process and regeneration air inlet conditions and outlet requirements call for different configurations that are suited to individual situations. For illustration purposes, two simple examples are shown in Figures 7.8 and 7.9.

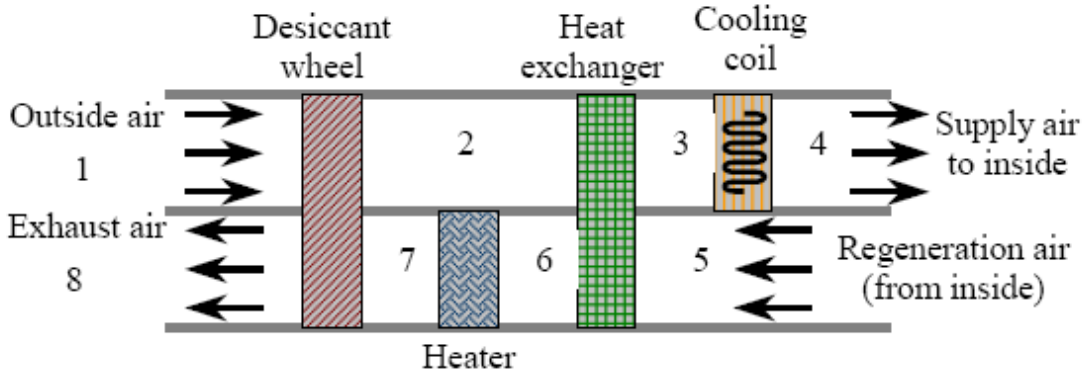

Figure 7.8: Ventilated Desiccant Dehumidification System Configuration (Chamra, et al., 2000)

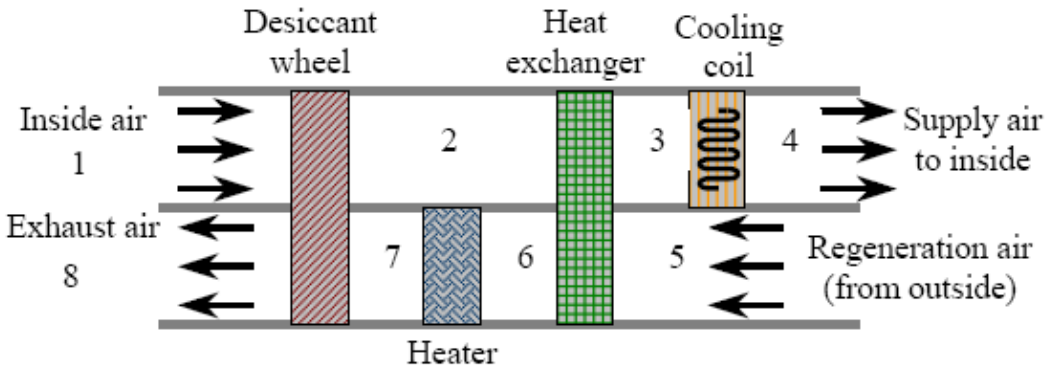

Figure 7.9: Ventilated Desiccant Dehumidification System Configuration (Chamra, et al., 2000)

Figure 7.8 illustrates a possible configuration for a desiccant system that is designed for operation in a ventilation situation; that is, 100 % outside air used to supply the conditioned space. The regeneration air for this illustration is taken completely from within the conditioned space and exhausted outside. The outside air starts at State 1 at approximately 95 F db, 75 F wb. From State 1 to State 2, the sensible temperature increases and the moisture content decreases as the outside air passes through a desiccant wheel. From State 2 to State 3, the hot air rejects some heat to the regeneration air stream via a heat exchanger. Finally, the air stream is cooled to the design supply condition by passing through a conventional cooling coil (State 3 to State 4).

The regeneration air stream starts at approximately 75 F db, 40 % rh. From State 5 to State 6, this air stream acquires heat from the process air stream through a heat exchanger, and from State 6 to State 7 the regeneration stream is further heated to bring it to an appropriate temperature for desiccant

regeneration. Finally, the regeneration air is cooled and humidified as it extracts moisture from the desiccant wheel (State 7 to State 8). At State 8, the regeneration stream is exhausted to the outside.

Figure 8-9 illustrates a re-circulating configuration; 100 % of the process air is drawn from the conditioned space (and all is returned to the conditioned space). The regeneration air is 100 % outside air. The equipment arrangement is identical to that of the ventilation illustration in Figure 7.8, only the air stream conditions are different.

Cost Considerations

In many cases, the additional benefits provided by a desiccant system will lead to greater overall capital equipment cost. However, since the latent part of the cooling load is shifted from electrical energy to thermal energy, desiccant dehumidification systems can potentially have lower operating costs, particularly if waste heat can be utilized. In m-CHP systems, waste heat can be used to regenerate the desiccant. This makes desiccant dehumidification appealing to m-CHP applications, especially when an absorption chiller is incorporated into the system to provide the sensible cooling load.

Because the humidity and temperature can be controlled independently with a desiccant dehumidification and cooling system, the system performance is often more effective than that obtainable with conventional systems. Analysis of the sensible heat ratio (SHR) suggests the energy cost savings potential that a desiccant system may have. The SHR is the ratio of sensible cooling load to the

total cooling load (sensible load plus latent load). A sensible heat ratio close to unity implies that very little moisture is removed from the air, while a sensible heat ratio close to zero indicates that most of the load is latent cooling. Air-conditioned environments often have SHR values well below unity, which results in greater energy consumption for a sub-cooling system than that of a desiccant dehumidification and cooling system that meets the same temperature/humidity requirements.

Manufacturers

- Bry-Air, headquartered in Sunbury, Ohio, manufactures desiccant dehumifiers that can dry 100 to 30,000 CFM. The MiniPAC™ and Desiccant Dehumidifier Cassettes offered by Bry-Air are pictured in Figures 7.10 and 7.11.

Figure 7.10: MiniPAC Desiccant Dehumidifier by Bry-Air (http://www.bry-air.com/)

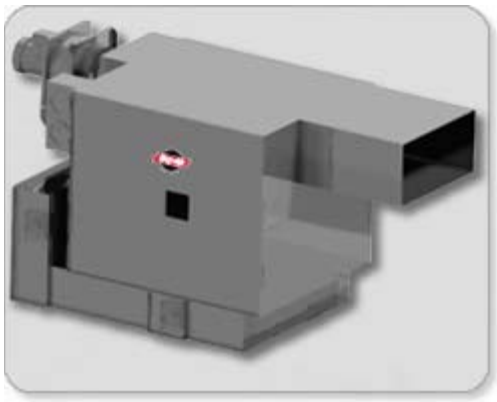

Figure 7.11: Desiccant Dehumidifier Cassettes by Bry-Air (http://www.bry-air.com/)

- Munters, located in, Amesbury, MA, manufactures desiccant dehumidifiers with flow rates ranging from 75 to 12,000 CFM. The HC-150, HC-300, MG90, and M120 are shown in Figure 7.12. The units shown can remove 4.1 – 9.5 lbm/hr of water vapor from the air.

Figure 7.12: Munters HC/M/MG Off the Shelf Desiccant Dehumidifiers (75-300 scfm) (www.muntersamerica.com)

- DehuTech, headquartered in Sweden, produces the DehuTech line of desiccant dehumidifiers. The DehuTech 160 is pictured in Figure 7-13.

Figure 7.13: DehuTech 160 (www.dehutech.com)

- Dri-Eaz located in Burlington, WA manufacturers a small line of desiccant dehumidifiers. The Dro-Eaz DriTec Pro150 pictured in Figure 7.14 processes 88 CFM to remove 27.5 pints/day of water vapor at 60% relative humidity and 68 F.

Figure 7.14: Dri-Eaz DriTec Pro150 (www.dri-eaz.com)

- Drykor, located in Fayetteville, Georgia manufactures a product line of dehumidifiers. Drykor's Alpha-Release Residential Comfort Conditioner provides cooling/heating, dehumidification, filtration of particles, and removal of bacteria and microorganisms. The Drykor RCC is shown in Figure 7.15.

Figure 7.15: Drykor Residential Comfort Conditioner (www.drykor.com)

- Dryomatic headquartered in Frederick, Maryland, manufactures industrial and commercial scale desiccant dehumidifiers, The model DCX Series rotary type desiccant dehumidifier is shown in Figure 7.16.

Figure 7.16: Dryomatic DCX Desiccant Dehumidifier (www.dryomatic.com)

CHAPTER VIII:

BIOFUELS

Introduction

In 2003, for the fourth year in a row, biomass was the leading source of renewable energy in the United States, providing 2.9 Quadrillion Btu (Quads) of energy. Biomass was the source for 47% of all renewable energy or 4% of the total energy produced in the United States (http://www.eere.energy.gov/). Agriculture and forestry residues, and in particular residues from paper mills, are the most common biomass resources used for generating electricity and for providing industrial process heat and steam as well as for a variety of biobased products. Agriculture and forestry residues are the organic byproducts of food, fiber, and forest production. In fact, 48% or 1.1 Quads of biomass energy was consumed by the pulp and paper industry. Current biomass consumption in the United States is dominated by industrial use, largely derived from wood. Use of liquid transportation fuels such as ethanol and biodiesel, however, currently derived primarily from agricultural crops, is increasing dramatically. In 2003 ethanol produced from corn reached 2.81 billion gallons.

Ethanol and biodiesel, made from plant matter instead of petroleum, can be blended with or directly substituted for gasoline and diesel, respectively.

Unlike gasoline and diesel, biofuels contain oxygen. Adding biofuels to petroleum products allows the fuel to combust more completely, thus reducing air pollution. (http://www.eree.energy.gov/biomass)

The purpose of this section is to provide introductory level information about biofuels and discuss the potential benefits of biofuels relating to m-CHP. The various methods of producing biofuels and issues relating to cost of biofuels will also be discussed.

Biomass

Biomass is any material of recent biological origin. Examples include crops and forests. Biomass as a solid has several disadvantages as compared to liquids such as petroleum or gases such as natural gas. Solid biomass generally has a lower energy density and results in a bulky fuel that is difficult to transport. Solid biomass also has limited applications, for example conventional engines and boilers do not accommodate solid fuels. The goal of many biomass processes is to convert solid fuel into more useful forms: gaseous or liquid fuels.

Mechanisms to perform this conversion include anaerobic digestion of wet biomass to produce methane and gasification of dry biomass to produce flammable gas mixtures of H_2, CO, and CH_4. Liquid fuels can be obtained through the fermentation of sugars to ethanol, thermochemical conversion of biomass to pyrolysis oils or methanol, and processing of vegetable oils to biodiesel.

Before beginning to discuss the methods of converting biomass to more useful forms, several terms that are relative to most conversion processes need to be defined.

- Carbohydrates: compounds that include sugars, cellulose, and a wide variety of other cellular products.
- Cellulose: the chief constituent of the cell walls of plants $(C_6H_{10}O_5)_X$
- Ester: Any class of organic compounds that react with water to produce alcohols and organic or inorganic acids.
- Glycerol: a clear, colorless, viscous, sweet-tasting liquid belonging to the alcohol family of organic compounds.
- Hemicellulose: complex carbohydrates that surround the cellulose fibers of a plant cell.
- Hydrolysis: the breaking point of a hydrogen bond in long-chained organic molecules.
- Lignin: complex oxygen-containing organic substance that, with cellulose, forms the chief constituent of wood.
- Protein: any group of nitrogenous organic compounds of high molecular weight synthesized by plants and animals that are required for life processes.
- Starch: a white granular organic chemical produced by all plants
- Sugar: any number of sweet, colorless, water-soluble compounds present in the sap of seed plants and the milk of mammals and making up the simplest group of carbohydrates.
- Triglycerides: esters in which three molecules of one or more different fatty acids are linked to the alcohol glycerol.
- Biogas: the product of anaerobic digestion containing CH_4 and CO_2, typically 55-75% methane by volume.

- Waste material: any material of recent biological origin discarded because it has no apparent value or represent nuisances/pollutants to the local environment, (e.g. agricultural residues, yard waste, municipal solid waste, sewage, and food processing waste).

- Energy crop: plants grown specifically for energy and harvested/planted periodically, (e.g. wood and herbaceous annuals/perennials).

The last two items defined, waste materials and energy crops, are considered the main categories of biomass feedstocks. Waste materials have the advantage of low cost; however, this advantage is often negated as waste materials have a large variability and can be complex to convert to a more useful fuel. Energy crops contain significant amounts of oils, sugars, starches, and lignocellulose, increasing the energy value. Strategies that do not include harvesting the lignocellulose waste the greatest portion of the energy crop.

Anaerobic Digestion

Anaerobic digestion is the decomposition of organic waste to gaseous fuels by bacteria in an oxygen-free environment. The process occurs in three steps. The first step is hydrolysis and fermentation where bacteria break down carbohydrates, proteins, and fats into simple acids, alcohols, and neutral compounds. Hydrogen (H_2) and carbon dioxide (CO_2) are the products.

Complex products are degraded into acetate, hydrogen (H_2), and carbon dioxide (CO_2) during the second process, transitional acetonic dehydrogenation. Any oxygen (O_2) that was present after the anaerobic digestion is consumed during the transitional acetonic dehydrogenation. The final step is

methanogensis during which acetate is converted into methane by methane-forming bacteria. The basic anaerobic process is illustrated schematically in Figure 8.1.

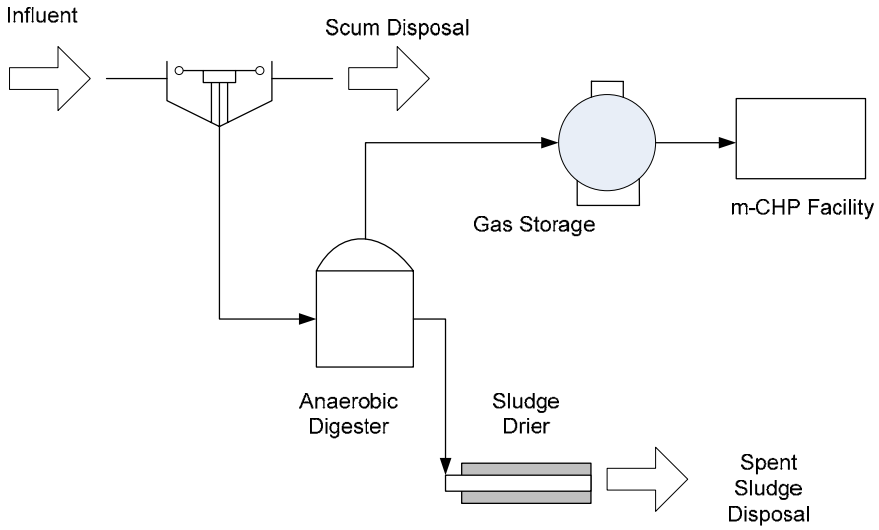

Figure 8.1: Basic Anaerobic Process (Goswami, et al, 2000)

Typically, the thermodynamic efficiency of converting the dry matter to methane is about 60% with methane yields ranging between 8,000 – 9,000 ft^3/ton of volatile solids added to a digester.

Thermal Gasification

Thermal gasification is the conversion of solid carbonaceous fuels into flammable gas mixtures called producer gas. Producer gas is a mixture of carbon monoxide (CO), hydrogen (H_2) methane (CH_4), nitrogen (N_2), carbon dioxide (CO_2), and higher hydrocarbons. The producer gas can be burned directly or used as a feedstock for liquid fuels. Gasification occurs through the parallel processes of combustion and pyrolysis. Combustion is the rapid

oxidation of fuel. Combustion is an exothermic reaction resulting in the release of large quantities of heat. Pyrolysis is the thermal degradation of a solid fuel into a variety of simple gases and organic vapors.

Heat is supplied to drive the reactions in the thermal gasification process. As heat is added, moisture is removed at 212 F (100 C). When the temperature increases to 752 F (400 C), the complex structure of the biomass starts to breakdown and gases, vapors, and liquids are released. Many of the components that are released are flammable and contribute to the heating value of the product gas released from the gasifier. After the components are released, a porous solid composed of carbon and ash, known as char, remains. The fuel's volatile percentage corresponds roughly to the pyrolysis yields, while fixed carbon and ash determine the char yield. As the temperature approaches 1292 F (700 C), the char begins to react with oxygen, carbon dioxide, and water vapor to produce more flammable gas. The primary reactions are as follows:

Carbon-oxygen Reaction $2C + O_2 \rightarrow 2CO$

Boudouard Reaction $C + CO_2 \rightarrow 2CO$

Carbon-water Reaction $C + H_2O \rightarrow H_2 + CO$

Water-shift Reaction $CO + H_2O \rightarrow H_2 + CO_2$

Hydrogenation Reaction $C + 2H_2 \rightarrow CH_4$

The gasification reactions are reversible and result in a complex equilibrium dependent upon the temperature, pressure and proportion of fuel and oxygen as well as steam added to the gasifier. Methane formation is favored in

the conditions of low temperature, high pressure, low oxygen concentration, and high water vapor content. Table 8.1 presents the gas compositions from various types of gasifiers. The higher heating value (HHV) is an important value when addressing the usefulness of a fuel. Higher heating values for a fuel include the full energy content as defined by bringing all products of combustion to 77 F (25 C). As the HHV increases, the fuel becomes more useful.

Table 8.1: Producer Gas Constituents from Various types of Gasifiers (Goswami, et al, 2000)

Gaseous Constituents (vol. % dry)							Gas Quality	
Gasifier Type	H_2	CO	CO_2	CH_4	N_2	HHV (MJ/m^3)	Tars	Dust
Air-blown fluidized bed	9	14	20	7	50	5.4	Medium	High
Air-blown downdraft	17	21	13	1	48	5.7	Low	Medium
Oxygen-blown downdraft	32	48	15	2	3	10.4	Low	Low
Indirect-heated fluidized bed	31	48	0	21	0	17.4	Medium	High

Arrangements of downdraft, updraft, and fluidized bed gasifiers are shown schematically in Figures 8.2, 8.3, and 8.4, respectively.

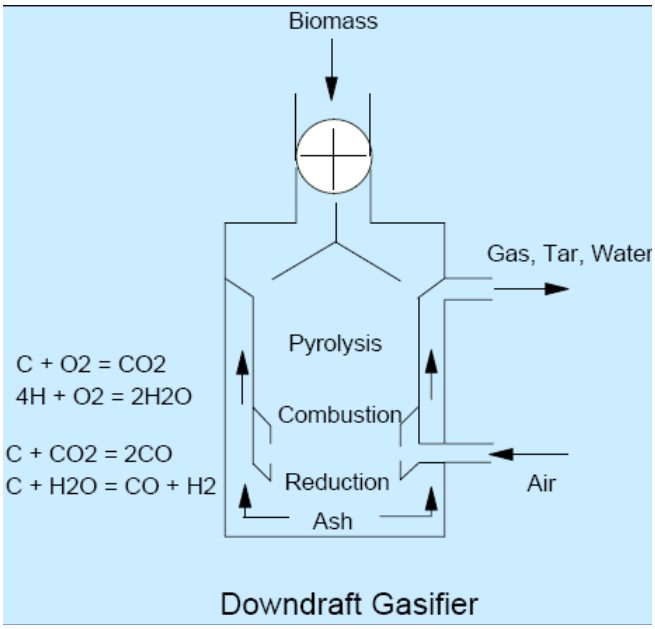

Figure 8.2: Schematic of a Downdraft Gasifier (Bricka, 2004)

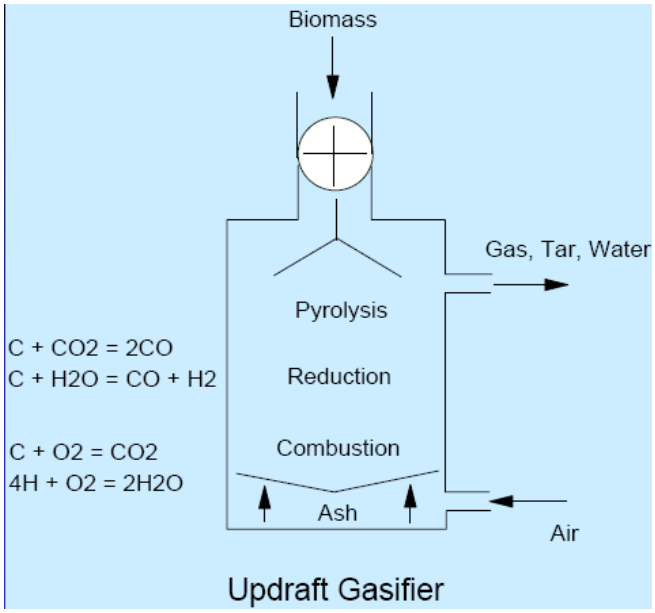

Figure 8.3: Schematic of an Updraft Gasifier (Bricka, 2004)

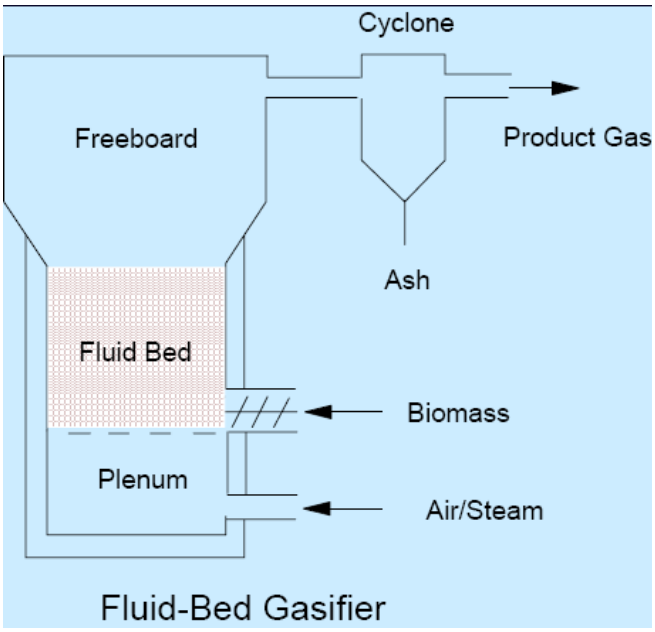

Figure 8.4: Schematic of a Fluid-bed Gasifier (Bricka, 2004)

Liquid Fuels from Biomass

Ethanol Fermentation

Ethanol (C_2H_5OH) can be burned in modified internal combustion engines, but is more commonly used as a five percent blend in gasohol. Ethanol is produced by fermentation. Fermentation is the decomposition of complex organic molecules into simple compounds through the action of microorganisms. The feedstock for ethanol production must be high in sugars. Examples of these feedstocks are sugar cane, sugar beets, and sorghum. Carbohydrates, such as starches, can serve as feedstocks if the carbohydrates can be broken down into sugars susceptible to fermentation. Cellulose and hemicellulose can be converted to fermentable sugars, though the process is relatively difficult. In the

United States, corn is the basis of the ethanol fuel industry. The typical yields of ethanol fermentation for a variety of energy crops are presented in Table 8.2.

Table 8.2: Ethanol Fermentation of Various Energy Crops (Goswami, et al, 2000)

Feedstock	Yield (Liters/ton)	Classification
Sorghum	80	Sugar crop
Sugar beets	90-100	Sugar crop
Sugar cane	75	Sugar crop
Corn	350-400	Starch crop
Wheat	400	Starch crop
Artichoke	90	Starch crop
Poplar	400	Lignocellulose crop
Corn Stover	400	Lignocellulose crop
Corn cobs	510	Lignocellulose crop
Wheat straw	490	Lignocellulose crop

As compared to methanol, ethanol can only be made from a much narrower range of feedstock. The properties pertaining to the use of ethanol as a fuel as compared to gasoline are shown in Table 8.3.

Table 8.3: Properties of Ethanol and Gasoline (Laraminie and Dicks, 2003)

Fuel	Ethanol	Gasoline
Chemical Formula	C_2H_5OH	C_8H_{18}
Molecular Weight	46.07	114.2
Freezing Point (C)	-114.1	-56.8
Boiling Point (C)	78.3	125.7
Enthaply of Combustion at 25 C (kJ/mol)	1275.9	5512.0
Heat of Vaporisation (kJ/kg)	839.3	368.1
Liquid density (kg/m^3)	789	702
Specific heat at STP (J/mol-K)	112.4	188.9
Autoignition temperature in air (C)	423	220

Chemical Synthesis of Methanol

Methanol (CH_3OH) is a liquid fuel that can be burned in modified internal combustion engines or blended with gasoline in a mixture that is 85 percent methanol and 15 percent gasoline. This methanol/gas mixture is also known as M85. Methanol is produced through the combination of carbon monoxide and hydrogen by the reaction

$$CO + 2H_2 \rightarrow CH_3OH$$

The carbon monoxide and hydrogen can be procured by the carbon-water reaction by gasifying biomass. Gasification often yields less hydrogen than the 2:1 ratio needed to produce methanol, the syn gas mixture is often reacted with steam to produce more hydrogen. Syn gas is an acronym for Synthetic gas. In general, Syn gases are composed primarily of hydrogen, carbon monoxide, carbon dioxide, perhaps methane, and possibly small amounts of other components (hydrogen sulfide, phenolics, etc.). The reaction of the syn gas and water vapor produces hydrogen and carbon dioxide according to the following reaction.

$$CO + H_2O \rightarrow CO_2 + H_2$$

The yield of methanol is 480 – 565 liter/ton. The process of thermal decomposition by gasification is essentially the same for all biomass feedstock. The properties pertaining to the use of methanol as a fuel as compared to gasoline are shown in Table 8.4.

Table 8.4: Properties of Methanol and Gasoline (Laraminie and Dicks, 2003)

	Methanol	Gasoline
Chemical Formula	CH_3OH	C_8H_{18}
Molecular Weight	32.04	114.2
Freezing Point (C)	-98.8	-56.8
Boiling Point (C)	64.7	125.7
Enthaply of Combustion at 25 C (kJ/mol)	638.5	5512.0
Heat of Vaporisation (kJ/kg)	1129	368.1
Liquid density (kg/m^3)	786	702
Specific heat at STP (J/mol-K)	76.6	188.9
Autoignition temperature in air (C)	464	220

Pyrolysis Oils

Pyrolysis is the thermal decomposition of organic compounds in the absence of oxygen. The products achieved by pyrolysis depend upon the rate and duration of heating. Liquid yields exceeding 70 percent are possible using fast pyrolysis conditions. Fast pyrolysis conditions allow a residence time of less than half a second and occur at temperature ranges of 450 – 600 C and also involve rapid quenching of the products. The rapid quenching process is essential if high-molecular weight gases are to be produced. The pyrolysis liquid obtained from fast pyrolysis is a low viscosity, dark brown liquid with concentrations of 15-20 percent water. Slow pyrolysis results in a black, tarry liquid.

The fast pyrolysis liquid is a complex mixture of hydrocarbons from the lignin in the feedstock. Pyrolysis liquids can be used as a direct substitute for heating oil. The heating value of pyrolysis oils falls in the range of 17-20 MJ/kg with an average density of 1280 kg/m^3. The yield of pyrolysis oil is approximately

135 gal/ton of feedstock. The fast pyrolysis process is illustrated schematically in Figure 8.5.

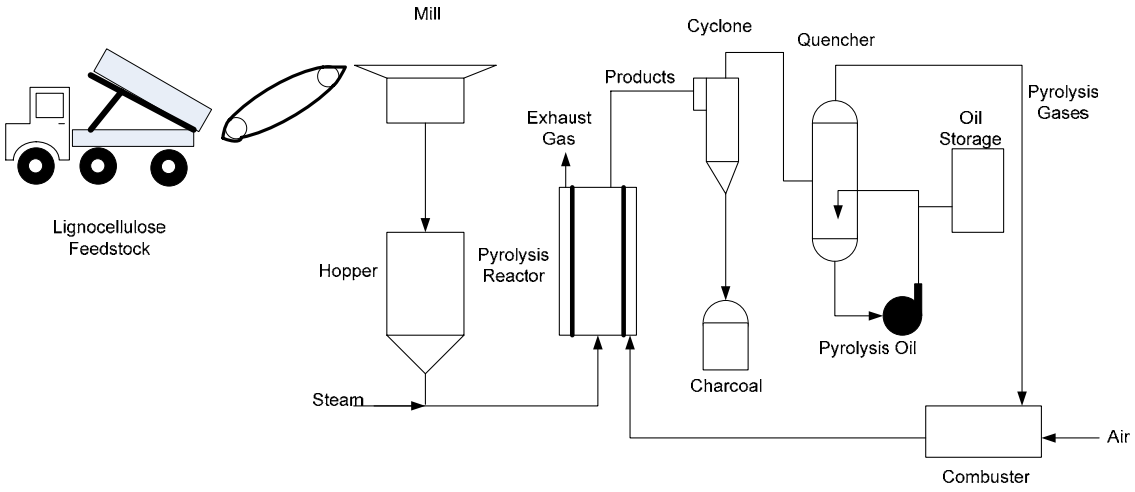

Figure 8.5: Fast Pyrolysis Production Process (Goswami, et al, 2000)

Many difficulties are encountered in using pyrolysis liquids. Storage is difficult because of polymerization and corrosion. The high oxygen and water content render the liquids incompatible with conventional hydrocarbon fuels. The liquid quality of pyrolysis oils is also very poor, lower than Bunker C heavy fuel oil.

These qualities make upgrading pyrolysis oils to more conventional fuel desirable. Upgrading the pyrolysis liquids is possible through the use of hydrotreatment. Hydrotreating involves the addition of hydrogen at high pressure and uses a catalyst to result in high quality products with maximum fuel yield.

Vegetable Oils

Vegetable oil can be obtained using grains and seeds as the feedstock. Grains and seeds have relatively high concentrations of vegetable oils with high energy content. Unfortunately, the viscosity of most vegetable oils is about twenty times that of diesel fuel, and direct use as a fuel would lead to the coking of injectors and rings. Vegetable oils can be chemically modified into methyl or ethyl esters to produce excellent diesel fuel. These vegetable oil esters that are suitable for use as diesel fuel are also known as biodiesel. Biodeisel can be used in unmodified diesel engines with no operational problems. Feedstocks for biodiesel include soybean, sunflower, cottonseed, corn, peanut, safflower, waste cooking oils, and animal fat. The production of biodiesel from oil seed is illustrated in Figure 8.6.

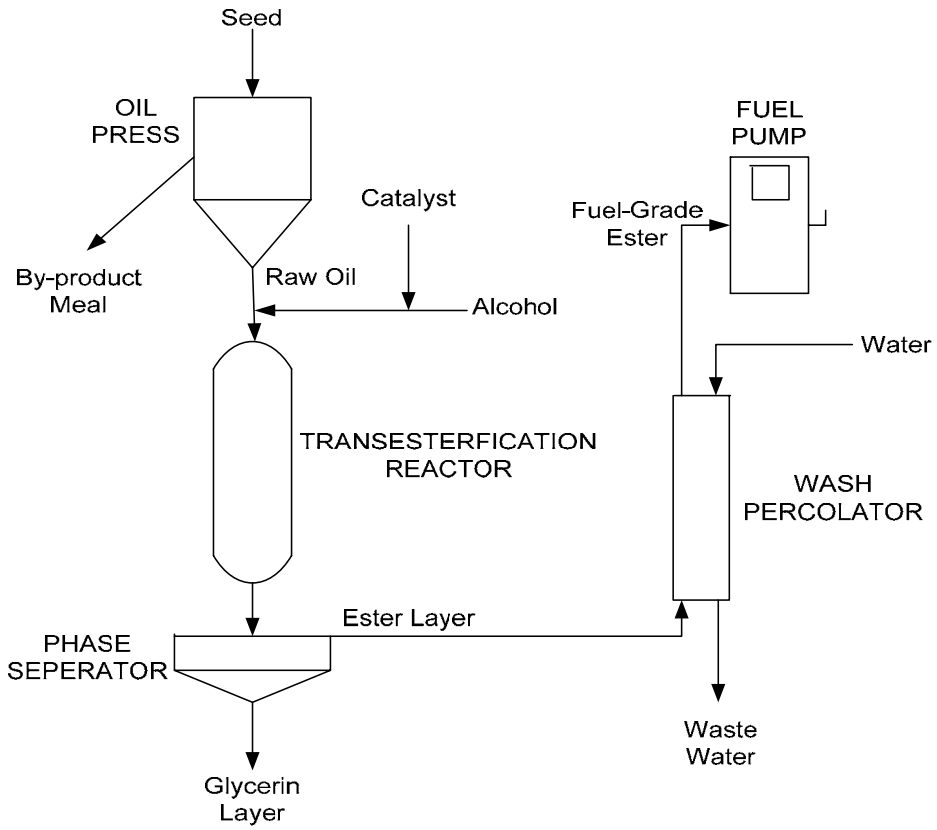

Figure 8.6: Biodiesel Production from Seed Oil (Goswami, et al, 2000)

A vital step in producing biodiesel from seed oils is shown in Figure 8.6 at the transesterfication reactor. Transesterfication is the process by which triglycerides in vegetable oil are reacted with methanol or ethanol to produce esters and glycerol. In the reaction, one triglyceride molecule [G1(FA)$_3$] reacts with three methanol molecules [MeOH] to produce three esters molecules [MeFA] and one glycerol molecule [G1(OH)$_3$] according to the reaction

$$G1(FA)_3 + 3MwOH \rightarrow 3MeFA + G1(OH)_3$$

where FA represents the fatty acid component.

Potential of Biofuels

Currently, the United States imports more than 53% of the petroleum it uses for transportation fuel. The U.S. Department of Energy (DOE) estimates that this will increase to 75% by 2010. Inevitably, this heavy dependence on imported oil makes oil supply vulnerable to international politics, economics, and military activities. The DOE, the U.S. fuels industry, automotive manufacturers, and the agricultural and forestry products industries are working together to ease our dependence on foreign oil and improve our energy security by bringing biofuels to the marketplace.

The United States has a vast biomass resource. Oil-bearing crops such as soybeans can be used to make biodiesel; residues from food and nonfood crops can be converted into liquid fuels such as ethanol. The nation's forests contain many small-diameter trees and underbrush that can be used to produce fuel.

In the 1960's, the discovery of oil outpaced oil consumption. Today, 75 million barrels per day are consumed while only 15 million barrels are discovered; a deficit that continues to grow. Figure 8.7 illustrates the oil consumption and production of industrialized areas.

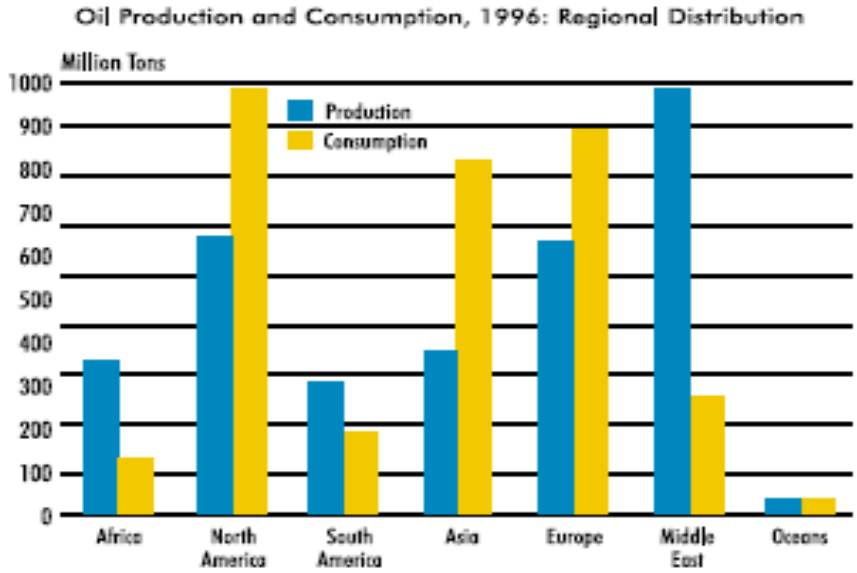

Figure 8.7: Oil Production and Consumption
(http://devafdc.nrel.gov/pdfs/energysecurity.pdf)

The reality that the consumption of fossil fuel based oils far exceeds the production of oils in all major areas except for Africa and the Middle East means that the potential for developing mass production of biofuels is very high. Potential uses for biofuels include automotive, power generation, mechanical lubrication, plastics production, and many others. Biofuels have an exceptionally high potential for use in an m-CHP system.

The local availability and potential decrease in resource costs are attractive for m-CHP systems. The fact that m-CHP systems are not mobile also increases the range of biofuels that could potentially be used because storage issues will be reduced. Biofuels would be an ideal fuel source for the external combustion Stirling Engine, and can be easily used in slightly modified reciprocating engines.

Economic Assessment

As the cost of fossil fuels, coal, and natural gas increases, the economic feasibility of adopting the use of biofuels increases. Also, as the technology and processes used to refine biofuels advances, biofuels become more attractive. Still, there are many obstacles to overcome before biofuels are an economically attractive solution.

To begin, collecting the biomass can be a time, cost, and labor intensive process. If waste material is used, the variability and complexity involved in converting the biomass into usable fuel can increase the capital and operational costs of the system. The variability of waste material also leads to collection and transportation issues. If an energy crop is used as the source of biomass, all the steps required to obtain the energy crop must be considered. First, the land (soil) must be prepared, the crop planted, fertilized, irrigated (if necessary), and finally the crop must be harvested. Each of these steps includes an input in the form of both energy and money.

There are also several issues to be addressed in harvesting the energy crop. As mentioned previously, harvesting strategies that do not include harvesting the lignocellulose waste the greatest portion of the energy crop. Also, there is the issue of contaminants in the harvested energy crop and their effect on the fuel processing equipment.

A major issue to be addressed for biofuels to become feasible is that the required infrastructure does not yet exist. To establish such an infrastructure would take a large capital investment and a significant amount of time.

Still, biofuels hold significant potential for future energy production, particularly in the area of m-CHP and other niche applications. One argument predicts that as time continues and advances in biofuel production are made, and as the cost of traditional fuels, such as natural gas and gasoline increases, the cost curves of the two fuels will intersect as shown in Figure 8.8. In Figure 8.8 the cost of each fuel is plotted as a function of time. At some unknown date, X, the cost of biofuels will become equal to or less than the cost of traditional fuels. At this point, biofuels will become an economically viable option for the masses. The curves in Figure 8.8 do not represent actual cost data, but are used only for representation.

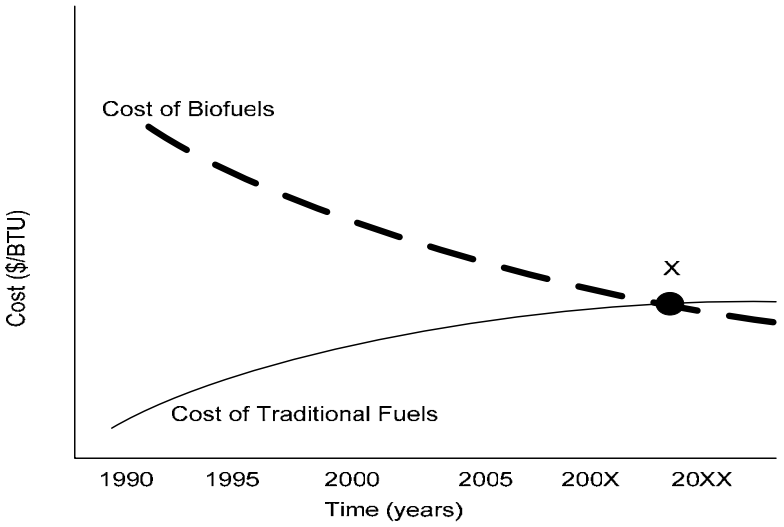

Figure 8.8: Theoretical Representation of Cost of Fuels as a Function of Time

A long-term economic assessment which encompasses all aspects and issues for producing biofuels as compared to traditional fuels has not yet been completed. Until such a study is done, much discussion of economic feasibility is generic and not quantitative. To give a better perspective, the cost information for the various production methods of biofuels is presented in Table 8.5.

Table 8.5: Cost Information for Production Methods of Biofuels (Goswami, et al, 2000)

Gaseous Fuels	Anaerobic Digester	$63,000 - $122,00 ton/day of capacity $5.10 - $6.10/GJ
	Gasification Plant	50 MW atmospheric pressure $15 million 50 MW pressurized $60 million
Liquid Fuels	Ethanol Plant	Typical of petrochemical plants. Have Capital Investment with economy of scale $0.26/liter (gasoline $0.20/liter) Lignocellulose basis $0.36/liter
	Corn Starch Facility	5,000 bb/day $0.55 - $1.10/liter capacity
	Methanol Plant	5,000 bb/day capacity cost $380 million $0.57/liter production cost
	Pyrolysis Liquid Plant	5,000 bb/day capacity cost $60 million $0.17/liter production cost
	Biodiesel	$0.33/liter production cost

CHAPTER IX:

CONCLUSIONS

m-CHP is a developing paradigm in energy systems. The driving potential behind m-CHP systems is the thermal efficiency that these systems can achieve and the significant portion of the energy market that lies within the “micro” regime. Projected system efficiencies of 80% are well above the overall thermal efficiencies produced by standard energy systems. m-CHP systems have the potential to increase the overall thermal efficiency, reduce the total power requirement, and provide higher quality, more reliable power than conventional systems. Larger homes, higher energy costs, volatile fuel markets, electricity blackouts, power security, power quality, and lower emissions are additional characteristics that make m-CHP attractive.

A variety of distributed power generation (DPG) technologies may be selected for an m-CHP system. Table 9.1 illustrates how these technologies compare in efficiency, cost, technology status, emissions, noise, and load matching flexibility. The technologies are ranked from those having the most positive characteristics to those having the most negative characteristics. For example, fuel cells have the quietest operation and, therefore, the best characteristics in the noise category, and reciprocating engines generate

significant noise and, therefore, the most negative characteristics in this category. The rankings in Table 9.1 are based on the technologies as a whole and may vary in some instances.

Table 9.1. Rankings for Distributed Power Generating Technologies

Rankings for DPG Technologies	
Category	Most Positive ⇒ Least Positive
Efficiency	Fuel Cells⇒ Reciprocating⇒ Stirling⇒ Microturbine⇒ Rankine
Technology Status	Reciprocating⇒ Microturbine⇒ Fuel Cells⇒ Stirling⇒ Rankine
Cost	Reciprocating⇒ Microturbine⇒ Fuel Cells⇒ Stirling⇒ Rankine
Emissions	Fuel Cells⇒ Stirling⇒ Microturbine⇒ Rankine⇒ Reciprocating
Noise	Fuel Cells⇒ Stirling⇒ Microturbine⇒ Rankine⇒ Reciprocating
Load Matching Flexibility	Reciprocating⇒ Fuel Cells⇒ Microturbine⇒ Stirling⇒Rankine

The thermally activated components discussed in this module are non-competing technologies. The selected use of either an absorption chiller or desiccant dehumidifier is based upon the needs of the application rather than performance. A system configuration requiring only latent cooling would incorporate an absorption chiller. If both cooling and dehumidification are required, both a desiccant dehumidifier and absorption chiller can be included in an m-CHP system.

Despite the potential benefits of m-CHP systems, numerous significant obstacles and challenges must be addressed if m-CHP is to be successful in the United States. Research must be conducted to validate m-CHP systems and components. Likewise, efforts must be made to reduce installed initial capital costs of m-CHP systems. These issues can be resolved with time and the application of good engineering practices. The more difficult issues to overcome are characteristics of the market to which m-CHP systems apply.

In order for m-CHP systems to succeed, maintenance and service support issues must be addressed. Large scale CHP systems are typically installed in large factories, hospitals, or other facilities which employ a full-time maintenance staff. Retaining a full-time maintenance staff for a single m-CHP system is neither practical nor economically feasible. Expecting the owner to maintain the system is also impractical because of technical complexity and safety issues. Still, providing professional, timely service and maintenance will be a crucial part of successful m-CHP system operation. More than one potential technology has become a distant memory because of poor maintenance and technical support. This situation leads to a very important question: Who will provide maintenance and support? Should this responsibility fall on utility providers, individual m-CHP system manufacturers, or independent maintenance contractors?

Another important issue to address is the inclusion and cooperation of local electrical utilities. Ideally, an m-CHP system would provide the exact amount of electrical power needed instantaneously, continually throughout the

day. While designing such a system is possible, unfortunately, the increase in system complexity and increased capital costs would be a detriment to early system installations. Initially, most m-CHP systems will likely be designed as constant-power output or base-load systems. This implies that at some point the power requirement will not be met, or that the requirement will be exceeded. Realistically, both cases will occur within a 24-hour period. For example, in the United States, the base electrical load for the average home is approximately 2 kW while the peak electrical demand is slightly over 4 kW. (EIA) If a 3 kWe m-CHP system were installed in this situation, part of the time more energy will be provided than could be used and for a portion of the time more energy will be required than could be provided.

One option is to size the system for base electrical load. This option requires that the system include an energy storage device or be connected to the electrical grid to provide the peak electrical load. Another option is to size the system for peak electrical load. This option requires that the excess energy be stored, transferred to the electrical grid, or simply rejected as a loss. In all instances, either energy storage or grid connectivity is required. Energy storage is expensive and increases the system size and initial costs. In many instances, a more economically attractive option is for the m-CHP system to be grid connected.

Grid connectivity will require the inclusion and cooperation of local electrical utilities to establish an infrastructure and pricing system to

accommodate m-CHP installations. Grid connectivity also requires the use of two-way metering. The Institute of Electrical and Electronics Engineers-United States of America (IEEE-USA) has developed a series of standards for interconnection of distributed energy resources with the electricity grid. The IEEE 1547 2003 Standard for Interconnecting Distributed Resources With Electrical Systems is the first in the 1547 series of planned interconnection standards. The standard establishes technical requirements for electrical power systems (EPS or electrical grids) interconnecting with distributed generators such as fuel cells, photovoltaics, microturbines, reciprocating engines, wind generators, large turbines, and other local generators. Additional IEEE interconnection standards activities are now designated under the 1547 series of standards.

Before a full-market drive for installation of m-CHP systems is attempted, an in-depth case study of an m-CHP system should be performed. Also, a full economic assessment including all capital costs and the potential effects of the volatile fuel market should be conducted. The selection and price of fuel to be used in an m-CHP system is very important. A small percent change in the market demand creates a large change in the cost of many fuels.

REFERENCES

Books

1. Moran, Michael J., and Shapiro, Howard N., *Fundamentals of Engineering Thermodynamics,* 4th edition, New York: John Wiley and Sons, 2000

2. Caton, Jerald A., and Turner, W. Dan, "Cogeneration," *CRC Handbook of Energy Efficiency*, New York: CRC Press, Inc., 1997.

3. Peltchers, Neil, *Combined Heat and Power Handbook: Technologies and Applications*, The Fairmont Press, Inc., Georgia, 2003

4. Hodge, B.K., and Taylor, Robert P., *Analysis and Design of Energy Systems*, 3rd edition, New Jersey: Prentice Hall, Inc. 1999.

5. Chamra, Louay, Parsons, Jim A., James, Carl, Hodge, B.K., and Steele, W. Glenn*, Desiccant Dehumidification Curriculum Module for Engineering/Technology HVAC Courses*, Mississippi State University, 2000.

6. Harold, Keith E., Klein, Sanford A., and Radermacher, Reinhard. *Absorption Chillers and Heat Pumps*, New York: CRC Press, Inc., 1996.

7. Shah, Ramesh K., "Recuperators, Regenerators and Compact Heat Exchangers," *CRC Handbook of Energy Efficiency*, New York: CRC Press, Inc., 1997.

8. Boyce, Meherwan P., *Handbook for Cogeneration and Combined Cycle Power Plants*, New York: ASME Press, 2002

9. Cengel, Yunus A., *Heat Transfer: A Practical Apprach*, 2nd edition, New York: McGraw Hill, 2003

10. Laraminie, James, and Dicks, Andrew, *Fuel Cell Systems Explained*, 2nd edition, West Sussex: Wiley, 200

11. Stull, D.R., et al., *JANAF Thermochemical Tables*, Michigan: Dow Chemical Company, 1965

12. Urieli, Isreal, and Berchowitz, David M., *Stirling Cycle Engine Analysis*, Great Britain: Adam Hilger Ltd.,1984

13. Senft, James R., *Ringbom Stirling Engines*, New York: Oxford University Press, 1993

14. Hardy, J.D, *Cooling, Heating, and Power for Building Instructional Module*, Mississippi State University, 2004

15. Goswami, D.Y., Kreith, F., and Kreider, J., *Principles of Solar Engineering*, 2nd edition, Taylor and Francis Pub., 2000.

16. Felder, Richard M., and Rausseau, Ronald W., *ElementaryPrinciples of Chemical Processes*, 2nd edition, New York: John Wiley and Sons, 1986

17. RS Means Mechanical Cost Data 24th Annual Edition, Kingston, Maryland: RS Means Company Inc. 2001

Journal Articles

1. "The micro-CHP Technologies Roadmap: Meeting 21st Century Residential Energy Needs" December 2003 United States Department of Energy Office of Energy Efficiency and Renewable Energy

2. Alanne, Kari, and Saari, Arto, 2003, "Sustainable Small-scale CHP Technologies for Buildings: The Basis for Multi-perspective Descision Making," Renewable & Sustainable Energy Reviews, Helsinki University of Technology, Hut, Finland

3. Harrison, J., 2003a, "Micro CHP in Rural Areas," EarthScan James & James. 1 January, 2003.

4. Harrison, J. 2003b, "Micro CHP in Europe" EA Technology. Presentation at the 2003 National Micro CHP Technology Pathways Workshop.

5. Harrison, J., 2003c, "Towards a Strategy for micro CHP in the USA Domestic Markets," EA Technology © June 2003.

6. Flin, D., 2005, “Domestic CHP in Europe,” Cogeneration and On-Site Power Production, Jan. – Feb. 2005, pp. 43 – 49.

7. Pehnt, P., Praetorius, B., Foscher, C., Schnieder, L., Cames, M., and VoB, J.P,, 2004, “Micro CHP – a Sustainable Innovation?,” Transformation and Innovation in Power Systems, Berlin/Heidelberg

8. Harrison, J. and Redford, S., “Domestic CHP: What Are the Potential Benefits,” Report for Energy Saving Trust, Capenhurst, Chester

9. “Micro Gas Turbines and Heat-Driven Cooling,” Australian National Training Authority, © 2003

10. “Commercial Micro-CHP Using Fuel Cells and Microturbines,” Emerging Technologies and Practices: 2004 American Council for an Energy-Efficient Economy

11. Basso, Thomas S. and DeBlasio, Richard, “IEEE 1547 Series of Standards: Interconnection Issues,” IEEE Transactions on Power Electronics, Vol. 19, No. 5, September 2004

Internet References

1. http://www.microchap.info, micro CHP website maintained by Jeremy Harrison

2. http://www.eia.doe.gov, DOE Energy Information Administration.

3. http://www.energy.ca.gov/distgen/, California Distributed Energy Resources Guide.

4. http://www.eere.energy.gov/, DOE Energy Efficiency and Renewable Energy (EERE).

5. http://www.eere.energy.gov/de/, DOE Distributed Energy Resources Distributed Energy Program.

6. http://en.wikipedia.org/wiki/Internal_combustion_engine, “Internal Combustion Engine,” Wikipedia, 10 May, 2005

7. http://www.siu.edu/~autoclub/frange.html, “Fundamentals of the Four Stroke Internal Combustion Engine,” 10 May, 2005

8. http://www.eren.doe.gov/der/chp/pdfs/chprev.pdf, “Review of Combined Heat and Power Technologies,” ONSITE SYCOM Energy Corporation, October 1999.

9. http://www.platts.com/Research, “Microturbines: Lessons Learned from Early Adopters,” E Source Multi-Client Market Research Studies, 2003

10. http://physics.about.com/cs/thermodynamic, Anderson, Joseph, “Determine the Efficiency of the Stirling Cycle,”9 June, 2005

11. http://www.energy.ca.gov/distgen/, California Distributed Energy Resources Guide.

12. http://www.eren.doe.gov, DOE Energy Efficiency and Renewable Energy Network (EREN).

13. http://en.wikipedia.org/Stirling_engine, “Stirling Engine,” Wikipedia, 13 April, 2005

14. http://www.howstuffworks.com, How Stuff Works

15. http://www.keveny.com/Vstirling.html, Keveny, Matt, 2000, “Two Cylinder Stirling Engine”

16. http://www.bnl.gov/est/files/pdf/No.%2003.pdf, Butcher, Tom, 2003, “MicroCHP The next Level in Efficiency,”

17. http://hyperphysics.phy-astr.gsu.edu/hbase/thermo/diesel.html, Georgia State University Physics Website

18. http://www.iit.edu/~smart/garrear/fuelcells.htm

19. http://www.fctec.com/fctec, The U.S. Department of Defense (DoD) Fuel Cell Test and Evaluation Center

20. http://www.ieeeusa.org/policy/positions/interconnection.html, IEEE-USA Position Statement on Standards for Interconnection of Distributed Energy Resources

21. http://www.oit.doe.gov, DOE Industrial Technologies Program

22. http://www.eere.energy.gov/biomass, DOE Biomass Program

Manufacturer Websites

Reciprocating Engines

www.generac.com
www.cat.com
www.cumminspower.com
www.deutzusa.com
www.kohlerr.com

Microturbines

www.capstoneturbine.com/
www.irpowerworks.com/
www.elliottmicroturbines.com
www.turbec.com/
www.bowmanpower.com

Stirling Engines

www.whispergen.com
www.microgen.com
www.enatec.com
www.stirling-engine.de/engl/
www.waoline.com

Rankine Cycle Engines

www.enginion.com
www.cogenmicro.com

Fuel Cells

www.cfcl.com.au
www.plugpower.com
www.baxitech.co.uk

Absorption Chillers

www.yazakienergy.com
www.robur.com
www.global.carrier.com
www.trane.com
www.york.com

Desiccant Dehumidifiers

http://www.bry-air.com/
www.muntersamerica.com
www.dehutech.com
www.dri-eaz.com
www.drykor.com
www.dryomatic.com